Sinan GENÇ PHOTOMETRIC MODELLING FOR EFFICIENT LIGHTING AND DISPLAY TECHNOLOGIES AGU 2016

PHOTOMETRIC MODELLING FOR EFFICIENT LIGHTING AND DISPLAY TECHNOLOGIES

A MASTER'S THESIS

By

Sinan GENÇ

December 2016

ABDULLAH GÜL UNIVERSITY

PHOTOMETRIC MODELLING FOR EFFICIENT LIGHTING AND DISPLAY TECHNOLOGIES

A THESIS
SUBMITTED TO THE DEPARTMENT OF
ELECTRICAL AND COMPUTER ENGINEERING
AND THE GRADUATE SCHOOL OF ENGINEERING AND SCIENCE
OF ABDULLAH GÜL UNIVERSITY
IN PARTIAL FULFILLMENT OF THE REQUIREMENTS
FOR THE DEGREE OF
MASTER OF SCIENCE

By
Sinan GENÇ
December 2016

SCIENTIFIC ETHICS COMPLIANCE

I hereby declare that all information in this document has been obtained in accordance with academic rules and ethical conduct. I also declare that, as required by these rules and conduct, I have fully cited and referenced all materials and results that are not original to this work.

Sinan GENÇ

REGULATORY COMPLIANCE

M.Sc. thesis titled "**PHOTOMETRIC MODELLING FOR EFFICIENT LIGHTING AND DISPLAY TECHNOLOGIES**" has been prepared in accordance with the Thesis Writing Guidelines of the Abdullah Gül University, Graduate School of Engineering & Science.

Prepared By

Sinan GENÇ

Advisor

Asst. Prof. Evren MUTLUGÜN

Head of the Electrical and Computer Engineering Program

Assoc. Prof. Vehbi Çağrı GÜNGÖR

ACCEPTANCE AND APPROVAL

M.Sc. thesis titled "**PHOTOMETRIC MODELLING FOR EFFICIENT LIGHTING AND DISPLAY TECHNOLOGIES**" and prepared by Sinan GENÇ has been accepted by the jury in the Electrical and Computer Engineering Graduate Program at Abdullah Gül University, Graduate School of Engineering & Science.

26/12/2016

JURY:

Prof. Bülent YILMAZ :…….

Assoc. Prof. M. Serdar ÖNSES :……

Asst. Prof. Evren MUTLUGÜN :…….

APPROVAL:

The acceptance of this M.Sc. thesis has been approved by the decision of the Abdullah Gül University, Graduate School of Engineering & Science, Executive Board dated ….. /….. / …….. and numbered ……..……. .

…….. /…….. / ……..

Graduate School Dean

Prof. İrfan ALAN

ABSTRACT

PHOTOMETRIC MODELLING FOR EFFICIENT LIGHTING AND DISPLAY TECHNOLOGIES

Sinan GENÇ
M.Sc. in Electrical and Computer Engineering
Supervisor: Asst. Prof. Evren MUTLUGÜN

December 2016

Using light emitting diodes (LEDs) as lighting devices has come to the sight as a compulsory step in terms of the energy efficiency. Almost a quarter of total consumed energy that generated whole around the world is used for lighting. Using incandescent bulbs as lighting devices is forbidden in most of Europe and light emitting devices are one of the most important choices in order to compensate that need. Their high performance in terms of both luminance levels and energy efficiency has opened a new research area to increase their performance. White light has different requirements based on an application area. Providing that necessities by engineering on light parameters is one of the main aims of this thesis.

In display technology, the development from cathode ray tubes to organic light emitting devices has increased the performance of both display quality and energy efficiency. Enhancement of the color scale that can be perceived by the human eye is the main purpose so that the reference color area increases systematically. The last announced reference, Rec.2020, has two thirds of the colors perceived by human eye. In this thesis, considering the current references such as National Television System Committee (NTSC) color gamut, the broadening of Rec.2020 is also presented as a new important figure of merit.

In this thesis, we have studied on the investigation of the parameters of the emitters, i.e., peak emission wavelength, full width at half maximum and peak intensity to achieve the desired quality white light. Although it is possible to get white light in each step, the high quality requirements have been implemented by four colors within the simulation

range of thesis which possess color rendering index value >90, correlated color temperature <4000K and luminous efficacy of optical radiation 380 lm/W_{opt}.

In addition, in terms of display technology, we have shown that using ultra narrow emitters is an optimal choice for achieving Rec.2020 color triangle. Using ultra-narrow emitters, it is possible to obtain 99,89% of the Rec.2020 that also almost covers the NTSC. As expected, using a fourth color component cyan has increased the reached area to 169,55% of NTSC on color space dramatically.

Keywords: Colorimetry, color gamut, display technology, lighting, high quality white light

ÖZET

VERİMLİ AYDINLATMA VE EKRAN TEKNOLOJİLERİ İÇİN FOTOMETRİK MODELLEMELERİN GERÇEKLEŞTİRİLMESİ

Sinan GENÇ
Elektrik ve Bilgisayar Mühendisliği Yüksek Lisans
Danışman: Yrd. Doç. Dr. Evren MUTLUGÜN

Aralık 2016

Aydınlatma elemanı olarak ışık saçan diyotların (LED) kullanımı, enerji verimliliği bağlamında zorunlu bir adım olarak ortaya çıkmıştır. Dünya çapında üretilen toplam enerjinin yaklaşık %25'i aydınlatma için kullanılmaktadır. Akkor telli ampullerin aydınlatma elemanı olarak kullanılması Avrupa'nın büyük bir kısmında yasaklanmış ve ışık saçan diyotlar en popüler seçenek olarak bu açığı doldurmuştur. Hem aydınlatma seviyesi hem de enerji verimliliği açısından yüksek performanslı oluşları, daha verimli hale getirilebilmeleri için yeni bir araştırma alanı ortaya çıkarmıştır. Yüksek kaliteli beyaz ışık kullanıldığı ortama göre farklı özellikler gerektirir ve beyaz ışığı oluşturan renk bileşenlerini optimize ederek bu gerekliliklerin sağlanması, bu tezin temel amaçlarından biridir.

Ekran teknolojisinde, tüplü televizyonlardan (CRT), organic ışık saçan diyot (OLED) ürünlere gelişme süreci, hem ekran kalitesi hem de enerji verimliliği performansını arttırmıştır. Ekranlardaki renk skalasının, insan gözüyle algılanabilen skalaya doğru genişlemesi temel amaç olduğundan, referans alınan skala sistematik bir şekilde genişlemektedir. Literatürdeki son referans, Rec.2020, insan gözüyle algılanabilen renklerin üçte ikisini kapsamaktadır. Bu tezde, kullanımda olan NTSC renk skalası gibi referanslar da dikkate alınarak Rec.2020 renk gamının genişletilmesi yeni bir amaç olarak tanımlanmıştır.

Bu tezde, istenilen kalitedeki beyaz ışığa ulaşabilmek için, renk bileşenlerinin tepe ışıma dalga boyu, ışıma genişliği ve tepe değeri gibi ışıyıcı parametrelerinin sahip olması gereken değerler araştırılmıştır. Her adımda beyaz ışık elde edilmesine rağmen, dört renk bileşeni ile oluşturulan beyaz ışık simülasyonu yüksek kaliteli beyaz ışık

gereklilikleri olan renk eşleme indisi >90, renk sıcaklığı <4000K ve optik yayılmanın ışıksal verimi >380lm/W_{opt} değerlerini aynı anda sağlamıştır.

Ek olarak, ekran teknolojisi bağlamında, Rec.2020 renk referansına ulaşabilmek için kolloidal kuantum noktacıklar gibi dar ışıyıcılar ile birlikte 10nm'den daha dar (ultra dar) ışıyıcıların da kullanılmasının uygunluğu belirtilmiştir. Ultra dar ışıyıcılar ile Rec.2020 üçgeninin %99.89'una ulaşılmış ve bu parametreler kullanılarak NTSC referansı da %99,99'dan daha büyük yüzde ile kapsanmıştır. Beklenildiği üzere, dördüncü renk olarak siyan mavisinin kullanılması NTSC referansına göre ulaşılabilen alanı %169,55'ye çıkarmıştır.

Anahtar kelimeler: Renk bilimi, renk gamı, ekran teknolojisi, aydınlatma, yüksek kaliteli beyaz ışık

Acknowledgements

"Do you like cooking?" was the question when we first talked about what we can do together with my advisor, Asst. Prof. Evren MUTLUGÜN. I like cooking and at the end of the conversation he made me believed that I can cook with colors. Then, I noticed cooking on MATLAB is definitely fun. I am really appreciative for his encouragement and support.

There are many helpful and friendly people from Teknopark times up to now. I thank to Mustafa, Hatice, Oğuzhan, Erhan and the others, the residents of A103 and the guys in Starbucks. I also thank to the fictional characters that all Jedi Knights, Sith Lords and droids from a galaxy far, far away, all heroes from MARVEL studios in particular to the Avengers in the leadership of Nick Fury and finally Behzat Ç. for his effort to make me watch himself instead of writing these lines. As Doctor Who said, there is an old Earth saying. A phrase of great power and wisdom and consolation to the soul in times of need, ALLONS-Y!

After about a year in same office, in Teknopark, I knew a woman well in Sümer. Her smile took my breath away and I fell in love. I want to thank my life, my wife, my woman, Hava, for her thoughtful moments in every fields of life.

Ayrıca, her zaman yanımda olan annem ve babam, Gülsen ve Hikmet'e, kardeşlerim Cihan ve Selin'e, hep bizimle olacak Pakize, Tipsiz, Bıdık ve İnci'ye –ve hatırlayamadıklarıma- çok teşekkür ediyorum.

Last but not least, I would like to thank TÜBİTAK and ARÇELİK A.Ş. for their support on realizing of the thesis within the concept of project numbered 114E107.

"But you know,
happiness can be found even in the darkest of times,
if one only remembers to turn on the light."

Albus Dumbledore

Table of Contents

1. **INTRODUCTION 1**

1.1 HUMAN VISUAL SYSTEM 3
1.2 EYE SENSITIVITY FUNCTION 6
1.3 BASIC COLORIMETRIC DEFINITIONS 7
1.4 BASIC UNIFORM COLOR SPACES 8
1.5 CORRELATED COLOR TEMPERATURE (CCT) 15
1.6 COLOR RENDERING INDEX (CRI) 18
1.7 LUMINOUS EFFICACY OF OPTICAL RADIATION (LER) 20

2. **HIGH QUALITY WHITE LIGHT GENERATION 23**

2.1 TRADITIONAL WHITE LIGHT SOURCES 24
2.2 REQUIREMENTS FOR EFFICIENT WHITE LIGHT 25
2.3 LIGHT EMITTING DIODES 26
2.4 SIMULATION STUDY 28
2.4.1 Two-color mixing 28
2.4.1.1 Defination of simulation parameters 28
2.4.1.2 Simulation methodology 29
2.4.1.3 Two-color mixing simulation 29
2.4.1.4 Two-color mixing results 34
2.4.2 Three-color mixing 42
2.4.2.1 Defination of simulation parameters 42
2.4.2.2 Simulation methodology 43
2.4.2.3 Three-color mixing simulation 43
2.4.2.4 Three-color mixing results 43
2.4.3 Four-color mixing 55
2.4.3.1 Defination of simulation parameters 55
2.4.3.2 Simulation methodology 56
2.4.3.3 Four-color simulation 56
2.4.3.4 Four-color mixing results 56

3. **INVESTIGATION OF COLOR QUALITY ON DISPLAYS 71**

3.1 COLOR GAMUT 71
3.1.1 The effect of FWHM on chromaticity coordinate *75*
3.1.2 Areal percantage vs. Coverage percentage *75*
3.1.3 CIE 1931-CIE 1976 relation *75*
3.2 ULTRA-NARROW EMITTERS FOR WIDE COLOR GAMUT 77
3.3 SIMULATION STUDY 78
3.3.1 Three-color combination *79*
3.3.2 Four-color combination *90*

4. **CONCLUSIONS 93**
5. **BIBLIOGRAPHY 95**
6. **APPENDIX A 101**
7. **APPENDIX B 103**
8. **APPENDIX C 106**
9. **APPENDIX D 108**

List of Figures

Figure 1.1 Wavelengths of electromagnetic radiation and visible light 2
Figure 1.1.1 Human visual system pathway 3
Figure 1.1.2 Structural anatomy of human eye 4
Figure 1.1.3 Anatomy of retina 4
Figure 1.1.4 Sensibility distribution of rodes and cones due to the wavelength .. 5
Figure 1.1.5 Sensibility distribution of rodes and cones due to the luminance level 5
Figure 1.2.1 CIE 1978 eye sensitivity function 7
Figure 1.3.1 Schematic of Gaussian distribution and variables to describe it…..8
Figure 1.4.1 r, g, b color matching functions 9
Figure 1.4.2 CIE RGB color space 11
Figure 1.4.3 x, y, z color matching functions 11
Figure 1.4.4 Wright lines on CIE 1931 color space 12
Figure 1.4.5 MacAdam ellipses on CIE 1931 color space 13
Figure 1.4.6 MacAdam ellipses on u,v color space 14
Figure 1.4.7 MacAdam ellipses on CIE 1976 color space 14
Figure 1.5.1 Isotemperature lines on CIE 1931 color space 15
Figure 1.5.2 Schematic of Robertson method calculation 16
Figure 1.5.3 The effect of CCT change on vision 17
Figure 1.6.1 Effect of CRI on color quality and vision 18
Figure 1.6.2 Test color samples 18
Figure 1.6.3 Spectra of test color samples 19
Figure 1.7.1 LER lines on CIE 1931 color space 21
Figure 1.7.2 The proposed white color region 21
Figure 2.1 Classification of basic light sources in terms of energy consumption 23
Figure 2.3.1 White LED spectra based on fluorescent material 26
Figure 2.3.2 RGB white LED spectra 26
Figure 2.3.3 White LED based on four color components 27
Figure 2.4.1.4.1 The peak emission wavelength-CRI relation for raw data 35

Figure 2.4.1.4.2 For raw data, (a) peak emission wavelength-CCT, (b) peak emission wavelength-LER relation 36

Figure 2.4.1.4.3 For filtered data (CCT<4000K and LER>380lm/W in white region), relations of (a) wavelength-CRI, (b) wavelength-CCT, (c) wavelength-LER in two-color mixing..... 37

Figure 2.4.1.4.4 For filtered data (CCT<4000K and LER>380lm/W in white region), relation of FWHM-CRI in two-color mixing..... 38

Figure 2.4.1.4.5 For filtered data (CCT<4000K and LER>380lm/W in white region), relation of Intensity-CRI in two-color mixing 38

Figure 2.4.1.4.6 Using filtered data (CCT<4000K, LER>380lm/W and CRI>40 in white region), the relation between peak emission wavelength and CRI in two-color mixing. Each dot pairs in blue and yellow with same CRI represent only one parameter set 39

Figure 2.4.1.4.7 Based on commercial blue LED, relation between spectrum parameters and CRI for filtered data by CCT and LER conditions in white region, in two-color mixing..... 41

Figure 2.4.2.4.1 Wavelength-CRI relation for three-color mixing for raw data. 44

Figure 2.4.2.4.2 Wavelength-CRI relation for CRI>85.1 in three-color mixing for raw data 45

Figure 2.4.2.4.3 For filtered data (CCT<4000K and LER>380lm/W in white region), relation of wavelength-CRI in three-color mixing..... 46

Figure 2.4.2.4.4 For filtered data (CCT<4000K, LER>380lm/W and CRI≥85.1), relations between peak emission wavelength and CRI/CCT/LER in three-color mixing 47

Figure 2.4.2.4.5 The relations between FWHM values and CRI in filtered data (CCT<4000K, LER>380lm/W and CRI≥85.1 in white region)48

Figure 2.4.2.4.6 LER-FWHM/Intensity relation for filtered data (CCT<4000K, LER>380lm/W and CRI≥85.1 in white region)..... 49

Figure 2.4.2.4.7 CCT-FWHM/Intensity relation for filtered data (CCT<4000K, LER>380lm/W and CRI≥85.1 in white region) 50

Figure 2.4.2.4.8 LER-CCT relation using filtered data (CCT<4000K, LER>380lm/W in white region)for three-color mixing 51

Figure 2.4.2.4.9 CRI-CCT relation using filtered data (CCT<4000K, LER>380lm/W in white region)for three-color mixing 51

Figure 2.4.2.4.10 LER-CRI relation using filtered data (CCT<4000K, LER>380lm/W in white region)for three-color mixing 52

Figure 2.4.2.4.11 Based on commercial blue LED, relation between peak emission wavelength and CRI in three-color mixing for raw data..... 53

Figure 2.4.2.4.12 Based on commercial blue LED, relation between FWHM/Intensity and CRI in three-color mixing for raw data54

Figure 2.4.3.4.1 Wavelength-CRI relation for high quality white light in four-color mixing 57
Figure 2.4.3.4.2 Wavelength-CCT relation for high quality white light in four-color mixing 58
Figure 2.4.3.4.3 Wavelength-LER relation for high quality white light in four-color mixing 59
Figure 2.4.3.4.4 FWHM-CRI relation for high quality white light 59
Figure 2.4.3.4.5 FWHM-LER relation for high quality white light 60
Figure 2.4.3.4.6 FWHM-CCT relation for high quality white light 61
Figure 2.4.3.4.7 Intensity-CRI relation for high quality white light 61
Figure 2.4.3.4.8 Intensity-LER relation for high quality white light 62
Figure 2.4.3.4.9 Intensity-CCT relation for high quality white light 63
Figure 2.4.3.4.10 Based on commercial blue LED, relation between peak emission wavelength and CRI/CCT/LER in four-color mixing 66
Figure 2.4.3.4.11 Based on commercial blue LED, relation between FWHM/Intensity and CRI in four-color mixing 67
Figure 2.4.3.4.12 Based on commercial blue LED, relation between FWHM/Intensity and CCT in four-color mixing 68
Figure 2.4.3.4.13 Based on commercial blue LED, relation between FWHM/Intensity and LER in four-color mixing 69
Figure 2.4.3.4.14 The spectrum of white light synthesized in laboratory 70
Figure 3.1.1 (a)CIE 1931 color space, (b)CIE 1976 color space 72
Figure 3.1.2 NTSC, Adobe RGB and sRGB color gamuts on CIE 1931 73
Figure 3.1.3 Relation between reference color gamuts……....74
Figure 3.1.1.1 The effect of FWHM change on chromaticity coordinate 75
Figure 3.1.3.1 The relation between CIE 1931 coverage and CIE 1976 coverage ratios 77
Figure 3.3.1.1 The extended lines to determine peak emission wavelengths for simulation ranges. 79
Figure 3.3.1.2 The effect of FWHM on chromaticity coordinates 80
Figure 3.3.1.3 The effect of FWHM on blue (a) and red (b)chromaticity coordinate 80
Figure 3.3.1.4 Possible chromaticity coordinate areas for our simulation 81
Figure 3.3.1.5 Rec.2020, NTSC and our simulated color triangles on CIE 1931 82
Figure 3.3.1.6 Filtered data providing higher than 99% Rec.2020 coverage ratio 83

Figure 3.3.1.7 For Rec.2020 coverage≥99%, NTSC coverages achieved 83

Figure 3.3.1.8 Relation of NTSC coverage and NTSC areal percentages for data have higher than 99% for Rec.2020 coverage 84

Figure 3.3.1.9 FWHM-Rec.2020 coverage relation for Rec.2020 coverage≥99% 85

Figure 3.3.1.10 Wavelength-Rec.2020 coverage ratio relation for commercial blue LED application using results that have more than 99% NTSC coverage 86

Figure 3.3.1.11 Relation of NTSC coverage and NTSC areal percentages using commercial blue LED 87

Figure 3.3.1.12 FWHM-Rec.2020 coverage relation for commercial blue LED application using results that have more than 99% NTSC coverage 88

Figure 3.3.1.13 For equal intensities, the emission spectra of the synthesized green and red components along with the blue InGaN LED 89

Figure 3.3.1.14 The relation of color gamut based on synthesized emitters and reference color triangles 90

Figure 3.3.2.1 Rec. 2020 coverage after addition of cyan component to the parameters of best set in three-color combination 91

Figure 3.3.2.2 Rec.2020 coverage after addition of cyan component to the parameters that have more than 99% coverage in three-color combination 92

List of Tables

Table 2.4.1.4.1 The parameter sets that provide the CCT and LER requirements in white region and have CRI>40 in two-color mixing 40

Table 2.4.2.4.1 Wavelength-CRI relation for three-color mixing for raw data .. 43

Table 2.4.2.4.2 The parameter sets that provide the CCT and LER requirements in white region and have CRI>85.1 in three-color mixing 53

Table 2.4.3.4.1 The parameter sets for hihg quality white light in four-color mixing 64-65

Table 3.1.1 The red, green and blue coordinates of NTSC, Adobe RGB and sRGB color spaces 73

Table 3.1.2 The red, green and blue coordinates of Rec.2020 color space 74

Table 3.3.1.1 The distribution of results considering the coverage ratio on Rec.2020 82

To the Montana Gang,
bad boys of the city,
and
Kadiköy streets where we still learn about
life and women.

Chapter 1

Introduction

Light. An electromagnetic radiation that provides the ability of sight. In semiconductors, the recombination of an electron and a hole emits energy in the form of photons. This radiation can be visible to the human eye depending on the energy of it. The light can be classified by its frequency or wavelength as can be seen in Figure 1.1. The visible light has a range of approximately 400nm to 700nm on the wavelength scale of light. It starts with blue and continues with cyan, green, yellow, orange and red colors respectively.

The number of colors that we can distinguish is ten million according to Judd and Wyszecki [1]. However, it is impossible to identify all colors exactly. There are three different components to describe the color; the source of light, the objects illuminated by the source and the observers. The eye and the brain that we use to see, define colors, as observers constitute the basics of human visual system. Before describing the structure of human eye, it is important to characterize the nature of the light, which stimulates the visual system.

The Sun, which is the main light source, emits electromagnetic waves through the world and photons illuminate our surroundings. Light has a spectrum which includes all visible colors and density of them. The daylight has all colors in it so that the well-known experiment in which white light comes from one side and at the opposite side different colors occur separately by the effect of interference.

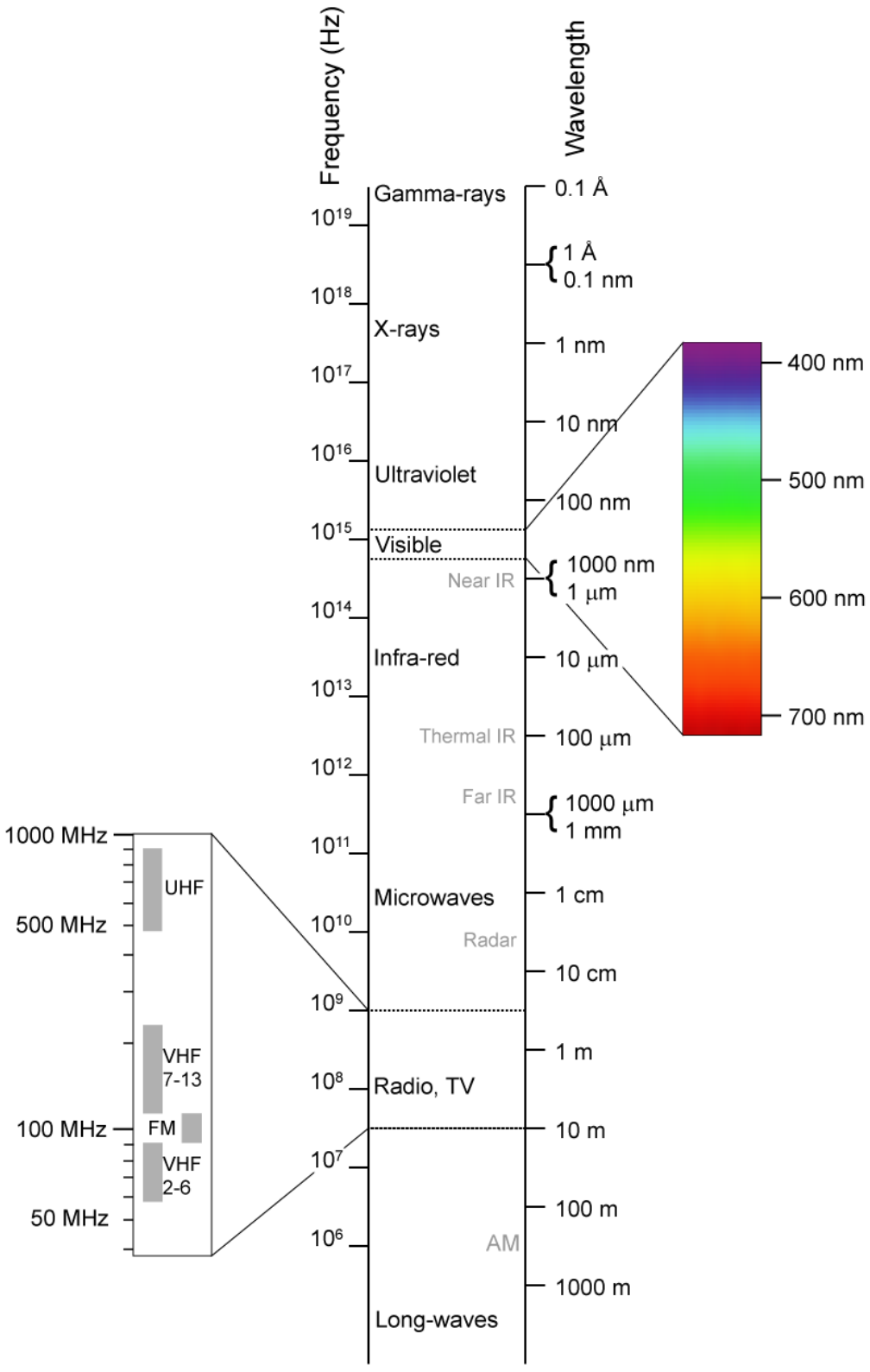

Figure 1.1 Wavelengths of electromagnetic radiation and visible light [2]

1.1 Human Visual System

The source of the light is an illuminant, such as Sun. The radiated light or spectrum comes to our surrounding. At this point the human visual system takes the leading role. The process of vision in humans can be named as both electrical and chemical activities of nerve cells in a part of brain. The occipital lobe, located at the back of the head, includes visual cortex. Before the signals reach to the brain, they have been collected in the retina and transferred by the optic nerve to the lateral geniculate nucleus (LGN). The brain gets the signals from the LGN. The whole system from eyes to brain that can be seen in Fig. 1.1.1, is called as visual pathway [3].

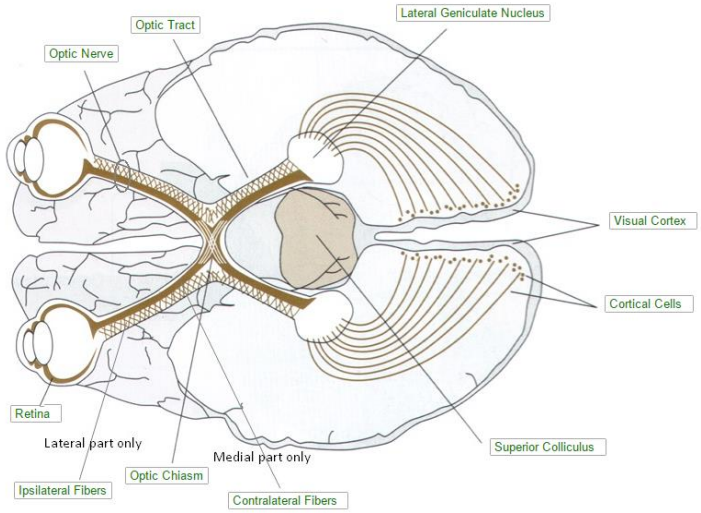

Figure 1.1.1 Human visual system pathway [4]

The critical part in terms of the vision is the retina where the light is received and analyzed. The light sensitive part of the eye, retina, covers the internal surface of the eyeball as can be seen in Fig. 1.1.2.

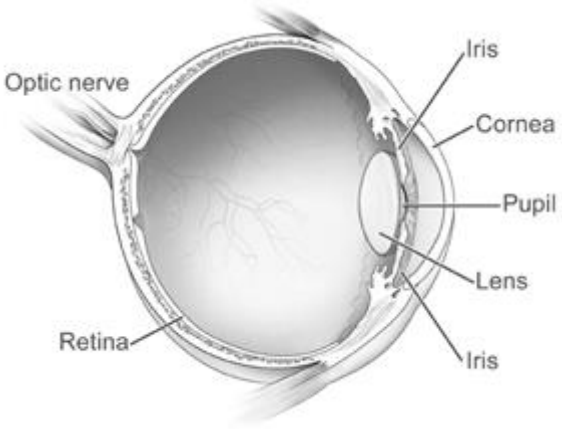

Figure 1.1.2 Structural anatomy of human eye [5]

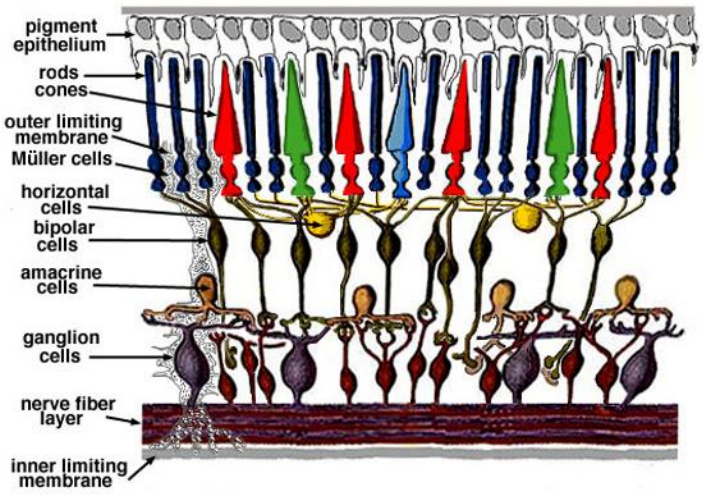

Figure 1.1.3 Anatomy of retina [6]

The retina includes rod cells and cone cells the light-sensitive part and also ganglion cells and nerve fibers that transmit the information of vision to the brain as given in Fig. 1.1.3. Rods are much more in number than the cones and they are also more light sensitive over the entire visible range [7]. Three types of cone cells are responsible for three different visible ranges, red, green and blue lights as given in Fig. 1.1.4.

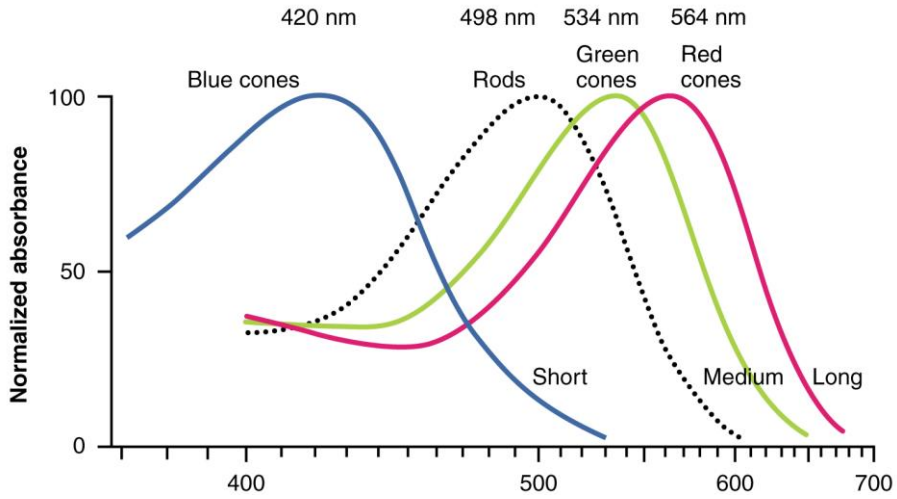

Figure 1.1.4 Sensibility distribution of rods and cones due to the wavelength [8]

Due to the luminance level of the environment, the vision regime is divided into three regimes; photopic, mesopic and scotopic [9]. In photopic region, where the luminance level is higher than 3 cd/m^2 such as daylight conditions the vision is provided via cones. The scotopic regime, where the luminance level lower than 0,003 cd/cm^2, occurs at night conditions and rod cells are dominant. Although the rods are more sensitive than cones, the color discrimination is lost in the scotopic vision regime. The objects are in colors only at different levels of grey. The mesopic vision that happens at the luminance level lower than photopic and higher than scotopic where both rods and cones are active as can be seen in Fig. 1.1.5.

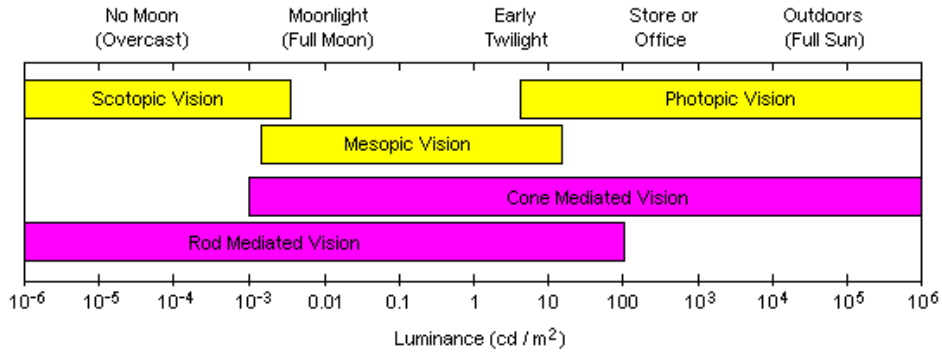

Figure 1.1.5 Sensibility distribution of rods and cones due to the luminance level [10]

1.2 Eye Sensitivity Function

The quality of the white light is also linked with the human eye. A high quality white light must match with the human eye sensitivity function as much as possible. The sensitivity of human eye is limited with visible wavelength range so that the radiated light by the source may not be perceived for some wavelengths that mean all radiation of the source mat not contribute to the vision.

The relation between the light source and human eye sensibility is evaluated using eye sensitivity function *V(λ)*. In 1924, International Commission on Illumination (CIE) declared the photopic eye sensitivity function called CIE 1931 *V(λ)* function. In the USA, it is still in use as a photometric standard whereas a modified eye sensitivity function has already been declared.

In 1978, Judd and Vos, introduced a modified eye sensitivity function which is called CIE 1978 *V(λ)* function to regulate the relation in blue and violet spectral region as can be seen in Fig. 1.2.1 [9]. The peak point of the function is located in 555nm with a normalized peak point value. If the spectrum of a light source matches with the eye sensitivity function or located in the area under it, the compatibility between the radiated light and perceived light would be maximum. The harmony of that relation will be explained in luminous efficacy of optical radiation (LER) part.

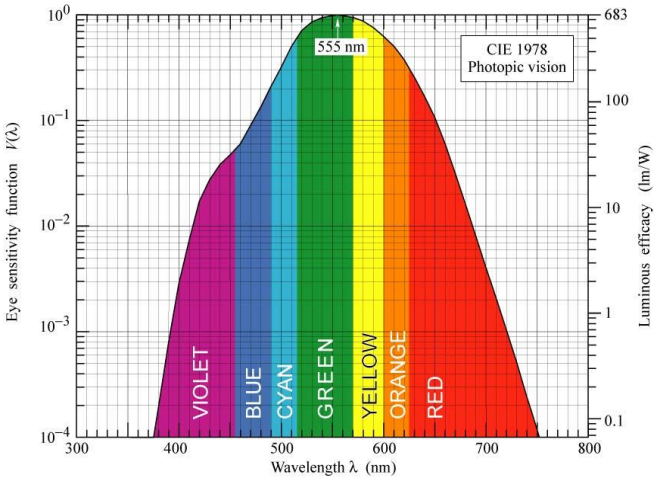

Figure 1.2.1 CIE 1978 eye sensitivity function [11]

1.3 Basic Colorimetric Definitions

When an object is illuminated by Sun or an external light source, the object absorbs some part of the spectrum of the light and reflects the remaining depending on its refractive index. Our eyes get only the reflected part of the spectrum and we see the object as the color in combination of that reflected part. The reflected part has peak or peaks in spectrum that represent the color components [12].

Apart from peak emission point, the full width at half maximum (FWHM) and intensity are the other variables for spectrum. In representation of an emitter, the emission spectrum of the illuminant is described as a Gaussian given in Fig. 1.3.1.

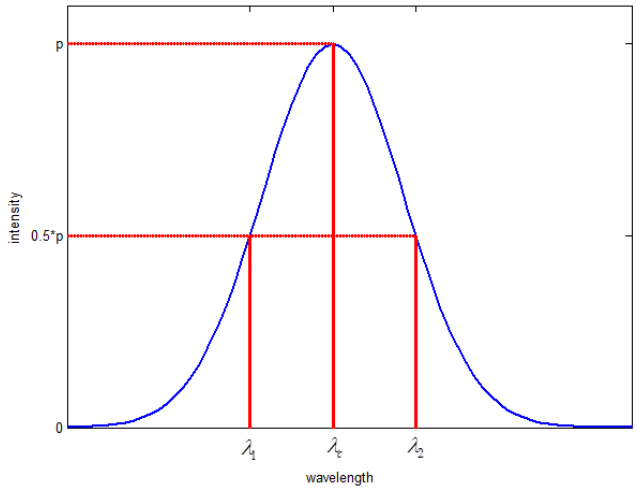

Figure 1.3.1 Schematic of Gaussian distribution and variables to describe it

These three variables are used to describe color. Using peak emission wavelength and FWHM, the chromaticity coordinates are identified. After calculation of chromaticity coordinates the point of the spectra on color space is identified.

The color matching functions described by CIE are the numerical definition of chromatic response that means spectral sensitivity curves of three color detector. They are used as a reference in the calculation process of chromaticity coordinates. All data corresponding to the functions are given in Appendix A. Another parameter tristimulus values that will be described in detail in next parts are the amounts of the components in an additive color model [13].

1.4 Basic Uniform Color Spaces

Color space organizes all visible colors by human eye. The colors are grouped and placed on different color spaces in different scales. In an additive color model, the test stimulus (F) can be defined as the amounts of three primaries R, G, B of the stimuli [R], [G] and [B]. Thus the color matching equation can be defined as in Eq. 1.4.1 which is called Grassmann's Equation [13]. The [R], [G], and [B] can be thought as basis vectors in three dimensions.

$$F = R[R] + G[G] + B[B] \tag{1.4.1}$$

In CIE RGB color space, the identification of a color spectrum is same with the equation described above. The effect is calculated through the visible wavelength range. The multiplication of the light source's spectrum with red, green and blue color matching functions is integrated separately and the yield of that process is amount of the primaries, R, G, B in light source's spectrum. The equations of these steps are given in Eq. 1.4.2 to Eq. 1.4.4

$$R = \int_{380}^{780} \bar{r}(\lambda) \mathrm{P}(\lambda) \mathrm{d}\lambda \tag{1.4.2}$$

$$G = \int_{380}^{780} \bar{g}(\lambda) \mathrm{P}(\lambda) \mathrm{d}\lambda \tag{1.4.3}$$

$$B = \int_{380}^{780} \bar{b}(\lambda) \mathrm{P}(\lambda) \mathrm{d}\lambda \tag{1.4.4}$$

where P(λ) is the spectral distribution of the light source that will be analyzed and $\bar{\mathrm{r}}(\lambda)$, $\bar{\mathrm{g}}(\lambda)$, and $\bar{\mathrm{b}}(\lambda)$ are the color matching functions given in Fig. 1.4.1.

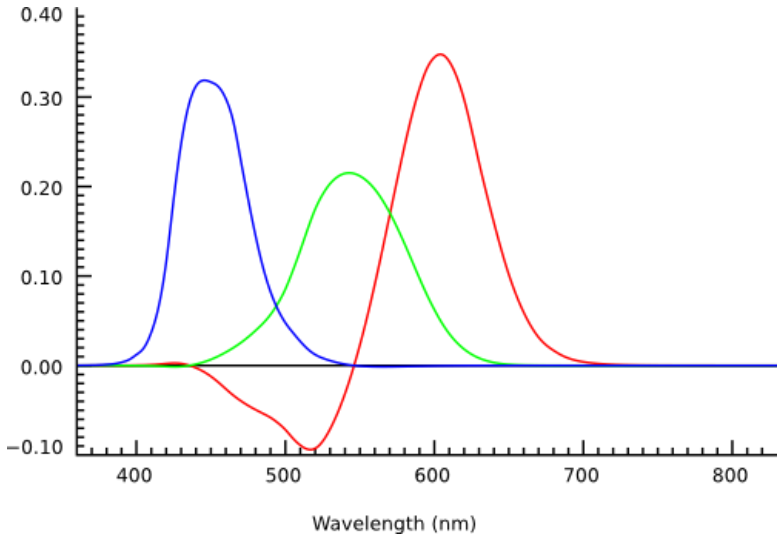

Figure 1.4.1 r, g, b color matching functions [14]

The red color matching function can be seen odd at first sight due to its negative part. The reason of that negative part is the following. Exactly matching a monochromatic light is impossible using monochromatic reference stimuli. The

test light is always too saturated compared to the reference. Thus, to match the test light, the saturation is lowered by adding red, and then the combination is matched using blue and green components [15]. The Grassmann's equation is then modified as,

$$\mathrm{F} + \mathrm{R}[\mathrm{R}] = \mathrm{G}[\mathrm{G}] + \mathrm{B}[\mathrm{B}] \tag{1.4.5}$$

$$\mathrm{F} = -\mathrm{R}[\mathrm{R}] + \mathrm{G}[\mathrm{G}] + \mathrm{B}[\mathrm{B}] \tag{1.4.6}$$

The amount of the three primaries to match the spectra is used to place the color into the unit plane where r, g, and b are the chromaticity coordinates and calculated as given in Eq. 1.4.7 to 1.4.9.

$$r = \frac{R}{R+G+B} \tag{1.4.7}$$

$$g = \frac{G}{R+G+B} \tag{1.4.8}$$

$$b = \frac{B}{R+G+B} \tag{1.4.9}$$

The two of chromaticity coordinates are enough to locate the color since the summation of them are equal to unity and since knowing two of them is sufficient to locate it in the color space. So, the color is specified on the CIE 1931 RGB color space as shown below.

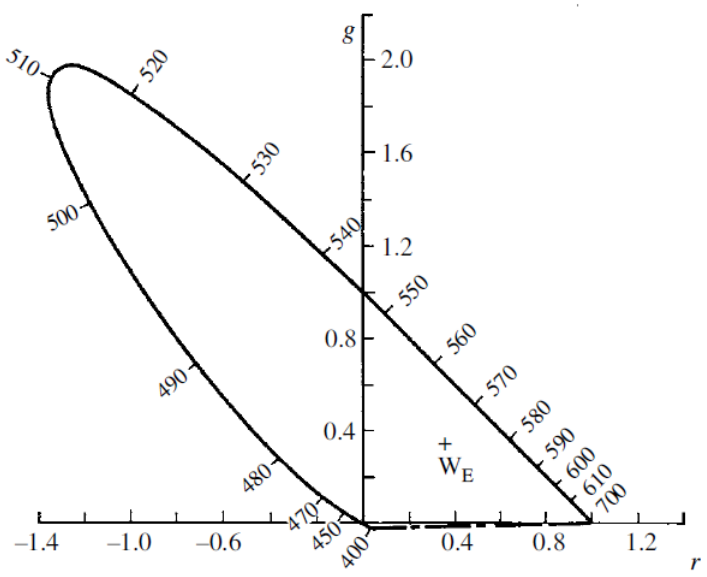

Figure 1.4.2 CIE RGB color space [16]

The RGB system has negative parts in color matching functions and in earlier times it caused complexity in calculations. So, the CIE declared a new color system CIE XYZ and also the conversation between CIE RGB and CIE XYZ. The logic is same in CIE XYZ with RGB but this time the color matching functions has only positive values as given in Fig. 1.4.3.

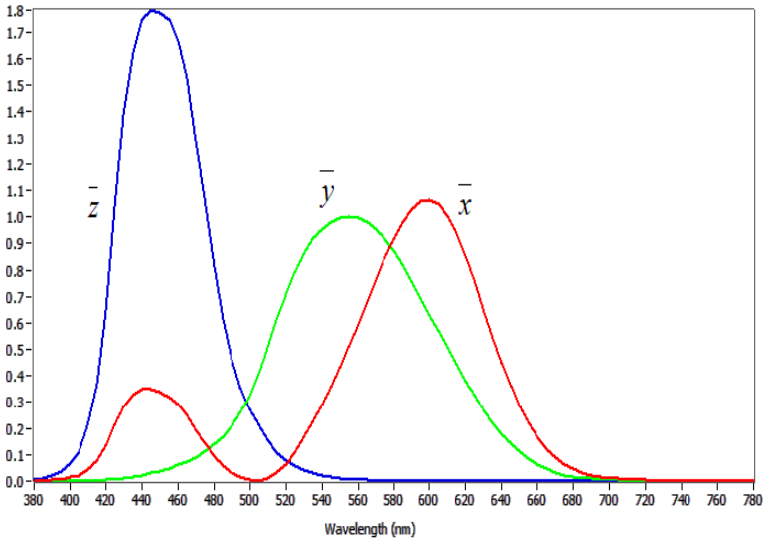

Figure 1.4.3 x,y,z color matching functions [17]

In CIE XYZ, the chromaticity coordinates are calculated using tristimulus values X, Y and Z as given in Eq. 1.4.10 to 1.4.12 and x and y are enough to place the test color on color space.

$$x = \frac{X}{X + Y + Z} \tag{1.4.10}$$

$$y = \frac{Y}{X + Y + Z} \tag{1.4.11}$$

$$z = \frac{Z}{X + Y + Z} \tag{1.4.12}$$

CIE XYZ is most commonly used color system on which colors are placed in x and y axis. The main aim of colorimetry is to distinguish the colors so on color space it is a critical issue to classify and place the colors. Although CIE 1931 color space is still used to be able to compare the new studies with studies done before, the nonuniformity is an important problem for the studies [18]. In 1941 Wright reported some coordinates that have same luminance and same perceived difference and showed them using lines called Wright lines shown in Fig. 1.4.4 [19].

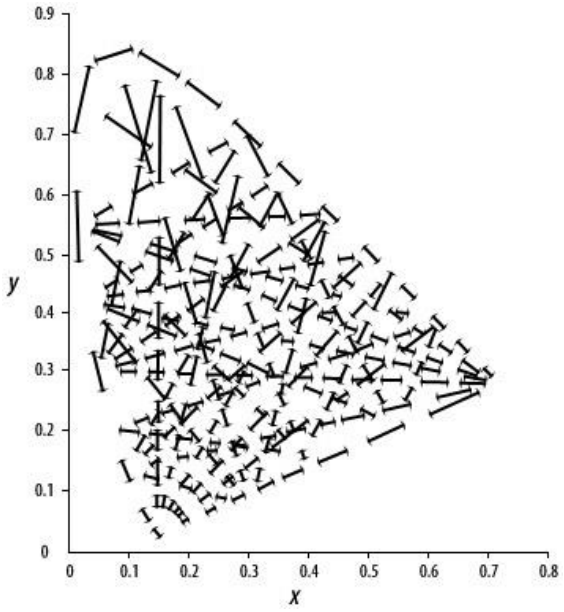

Figure 1.4.4 Wright lines on CIE 1931 color space [20]

The investigation of these lines was followed by David MacAdam as shown in 1942 [21], the just-noticeable color difference varies in different areas on color space as ellipses not as lines as Wright reported. This means that the difficulty to distinguish two colors, changes depending on the area in the color space. In Fig. 1.4.5, the MacAdam's determination is shown as ellipses which ten times extended to provide a better visualization.

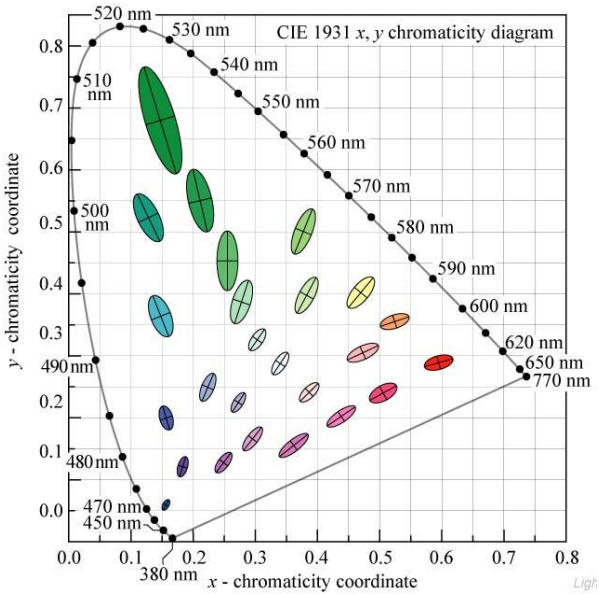

Figure 1.4.5 MacAdam ellipses on CIE 1931 color space [22]

The investigation of nonuniformity on CIE 1931 color space triggered the researchers to search more uniform color spaces. The equal difference distances must be equal in all directions, i.e. using circles instead of ellipses, was the idea of MacAdam [23]. MacAdam's proposed idea was recommended by CIE as 1960 UCS diagram as shown in Fig. 1.4.6.

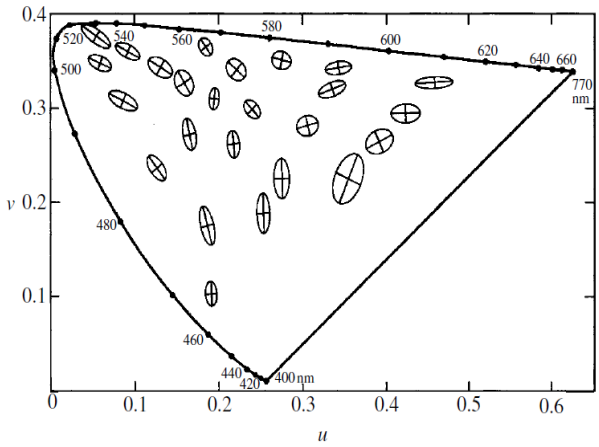

Figure 1.4.6 MacAdam ellipses on u,v color space [24]

The u,v color space was more uniform but the nonuniformity still holds. In 1971 Eastwood announced a better color space in terms of uniformity (u', v') and the only change was the multiplication of v values in u,v diagram by 1,5 [12]. The better circles can be seen in Fig. 1.4.7.

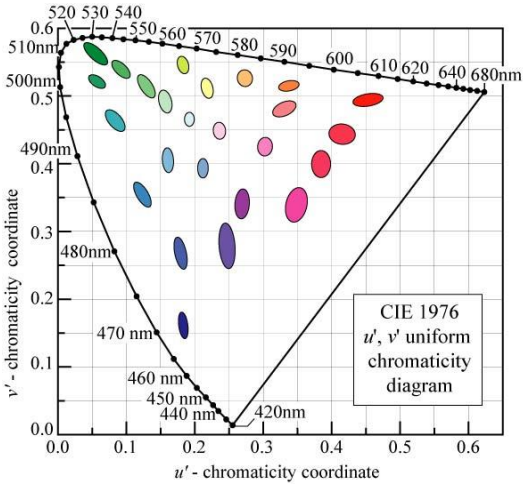

Figure 1.4.7 MacAdam ellipses on CIE 1976 color space [22]

Although CIE declared and recommended 1976 u'v' diagram because of its better uniformity, most of the studies still use CIE 1931 xy declaration to be able to compare their results with the early studies. The declaration of CIE 1976 caused a serious problem in terms of the display color quality calculations. The results announced in the literature have been given in either CIE 1931 or CIE 1976. In Chapter 3, the detailed information is given. In this thesis, all

calculations and percentages are given in CIE 1931 xy color space if it is not specified in other means.

1.5 Correlated Color Temperature (CCT)

Color temperature is a basic metric for visible light and in the application areas such as lighting, publishing, photography etc. and it has a high importance. Color temperatures over 5000K are named cool colors (bluish white), while lower temperatures are named as warm colors (yellowish white through red) [25]. The former is used commonly in public areas to increase the feeling of relaxation, and the latter is preferred to promote concentration in offices.

A Blackbody Radiator, which has definite temperatures and reflects all the lights perfectly is taken as a reference to calculate the color temperature of a spectrum. Most probably the color coordinate of the spectrum will not be lying on the Blackbody curve so that another term, correlated color temperature (CCT), is defined. The CCT means the temperature of the point, which is at the nearest distance to our coordinate on Blackbody. Isotemperature lines have been used to identify the calculation sensibility using micro reciprocal degree (MIRED) scale as can be seen in Fig. 1.5.1.

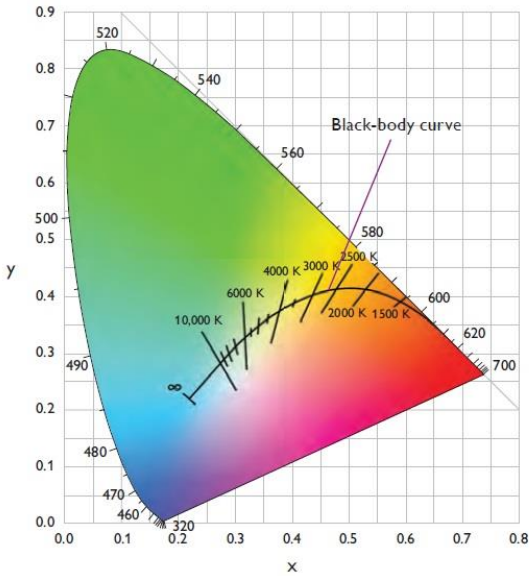

Figure 1.5.1 Isotemperature lines on CIE 1931 color space [26]

The CCT is commonly calculated using Robertson method [27]. In this method, isotherm lines are placed perpendicularly on the Blackbody using MIRED scale, which is one million over Kelvin degree [28]. The point on the isotherm and its temperature is used to calculate the temperature of the coordinate of the spectrum. Linear interpolation is used to calculate the coordinate's temperature. The equations 1.5.1 and 1.5.2 for the calculation and Fig. 1.5.2 for visualization are given below.

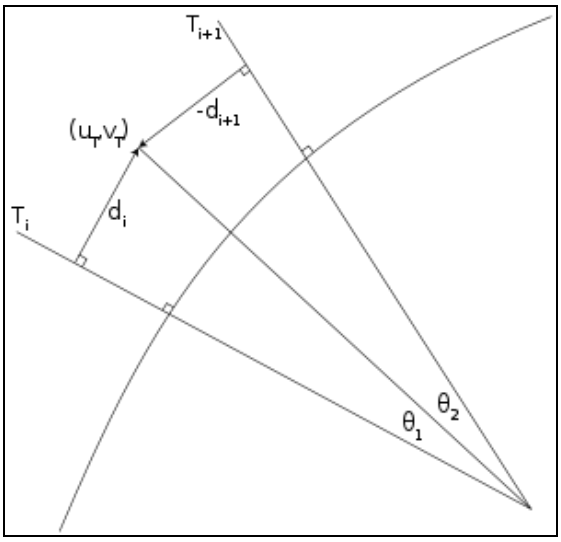

Figure 1.5.2 Schematic of Robertson method calculation [29]

$$\frac{1}{T_c} = \frac{1}{T_i} + \frac{\theta_1}{\theta_1 + \theta_2}\left(\frac{1}{T_{i+1}} - \frac{1}{T_i}\right) \tag{1.5.1}$$

where T_i and T_{i+1} are the color temperatures of the nearest two isotherms and CCT (T_c), is between them. If the distance between isotherm lines is narrow enough, it can be assumed that $\theta_1 / \theta_2 \approx \sin\theta_1 / \sin\theta_2$. So,

$$\frac{1}{T_c} = \frac{1}{T_i} + \frac{d_i}{d_i + d_{i+1}}\left(\frac{1}{T_{i+1}} - \frac{1}{T_i}\right) \tag{1.5.2}$$

The distance d_i can be calculated using the Eq. 1.5.3 given below.

$$d_i = \frac{(v_T - v_i) - m_i(u_T - u_i)}{\sqrt{1 + m_i^2}} \tag{1.5.3}$$

where m_i is the slope of isotherm line.

The CCT can be calculated for any of color coordinate as can be seen from the equations. However, CIE only recommends that the correlated color temperature approach must be used if the chromaticity of the spectrum differs more than $5x10^{-2}$ unit, which is the distance from the locus [27].

In this thesis, the CCT values are analyzed between 0K and 25000K. If the color temperature was below 0K or above 25000K or closer to the locus more than $5x10^{-2,}$ then it was defined as out of range.

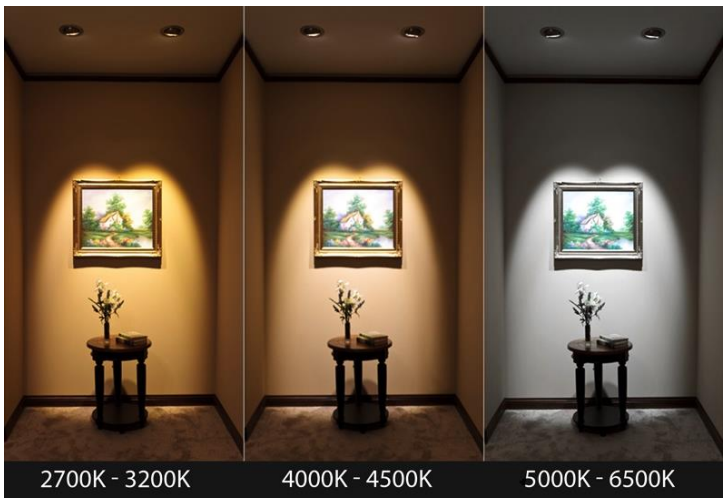

Figure 1.5.3 The effect of CCT change on vision [30]

The correlated color temperature effect on vision and color quality has been given in Fig. 1.5.3. The reference white light is generally chosen as D65 Illuminant, which is defined as the Daylight illuminant for a display. Although D65 has 6500K, for a better display lighting, a CCT below 4000K is preferred [31].

1.6 Color Rendering Index (CRI)

Color Rendering Index (CRI) gives information about the color reproduction ability of a light source and helps us to decide which light source is better for lighting. In other words the CRI gives us the discrimination chance of different colors. A value closer to 100 means that the light source has best CRI and preferably applicable as lighting [32,33,34]. The effect of CRI on vision and also color quality has been given in Fig. 1.6.1.

Figure 1.6.1 Effect of CRI on color quality and vision [35]

The calculation of CRI is a bit complicated process that needs a reference light source and sample colors. Although the calculation of a CRI value is a mathematical process, the color samples are defined in Munsell color space means they are real colors, they can be exactly found in nature. While the first eight of color samples that are used to calculate CIE General CRI, are mid-saturated and give approximately same brightness, the other six that are more saturated, give exact information about CIE Special CRI [36]. In Fig. 1.6.2 and Fig. 1.6.3 the sample colors and their spectra are given respectively.

Figure 1.6.2 Test color samples [37]

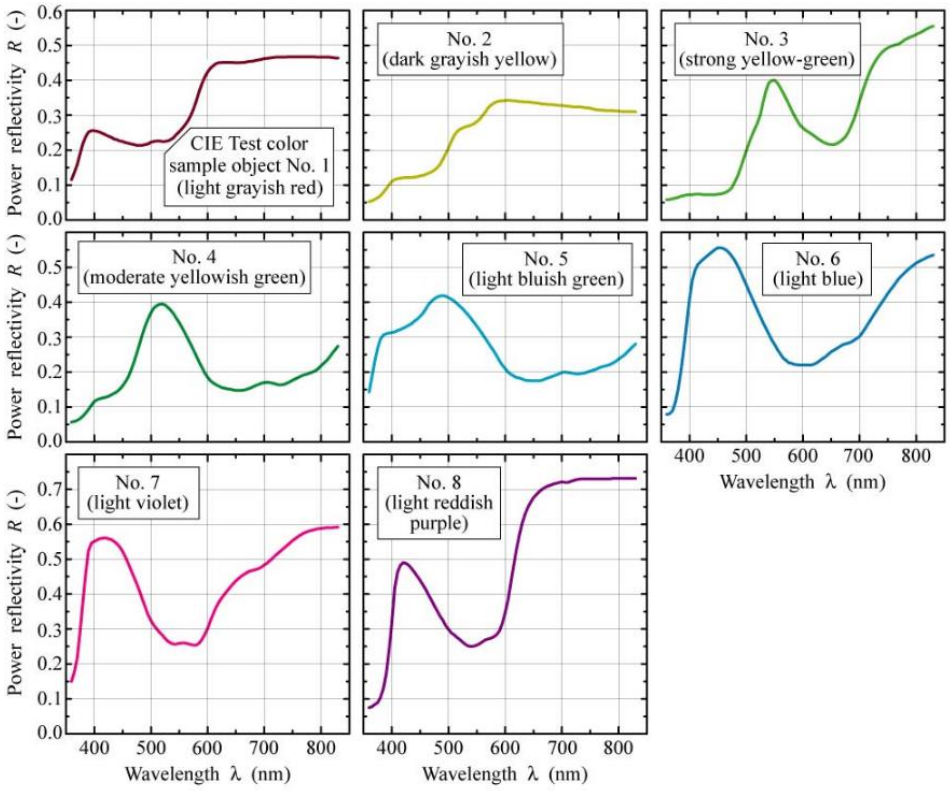

Figure 1.6.3 Spectra of test color samples [38]

In calculation steps, first 8 of all test colors are illuminated by the reference illuminant. The average of all results is assumed as best CRI value, 100. Then our light source is used to illuminate the test colors and the average of differences gives the CRI value.

Illumination of the test colors by the light sources requires a color temperature value and due to that value there are different references such as Blackbody Radiator or CIE Daylight Illuminants. The Blackbody is the reference when the CCT is below 5000K. If the CCT is above 5000K CIE Daylight Illuminant reference is used. Constants are different for below and above 7000K which is approximately the limit for the human eye to distinguish the colors. The CRI value for the CCT above 25000K is undefined.

In lighting technology, a better illuminant is the one that has a CRI value higher than 90. Therefore, in this thesis, the parameters of two/three/four primaries have been optimized to obtain an illuminant with a CRI value higher than 90.

1.7 Luminous Efficacy of Radiation (LER)

Luminous efficacy of optical radiation (LER) is one of the most important parameters to define a white color as high quality. The human eye is limited with a range spectrum in vision matter. The eye sensitivity function presents the most perceived light spectrum by human eye [38]. If the spectrum of the source has an overlap with the eye sensitivity function, the vision occurs at better condition. The measurement of the ability to calculate this effect, LER is used. Calculation of LER is defined as given in Eq. 1.7.1

$$LER = \frac{\Phi_{lum}}{P} = \frac{683 \int_{\lambda} V(\lambda)\,\mathrm{P}(\lambda)\,\mathrm{d}\lambda}{\int_{\lambda} \mathrm{P}(\lambda)\,\mathrm{d}\lambda} \qquad (1.7.1)$$

In calculation steps, the eye sensitivity function is used and the integration of the multiplication with the normalization constant (lm/W) over visible spectrum gives the luminous flux (Φ_{lum}). The division of luminous flux to the input power (P) gives the LER parameter.

In Fig.1.7.1, the values of the LER based on the chromaticity coordinates in CIE 1931 color space is given. An LER value higher than 380 lm/W_{opt} is preffered as limitation because that value is located in the point where white region starts in color space and also as it is stated in previous parts, it is better to have high LER as much as possible in conditions of high quality white light parameters.

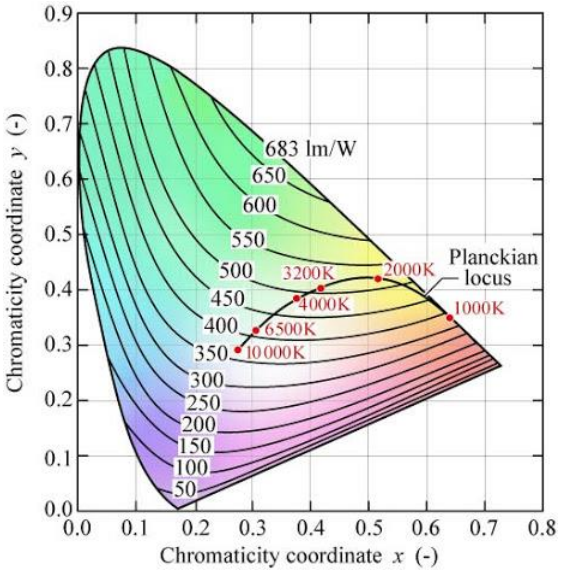

Figure 1.7.1 LER lines on CIE 1931 color space [11]

In calculation steps, all chromaticity coordinates were filtered considering the white region on CIE 1931 color space. As can be seen from Fig. 1.7.2, although the area does not have strict borders, it is assumed that if the coordinate is between 0.2-0.4 for x-axis and 0.25-0.45 for y-axis, the color is regarded as white light.

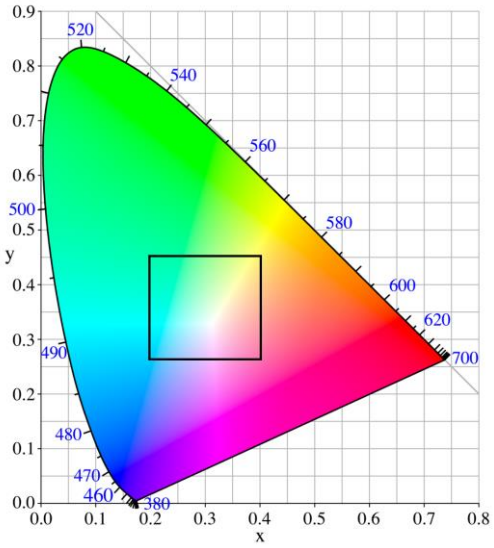

Figure 1.7.2 The proposed white color region

In the first chapter of the thesis, basic terms in colorimetry have been defined. In Chapter 2, the limitations and required parameters will be described for

appropriate and high quality lighting applications, and the spectral output parameters will be optimized for that need. The color parameters for the display applications will be investigated in Chapter 3. In that chapter, the parameters of the spectrum will be analyzed with the aim of achieving the maximum Rec.2020 color gamut. Finally in Chapter 4, the results of the thesis and future aspects of the technology will be discussed.

Chapter 2

High Quality White Light Generation

The limited supplies for the generation of electricity directed the humanity to save energy and search for alternative energy supplies. Since approximately 20% of the electricity generated annually is used for lighting, the use of energy efficient sources for lighting applications will save a huge amount of energy.

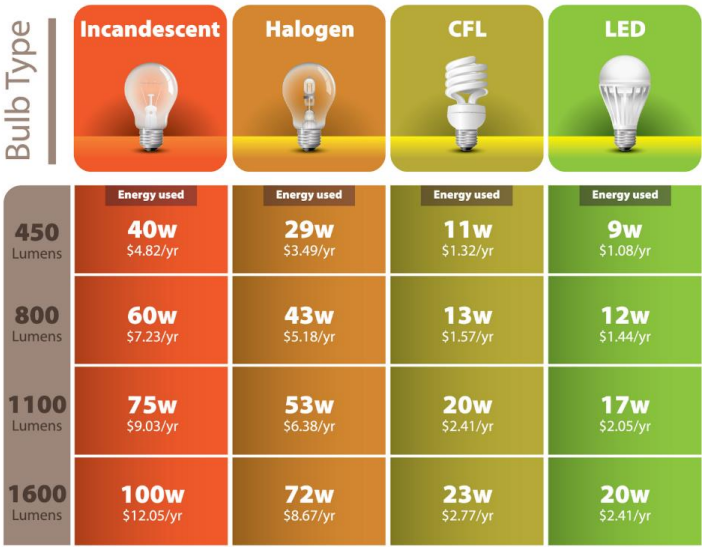

Figure 2.1 Classification of basic light sources in terms of energy consumption [39]

As can be seen in Fig. 2.1, using LED bulbs instead of traditional lighting devices will affect the energy consumption approximately five times compared to the incandescent bulbs. However, while trying to save the energy, it is critical to apply appropriate type of lighting sources to compensate the need. For instance, the requirement for lighting is different according to the application point of view. The lighting parameters are different for a library compared to a jewellery shop. The lighting requirement and performance also varies for indoor and outdoor applications.

The engineering of the color parameters, i.e. ensuring the limitations which define the white light as high quality, is very important. In thesis, the emitters defined as ultra-narrow correspond to the emitters with emission FWHM of 10nm-20nm and narrow emitters correspond to the emitters with FWHM of 30nm-60nm. Due to the ease in controlling their size and size distribution colloidal quantum dots exhibiting narrow emission spectra, are promising devices for lighting applications [40]. The emitters have been simulated using Gaussian distribution to mimic the emission of quantum dots. The parameters to be engineered had been defined in previous steps. Changing the spectral input parameters that are peak emission wavelength, FWHM and intensity, affects the chromaticity coordinate of the color in color space and the combination of color components in different densities influences the performance of the white color.

As have been mentioned before, the optimization of the parameters of lighting is very critical as it would lead to energy saving applications for sustainable Earth.

2.1 Traditional White Light Sources

Although they are inefficient and not have enough quality for a good vision, the white light sources had a great improvement from kerosene to fluorescent lamps. The kerosene is the most primitive white light source. However, in countries where the electricity supplies are not enough, it is a currently used light source [41].

The incandescent lamps are used widely throughout the world and illuminate the objects perfectly, that means they offer high color rendering ability, although they have very low power conversion efficiency (PCE) [42]. In addition to low power conversion they also possess low luminous efficacy of optical radiation (LER) [43].

On the other hand, fluorescent lamps' low photometric performance still holds. Although they exhibit both low LER and PCE, fluorescent lamps have five

times better in terms of luminance level and power efficiency than incandescent lamps [42].

The invention of LEDs presented the light as the main output whereas there is heat dominantly and light seems as a byproduct in the application of incandescent or fluorescent lighting applications. The power conversion efficiency of LEDs is much better and thanks to their small size, precise lighting applications provide ability to light only required areas. Thus, energy saving ratio increases.

2.2 Requirements for Efficient White Light

White light has to follow some requirements in order to be classified as high quality. The most important requirements are the color rendering ability and luminous efficacy of optical radiation [44]. The former is evaluated using the CRI and for an indoor lighting application it must be at least 90 [45]. In addition to the CRI, the correlated color temperature of the source is another figure of merit. Having a CCT value <4000K is desirable for indoor applications. Luminous efficacy of optical radiation is also required to be as high as possible. The target level has been chosen to be minimum 380 lm/W_{opt} [46].

A high quality white light has to provide these requirements in addition to the color coordinates falling into the white region of the CIE diagram. Missing any of them will affect the desired quality so that it would not be possible to name the generated white light as high quality. In this thesis, if a parameter set ensures all of the necessities it is named as high quality white light otherwise it would be a meaningless parameter set.

2.3 White Light Emitting Diodes

The optimization of the white light spectrum is a complicated task due to the application area where the need changes. For instance, indoor lighting requires much spectral overlap with the eye sensitivity function and high color rendering,

whereas outdoor lighting requires higher luminance levels and high rendering index especially while driving.

As the primary components of white light, red, green and blue have different densities in white, and they affect the color quality parameters, color temperature, color rendering index and luminous efficacy of optical radiation. Furthermore, as explained in Chapter 1, the FWHM and peak emission wavelength parameters affect these primaries individually.

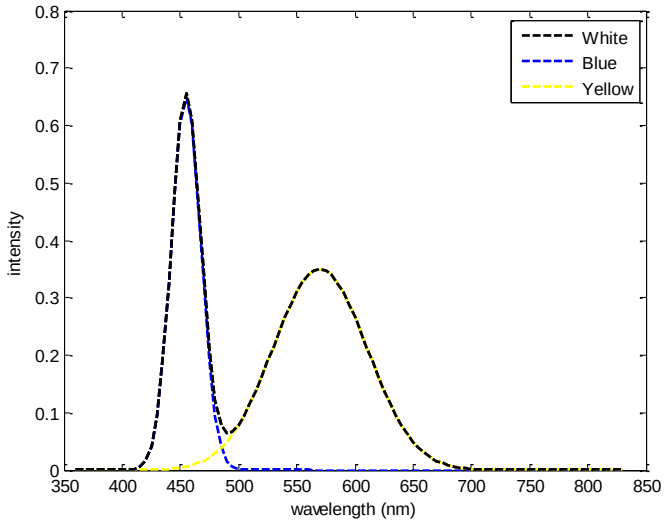

Figure 2.3.1 White LED spectra based on fluorescent material

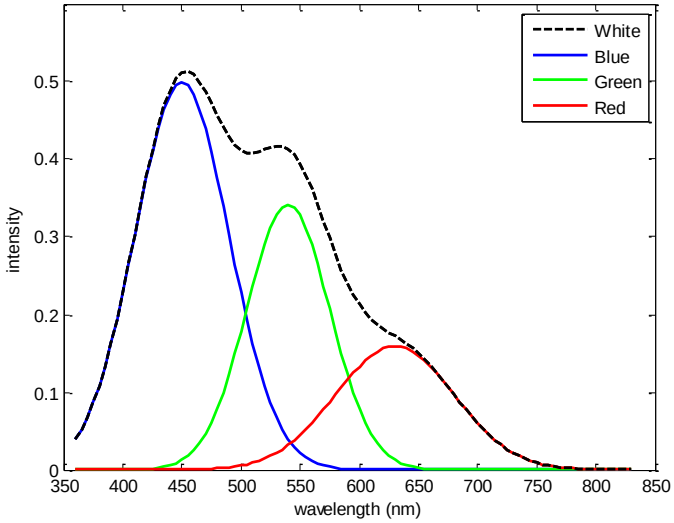

Figure 2.3.2 RGB white LED spectra

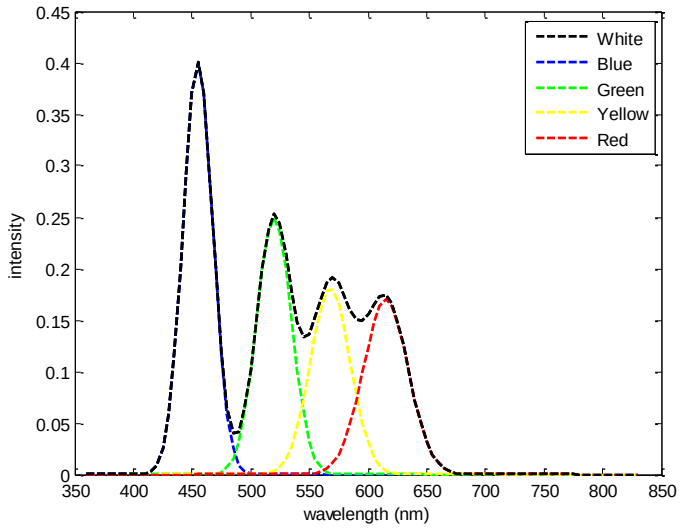

Figure 2.3.3 White LED based on four color components

Different from three color mixing of red, green and blue, white light can be achieved using only blue and yellow emission pair or with an additional color component, i.e. yellow to the three primaries as can be seen from Fig. 2.3.1 to Fig. 2.3.3.

The first combination, blue and yellow emissions have been thought as white LEDs based on phosphor emitters [47,48]. Application of yellow fluorescent material on blue LED is the main design of that combination. RGB LEDs have red, green and blue components apply the second opportunity (three-color combination) to get white [49]. However, their high cost and poor efficiency had directed the industry to use of narrow emitters i.e. quantum dots to enhance the white light. On a blue LED, hybridizing the mixture of red and green emitters as a film layer increases the efficiency of LED dramatically [50,51,52,53].

The engineering of the FWHM and peak emission wavelength of the individual component of the white light can be achieved with quantum dots, thanks to their chemical composition and size. Furthermore, it is possible to tune the spectral

intensity of the individual emitter by concentration of the emitters to meet the requirement of the optimal white light.

2.4 Simulation Study

High quality white light is described using limits for parameters, CCT, CRI and LER. The CCT below 4000K is assumed as proper levels for lighting applications. A CRI value more than 90 is another limit to obtain a high quality white light source. The last parameter, LER, has to be higher than 380lm/W_{opt} to identify the source as high quality. All of these limits and their reasoning have been given in the previous chapter.

High quality white light has to provide all three limitations that are CCT<4000K, CRI>90 and LER>380lm/W_{opt} all together in the pre-defined white region. For instance, having a CRI higher than 90 and CCT 3598K whereas LER 365lm/W_{opt} does not proper to classify the white as high quality.

2.4.1 Two-color mixing

Two-color mixing generally represents an LED most probably blue with a phosphor deposited material application onto it. Cerium(III)-doped YAG (Yttrum Aluminium Garnet) is often used as coating material onto blue LEDs. It absorbs blue light from the LED and emits broad range of color from green to red. The white LED types designed on this process called phosphor-based or phosphor-converted white LEDs [47]. Due to the simplicity of fabrication process, phosphor based white light generation is still used widely.

2.4.1.1 Definition of simulation parameters

In simulation process the design on a blue LED with a phosphor material in yellow region has been assumed. The blue region has been simulated with a peak emission wavelength range between 400nm to 490nm and having an emitter with FWHM from 10nm to 60nm. The phosphorescent material has been

identified with a peak emission wavelength between 500nm to 700nm, which is the rest of the visible spectrum, simulated with 10nm intervals. The same FWHM range applies for the phosphorescent material simulated with 10nm intervals.

2.4.1.2 Simulation methodology

The range of parameters has been defined in the previous part. Intensities of these two color components have been used from 10% to 90% in a collaterally way. Using these parameter ranges for our starting and ending nested 'for' loop values, all probabilities have been investigated. Starting from blue peak emission wavelength, blue FWHM, blue intensity, yellow peak emission wavelength, yellow FWHM, and yellow intensity respectively have been run on MATLAB using nested for loops. As mentioned in the previous part, the intervals were 10nm for peak emission wavelength and 10nm for FWHM.

In the output of the nested loops, using parameter sets that include three spectrum variables which are peak emission wavelength, FWHM and intensity for each color component, white coordinate that has x-axis value and y-axis value, CCT, CRI and LER values have been calculated. Thus, an output parameter set in two-color mixing has 6 inputs and 5 outputs.

Filtering output parameters using requirements of high quality white light, the relation between inputs and outputs has been investigated in this thesis. For instance the relation between blue peak emission wavelength and CRI can be demonstrated using related columns after eliminating the results in terms of CCT<4000K and LER>380lm/W_{opt} requirements.

2.4.1.3 Two-color mixing simulation

In the simulation steps, using the related parameter set, the chromaticity coordinate of the spectrum is calculated first. The calculation process of

chromaticity coordinate has been explained in Chapter 1 and MATLAB code for the calculation has been given below and also in Appendix D.

It is worth mentioning here that again, the sample calculation given below, is only for one parameter set. Nested loops have been used to calculate all possible parameter sets according to the ranges defined. In the whole simulation process, the steps that are given below to calculate white light quality parameters have been iterated in the analysis. The number of iterations can be calculated by multiplying the lengths of ranges which belong to the spectrum parameters that are peak emission wavelength, FWHM, and intensity for each color components.

```
wlb=460; %blue peak emission wavelength (nm)
FWHMblue=25; %blue FWHM (nm)
peakb=0.40; %blue intensity
wavel=360:5:830; %sampled visible spectrum range

gaussb=normpdf(wavel,wlb,FWHMblue/2.3548);
%gaussian definition
gaussb=peakb*gaussb./max(gaussb); %applying
intensity
spdb=gaussb';

Xb = trapz(wavel,spdb.*xcol'); %R tristimulus val
Yb = trapz(wavel,spdb.*ycol'); %G tristimulus val
Zb = trapz(wavel,spdb.*zcol'); %B tristimulus val
xb = Xb/(Xb+Yb+Zb); %x-axis coordinate
yb = Yb/(Xb+Yb+Zb); %y-axis coordinate
```

where "`xcol`", "`ycol`", and "`zcol`" are the x,y,z color matching functions from table and `xb,yb` are chromaticity coordinate of blue color.

After having the Gaussian distribution of a color component which has been represented by "gaussb" above, to get white spectrum each color components' spectrum is summed in element wise way in which the summation occurs wavelength by wavelength. Thus, the color spectrum of white would be originated as given below.

```
gaussw=gaussb+gaussy; %blue and yellow summation
```

The same steps, which are multiplication through visible wavelength range with color matching functions and then having tristimulus values, give the chromaticity coordinate of white light.

The next step, calculation of CCT is commonly done by Robertson method that has been given in Appendix D as MATLAB code.

The CCT value can also be calculated using the McCamy equation which has been given below:

```
     n=(x-0.3320)/(0.1858-y); %chromaticity coordinate
footprint on axes
     CCT= 449*n^3+3525*n^2+6823.3*n+5520.33; %McCamy
equation
```

Although is it easier to calculate CCT using McCamy's equation, it has around 1% error rate compared to the classical way which is Robertson Method.

Considering the CCT value, the reference illuminant has to be selected to calculate the CRI. Using the limitations that has been given in Chapter 1, which are 5000K, 7000K and 25000K, the reference would be the Backbody Radiator itself, a standard illuminant or CIE Daylight Tables respectively. If the CCT is above 25000K, the coordinate is regarded out of range to calculate CRI. The definition of reference has been done in MATLAB using the code given below.

```
if (Tc < 5000) %reference is Backbody Radiator
    c1 = 3.7418e-16;
    c2 = 1.4388e-2;
    spdref = c1 * (1e-9*wavel).^-5 ./ (exp(c2./
(Tc.* 1e-9*wavel)) - 1);
else
    if (Tc <= 25000)

        S0=CIEDay(:,2); % The table has been given in
Appendix C.
        S1=CIEDay(:,3);
        S2=CIEDay(:,4);

        if (Tc <= 7000)% Reference is D65 illuminant
            xd = -4.6070e9 / Tc.^3 + 2.9678e6 /
```

```
Tc.^2 + 0.09911e3 / Tc + 0.244063;
        else
            xd = -2.0064e9 / Tc.^3 + 1.9018e6 /
Tc.^2 + 0.24748e3 / Tc + 0.237040;
        end
        yd = -3.000*xd*xd + 2.870*xd - 0.275;
        M1 = (-1.3515 - 1.7703*xd + 5.9114*yd)
 / (0.0241 + 0.2562*xd - 0.7341*yd);
        M2 = (0.0300 - 31.4424*xd + 30.0717*yd)
 / (0.0241 + 0.2562*xd - 0.7341*yd);
        spdref = S0 + M1*S1 + M2*S2;
        spdref = interp1(wl,spdref,wavel);
        spdref(isnan(spdref)) = 0.0;
    else
        R = -1;
        Ra=-1;
disp('CCT is higher than 25000K so the CRI have not
been calculated.\n');
    end
end
```

Up to now, the chromaticity coordinate and CCT parameter have been calculated and the reference illuminant, to calculate CRI, has been selected. The next step will be the calculation of the chromaticity coordinate of each test color sample by both reference illuminant and test light which is the white spectrum, separately.

```
    % Interpolating of TCS values from 5 nm to spd
increments
    for i = 1:14
        TCS_1(:,i) =
interp1(TCS(:,1),TCS(:,i+1),wavel,'linear',0);
    end

    % u, v chromaticity coordinate under test
illuminant, (uk, vk) and reference illuminant, (ur,
vr)
    X = trapz(wavel,spdw .* xcol);
    Y = trapz(wavel,spdw .* ycol);
    Z = trapz(wavel,spdw .* zcol);
    Yknormal = 100 / Y;
    Yk = Y*Yknormal;
    uk = 4*X/(X+15*Y+3*Z);
```

```
        vk = 6*Y/(X+15*Y+3*Z); X = trapz(wavel,spdref .*
    xcol);
        Y = trapz(wavel,spdref .* ycol);
        Z = trapz(wavel,spdref .* zcol);
        Yrnormal = 100 / Y;
        Yr = Y*Yrnormal;
        ur = 4*X/(X+15*Y+3*Z);
        vr = 6*Y/(X+15*Y+3*Z);
        for i = 1:14
            X = trapz(wavel,spdw .* TCS_1(:,i) .* xcol);
            Y = trapz(wavel,spdw .* TCS_1(:,i) .* ycol);
            Z = trapz(wavel,spdw .* TCS_1(:,i) .* zcol);
            Yki(i) = Y*Yknormal;
            uki(i) = 4*X/(X+15*Y+3*Z); %u coordinate by
    test il.
            vki(i) = 6*Y/(X+15*Y+3*Z); %v coordinate by
    test il.

            X = trapz(wavel,spdref .* TCS_1(:,i) .*
    xcol);
        Y = trapz(wavel,spdref .* TCS_1(:,i) .*
ycol);
        Z = trapz(wavel,spdref .* TCS_1(:,i) .*
zcol);
        Yri(i) = Y*Yrnormal;
        uri(i) = 4*X/(X+15*Y+3*Z); %u coordinate by
ref. il.

        vri(i) = 6*Y/(X+15*Y+3*Z); %v coordinate by
ref. il.
    end
    % Color tolerance
    DC = sqrt((uk-ur).^2 + (vk-vr).^2);

    % Color shift
    ck = (4 - uk - 10*vk) / vk;
    dk = (1.708*vk + 0.404 - 1.481*uk) / vk;
    cr = (4 - ur - 10*vr) / vr;
    dr = (1.708*vr + 0.404 - 1.481*ur) / vr;

    for i = 1:14
        cki = (4 - uki(i) - 10*vki(i)) / vki(i);
        dki = (1.708*vki(i) + 0.404 - 1.481*
    uki(i)) / vki(i);
        ukip(i) = (10.872 + 0.404*cr/ck*cki
    - 4*dr/dk*dki) / (16.518 + 1.481*cr/ck*cki -
dr/dk*dki);
```

```
        vkip(i) = 5.520 / (16.518 + 1.481*cr/ck*
    cki - dr/dk*dki);
    end

    %  Into 1964 Uniform space coordinates.
    for i = 1:14
        Wstarr(i) = 25*Yri(i).^.333333 - 17;
        Ustarr(i) = 13*Wstarr(i)*(uri(i) - ur);
        Vstarr(i) = 13*Wstarr(i)*(vri(i) - vr);

        Wstark(i) = 25*Yki(i).^.333333 - 17;
        Ustark(i) = 13*Wstark(i)*(ukip(i) - ur);
        Vstark(i) = 13*Wstark(i)*(vkip(i) - vr);
    end

    % Delta E calculation
    deltaE = zeros(1,14);
    R = zeros(1,14);
    for i = 1:14
        deltaE(i) = sqrt((Ustarr(i) - Ustark(i)).^2
    + (Vstarr(i) - Vstark(i)).^2 + (Wstarr(i) -
Wstark(i)).^2);
        R(i) = 100 - 4.6*deltaE(i);
    end
    Ra = sum(R(1:8))/8; %Average to calculate general
CRI
    fprintf(1,'CRI(x,y) = %.1f\n',Ra);
         Vstarr(i) = 13*Wstarr(i)*(vri(i) - vr);
```

Finally to find the LER of the white light, the code that is given below, is used on MATLAB.

```
LER=683*(trapz(wavel,spdw'.*esf))/trapz(wavel,spdw);
```

where “esf” stands for CIE 1978 eye sensitivity function.

2.4.1.4 Two-color mixing results

In results, the analysis process has been done using two different approaches. In the first one, the relations between inputs and outputs have been presented using all filtered results which provide CCT and LER requirements and white region borders whereas CRI results have not been eliminated considering the necessity level. The reason for that process is that the two-color mixing is able to ensure CCT and LER requirements but not the CRI level>90.

For each input parameter, the outputs have been shown without considering the other inputs. For instance, as shown in Fig. 2.4.1.1, the peak emission wavelength of both blue and yellow components and CRI relation have been presented corresponding to their respective FWHM and intensity levels. The aim of that graph is to show the general trend of the relationship. Each horizontal line will intersect two points in blue and yellow dots which means that the combination of these dots gives that CRI level regardless of their FWHM and intensity levels. Due to the high number of data and input variable, the graphing process is a challenge therefore, in first approach the main aim is to narrow down the results towards proper ranges and present the general trend.

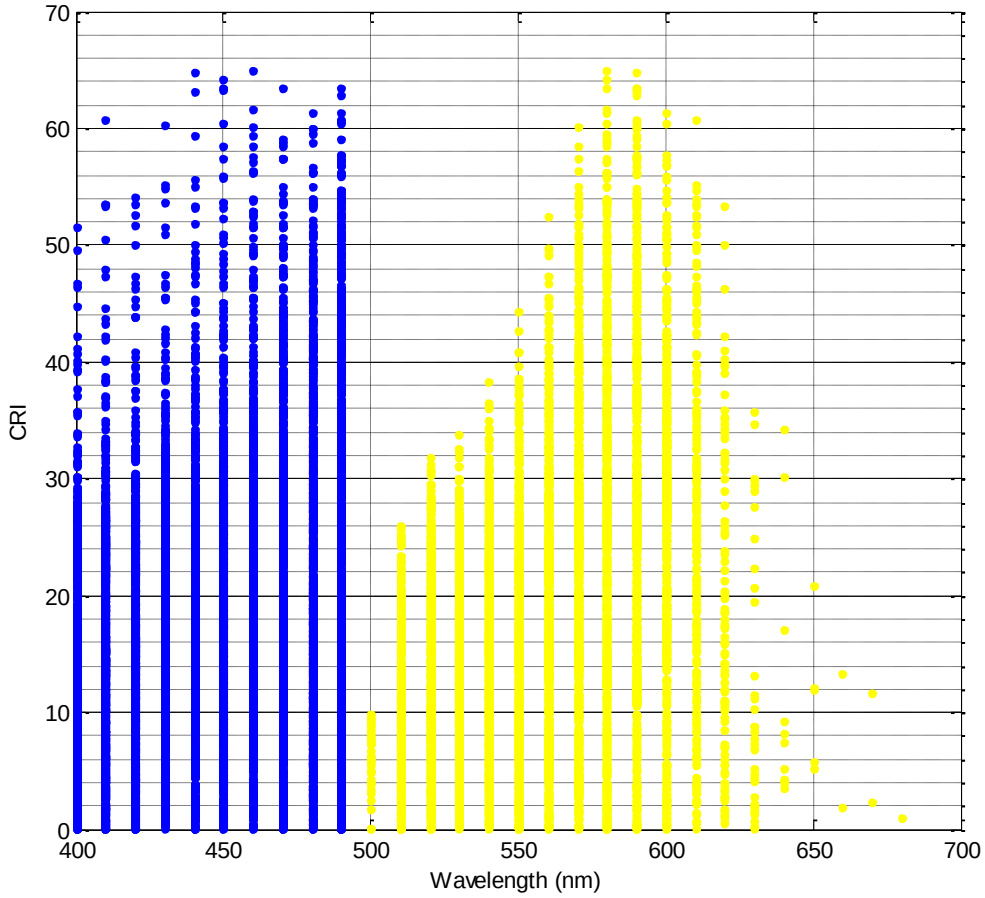

Figure 2.4.1.4.1 The peak emission wavelength-CRI relation for raw data

In Fig. 2.4.1.4.1, the relation between peak emission wavelength and CRI has been given for all calculated data and highest CRI result is 64,99. In results, as it

is expected there is no data set giving CRI higher than 90 although there were many appropriate results in terms of CCT and LER as can be seen in Fig. 2.4.1.4.2. For a good white light source, these parameters should be matched optimally all together.

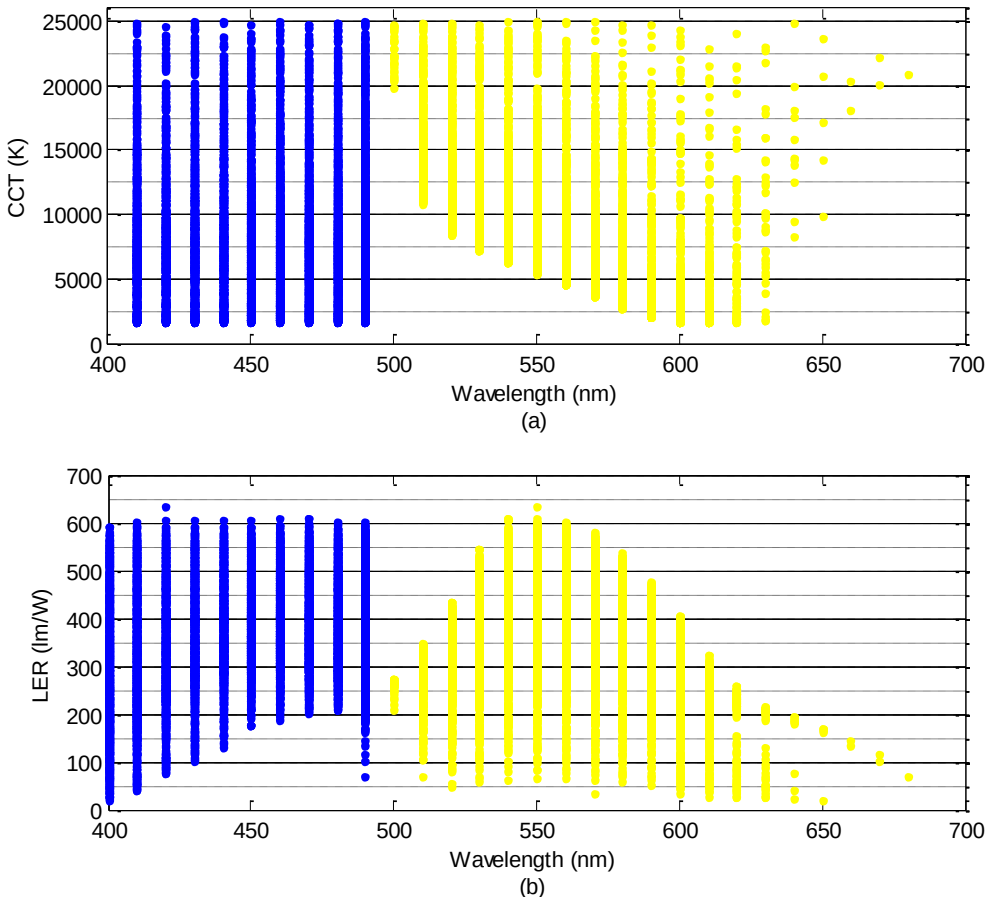

Figure 2.4.1.4.2 For raw data, (a) peak emission wavelength-CCT, (b) peak emission wavelength-LER relation

Maximum CRI level is lower than 90 in two-color mixing whereas the LER can be higher than 380lm/W_{opt} and CCT can get a value less than 4000K. Eliminating coordinates considering white region and filtering on CCT and LER requirements, the data is given in Fig 2.4.1.3. Using the 460nm-480nm as peak emission wavelength for blue and 580nm for yellow possess the most optimal results in terms of CCT and LER whereas the CRI could not be provided higher than 42.2. The main reason of this result is the area under color emission

spectra. All of meaningful filtered data sets belong to the narrow emitters; although for a high CRI value it is required to span a larger spectral content.

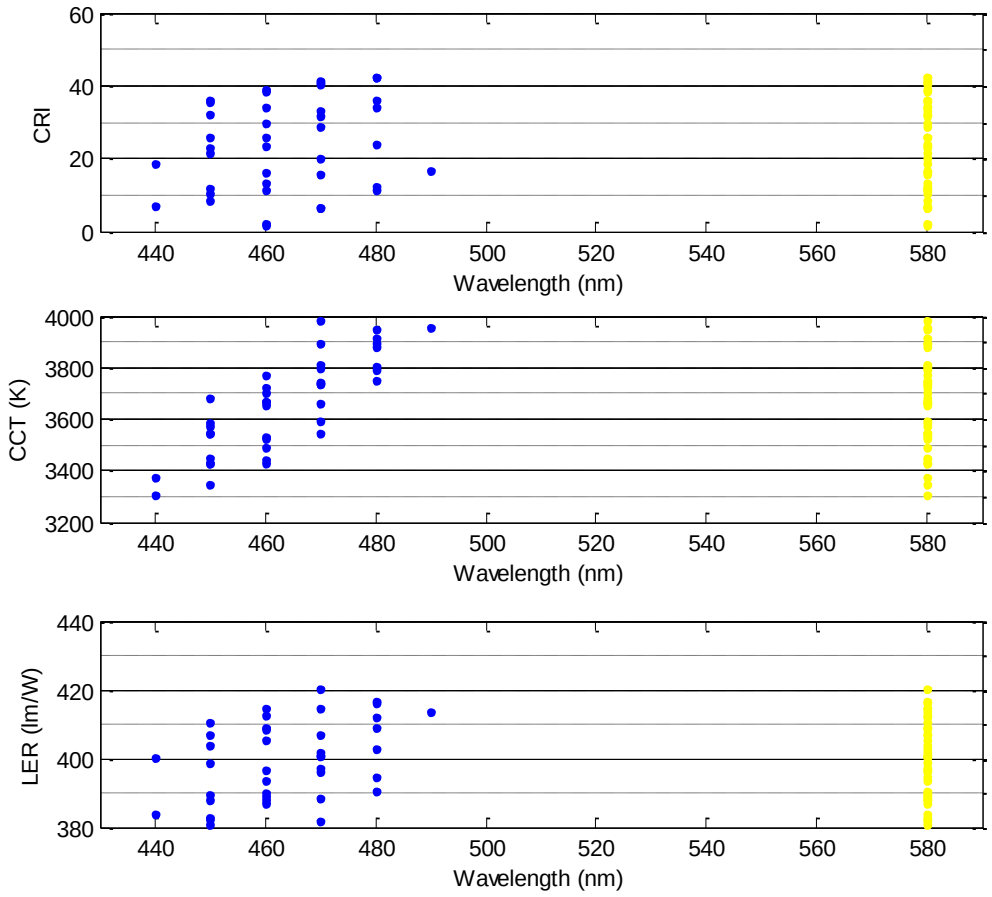

Figure 2.4.1.4.3 For filtered data (CCT<4000K and LER>380lm/W in white region), relations of (a) wavelength-CRI, (b) wavelength-CCT, (c) wavelength-LER in two-color mixing

In Fig. 2.4.1.4.4, the effect of FWHM on CRI has been presented. As mentioned before, the emitters that have more than 20nm FWHM belong to the narrow emitter class. The reason of having no proper results that have ultra-narrow FWHM is due to the area under the emission spectra. The color components under emission spectra are not sufficient to reveal more colors. As can be seen in Fig. 2.4.1.4.4, increasing the yellow emission FWHM, increases the achieved CRI.

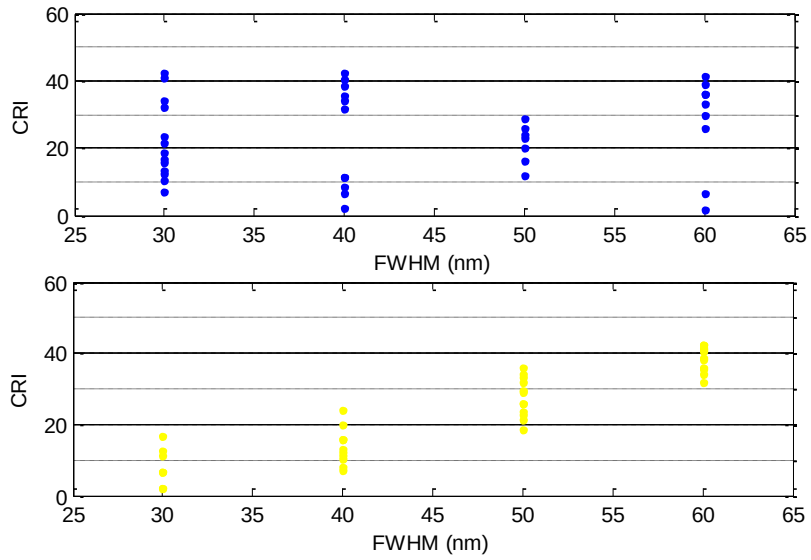

Figure 2.4.1.4.4 For filtered data (CCT<4000K and LER>380lm/W in white region), relation of FWHM-CRI in two-color mixing

In Fig. 2.4.1.4.5, the relation between intensities of two color components and CRI have been shown. Obtaining higher CRI requires less blue percentage compared to the yellow one in two-color mixing application. At least 50% yellow intensity is required to achieve a CRI that is higher than 40. The optimal combination can be defined as 30%-40% blue and 60%-70% yellow in two-color mixing to increase the performance of white light.

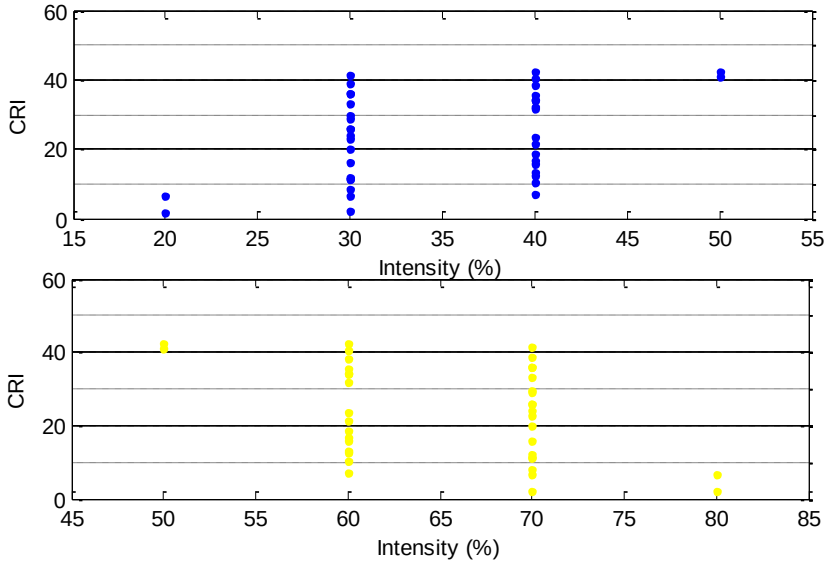

Figure 2.4.1.4.5 For filtered data (CCT<4000K and LER>380lm/W in white region), relation of Intensity-CRI, in two-color mixing

In the second approach, using the filtered data that provide CCT and LER limitations and white region, the relation between peak emission wavelength and CRI have been presented. Then, considering the highest CRI level, that is 42.2 in two-color mixing, a minimum CRI level have been chosen, which is 40 in this thesis. Using that minimum level, all data have been investigated to analyze the maximum levels of the study. The results that have at least CRI=40, have been used to show the parameter set situation.

In Fig. 2.4.1.4.6, using all two-color mixing simulation results, the data which filtered using CCT<4000K, LER>380lm/W and white region requirements, the relation between peak emission wavelength and CRI have been presented.

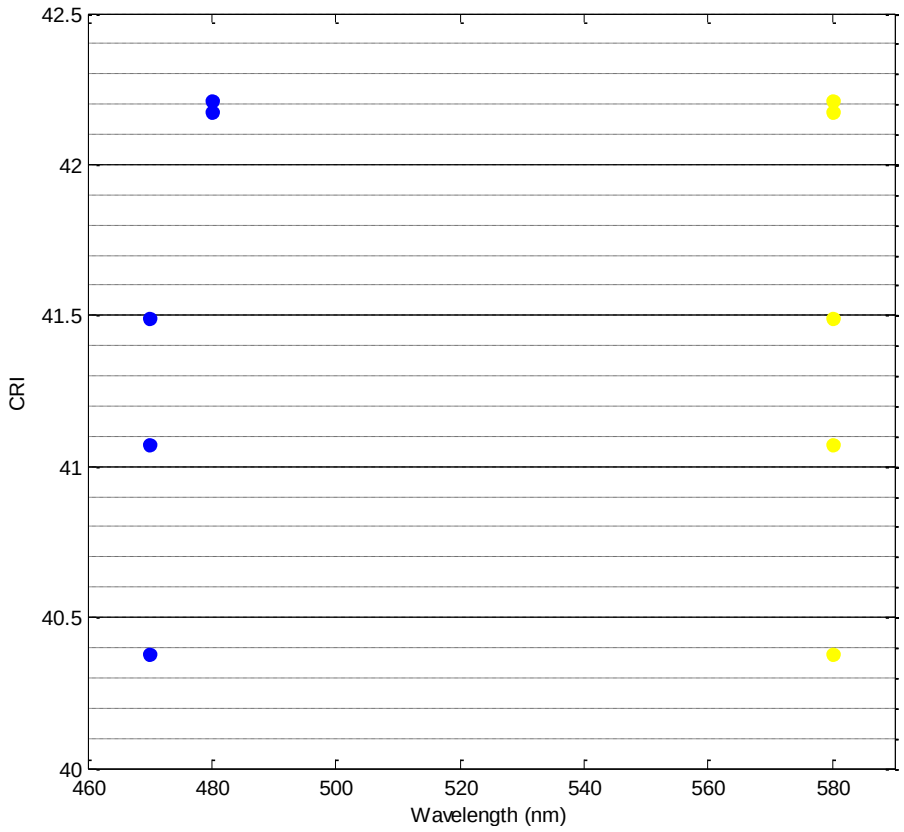

Figure 2.4.1.4.6 Using filtered data (CCT<4000K, LER>380lm/W and CRI>40 in white region) the relation between peak emission wavelength and CRI in two-color mixing. Each dot pairs in blue and yellow with same CRI represent only one parameter set.

After eliminating the results considering CRI>40, the values of spectrum variables that are peak emission wavelength, FWHM and intensity and CCT, CRI, LER values have been given in Table 2.4.1.4.1.

CRI	CCT (K)	LER (lm/W)	λ_{peak} blue (nm)	FWHM Blue (nm)	Int. blue (%)	λ_{peak} yellow (nm)	FWHM Yellow (nm)	Int. yellow (%)	x coordinate	y coordinate
40.4	3795	396	470	40	40	580	60	60	0.39	0.37
41.1	3981	382	470	30	50	580	60	50	0.38	0.36
41.5	3736	407	470	60	30	580	60	70	0.40	0.39
42.2	3917	394	480	30	50	580	60	50	0.39	0.40
42.2	3804	409	480	40	40	580	60	60	0.40	0.41

Table 2.4.1.4.1 The parameter sets that provide the CCT and LER requirements in white region and have CRI>40 in two-color mixing

In the technology market, the blue LEDs such as InGaN, have the peak emission wavelength around 450nm-460nm and FWHM varies between 20nm-30nm [47,60]. Filtering the raw data considering these limitations, optimal results is given in Fig. 2.4.1.4.7.

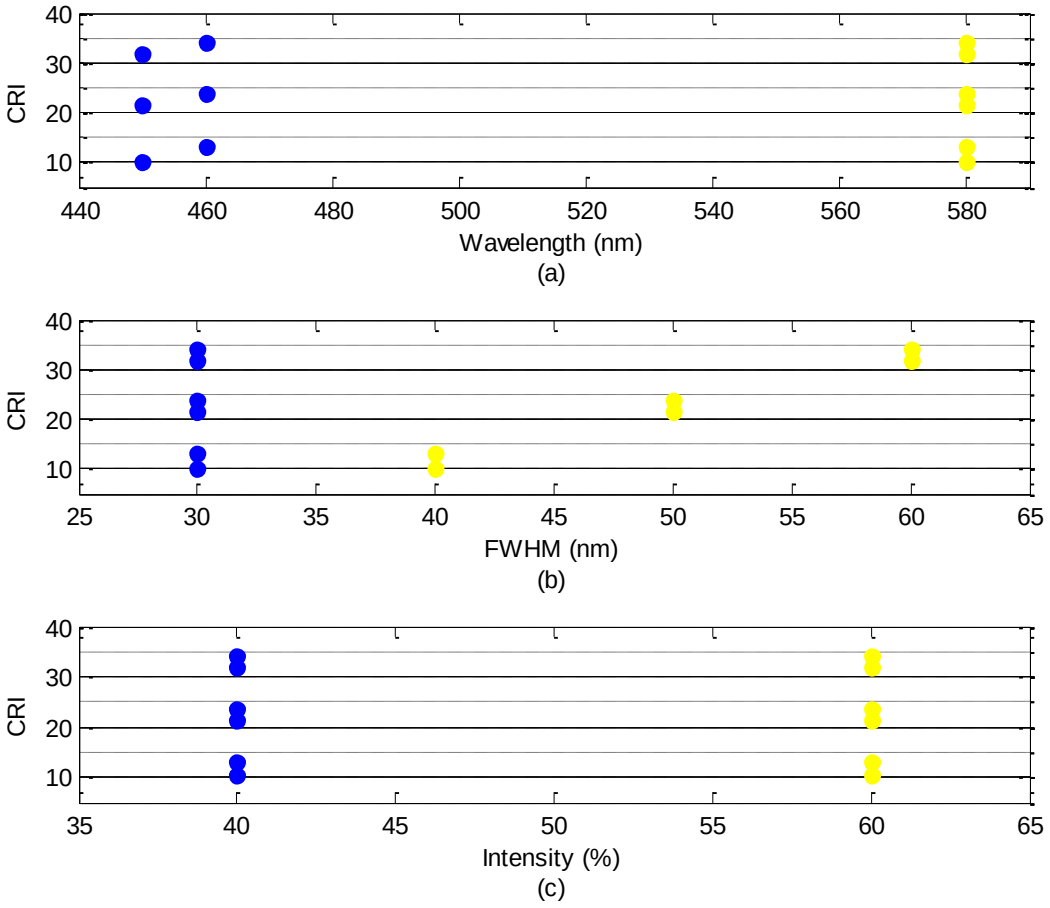

Figure 2.4.1.4.7 Based on commercial blue LED, relation between spectrum parameters and CRI for filtered data by CCT and LER conditions in white region, in two-color mixing.

As can be seen on Fig. 2.4.1.4.7, to get highest results for two-color mixing the peak emission wavelength has to be 580nm, and FWHM has to be around 40nm-60nm for yellow emitter. The intensity percentages have to be divided as 40% for LED and 60% for phosphor-included material. Maximum CRI level is 34 with the following parameters of, 460nm and 580nm peak emission wavelengths, 30nm and 60nm FWHM, 40% and 60% intensities for blue and yellow respectively as can be seen in Fig. 2.4.1.4.7.

In two-color mixing, the results analyzed in terms of limitations and the design could provide only CCT and LER requirements. Obtaining high quality white light requires higher CRI value. Having low number of color component in white and limitation in terms of visible region that can be reached causes that

issue. Thus, to improve the quality and obtain high quality white light a third component was added to simulation process and three-color mixing has been implemented to achieve the white light.

2.4.2 Three-color mixing

Using red, green and blue components to generate white is called three-color mixing. Satisfying the conditions of high quality white light requires optimized parameters for three primaries.

An RGB can be given as an example to this method. Arranging the spectral parameters of peak emission wavelength, FWHM and intensity of the emitters, the quality of white light can be engineered. Different from RGB LEDs, materials that emits red and green light when excited with blue LED, such as quantum dots can also be used to generate white light.

2.4.2.1 Definition of simulation parameters

In this part of the thesis, with the aim of searching all possibilities, visible wavelength range has been divided into three parts. The blue peak emission wavelength range is taken between 400nm and 490nm. Starting from 500nm to 590nm is called as green range and the rest part of the spectrum i.e. 600nm-700nm region has been run for red range, which is simulated with 10nm peak emission wavelength intervals for all components.

The FWHM of three components has been simulated between 10nm and 60nm to search both narrow and ultra-narrow emitters with 10nm intervals. The last parameter, intensity has been simulated with 10% intervals giving a total intensity of 100%. Due to the high computational bandwidth required, a more precise step size could not be applied for our simulation work.

2.4.2.2 Simulation methodology

As it has been done in two-color mixing, two approaches have been used in that part of the study. In the first approach, the aim is to analyze the general trend of the results whereas in the second approach, the results have been analyzed after filtering by a CRI value. The only difference is both first and second approach have been used together. The results have been analyzed for the general situation and also with a minimum level of CRI to make the understanding of high levels easier.

2.4.2.3 Three-color mixing simulation

The simulation process is the same with the one applied in two-color mixing. The one difference is to sum the three color components' spectrum instead of two. Using all MATLAB code that has been given in two-color mixing, works in three-color application with the white spectrum code given below.

```
gaussw=gaussb+gaussg+gaussr;  %blue, green and red summation
```

2.4.2.4 Three-color mixing results

In simulation process for three-color mixing, although having proper CCT and LER results, having CRI>90 was not possible as it was in two-color mixing. The maximum CRI value achieved is 85,105 where the CCT is 3999K and LER is 411.9lm/W. The main reason for that issue is the FWHM range which is up to 60nm is not enough to reach the condition of high quality white light.

	Ultra-narrow emitters	Narrow emitters
CRI>80	8.163 (7,4%)	19.782 (13,9%)
80>CRI>70	12.432 (11,3%)	27.493 (19,4%)
70>CRI	89.629	74.725

Table 2.4.2.4.1 The number of results for filtered data (CCT<4000K, LER>380lm/W) in three-color mixing

As can be seen in Table 2.4.2.5, an increment on FWHM provides more opportunity to find white light has a high CRI. If wider emission profiles are used, the ability to reach more colors increases because the area under the spectrum includes more colors.

In Fig. 2.4.2.4.1, CRI's success of three-color mixing has been analyzed roughly using all results which have been called as raw data. Most of the wavelengths were proper to get maximum CRI that was approximately 85,105 as can be seen in Fig. 2.4.2.4.1.

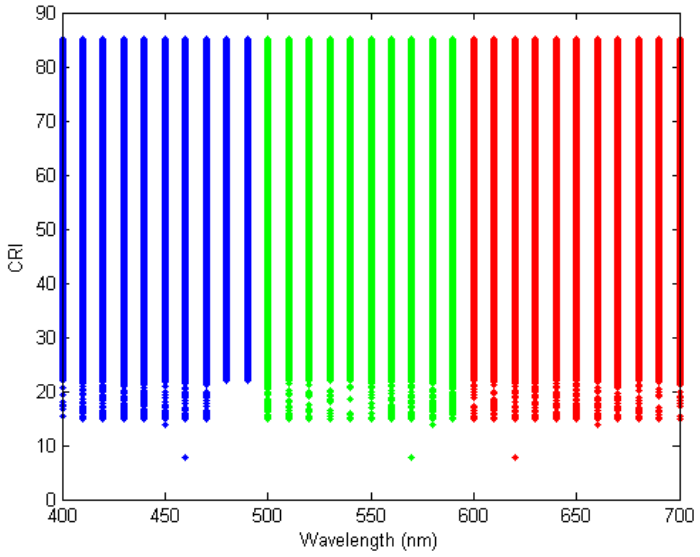

Figure 2.4.2.4.1 Wavelength-CRI relation for three-color mixing for raw data

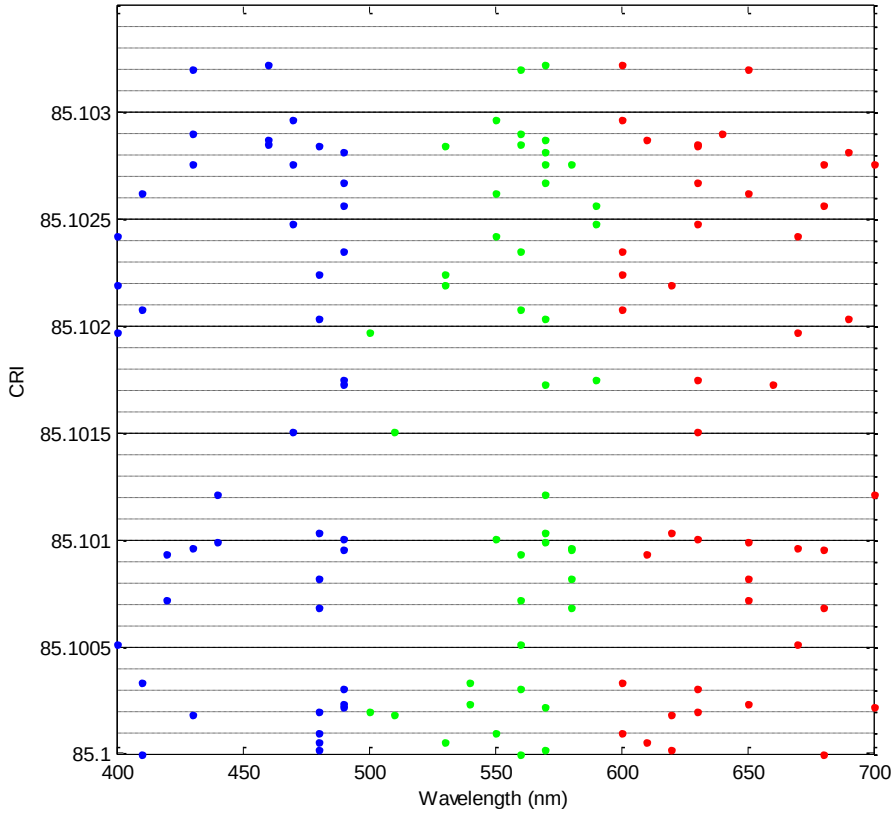

Figure 2.4.2.4.2 Wavelength-CRI relation for CRI>85.1 in three-color mixing for raw data

In Fig. 2.4.2.4.2, to make the visualization better, the results with CRI more than 85,1 have been showed. The dots in the same CRI level for blue, green and red region construct a parameter set. As can be seen more dots from bottom to top that located in 480nm-490nm for blue, 560nm-570nm for green and 600nm-610nm for red seems better to use to get a high performance in three color mixing. Although the probability of having higher quality white light in spectral zones having more dots is higher, the others can also be considered to possess higher results, too.

In Fig. 2.4.2.4.3., the data sets which are located in white region, having CCT<4000K and LER>380lm/W, as a function of the peak emission wavelength have been analyzed. The green region has some limitations whereas almost all of blue and red peak emission wavelength range is possible to get high performance white light. This shows that only peak emission wavelength parameter does not indicate any limitation individually to classify the white light

as high quality so that all spectral input parameters that are peak emission wavelength, FWHM and intensity have to be evaluated simultaneously.

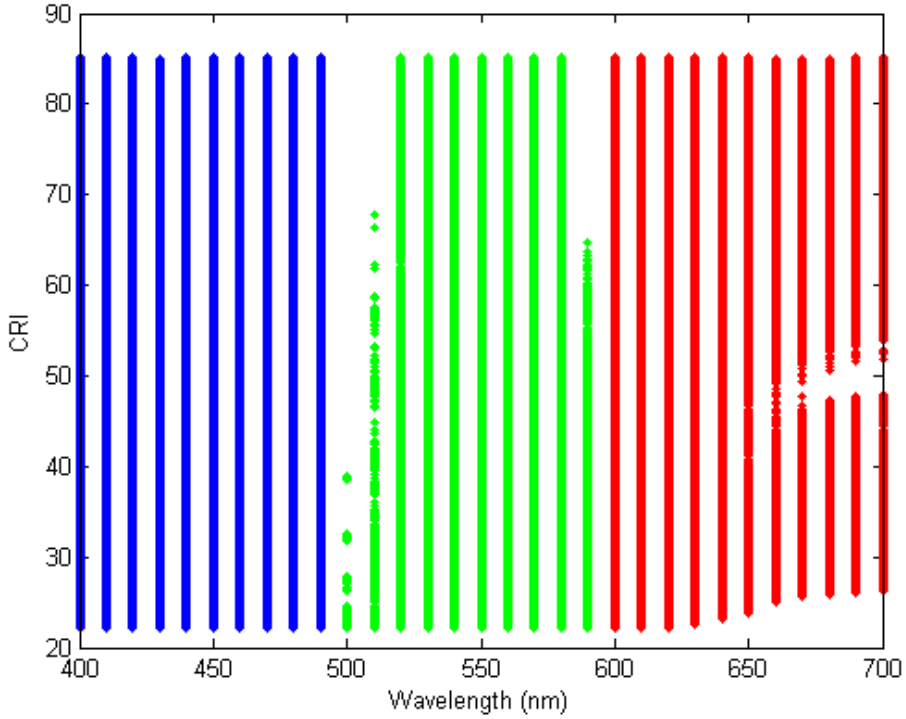

Figure 2.4.2.4.3 For filtered data (CCT<4000K and LER>380lm/W in white region), relation of wavelength-CRI in three-color mixing

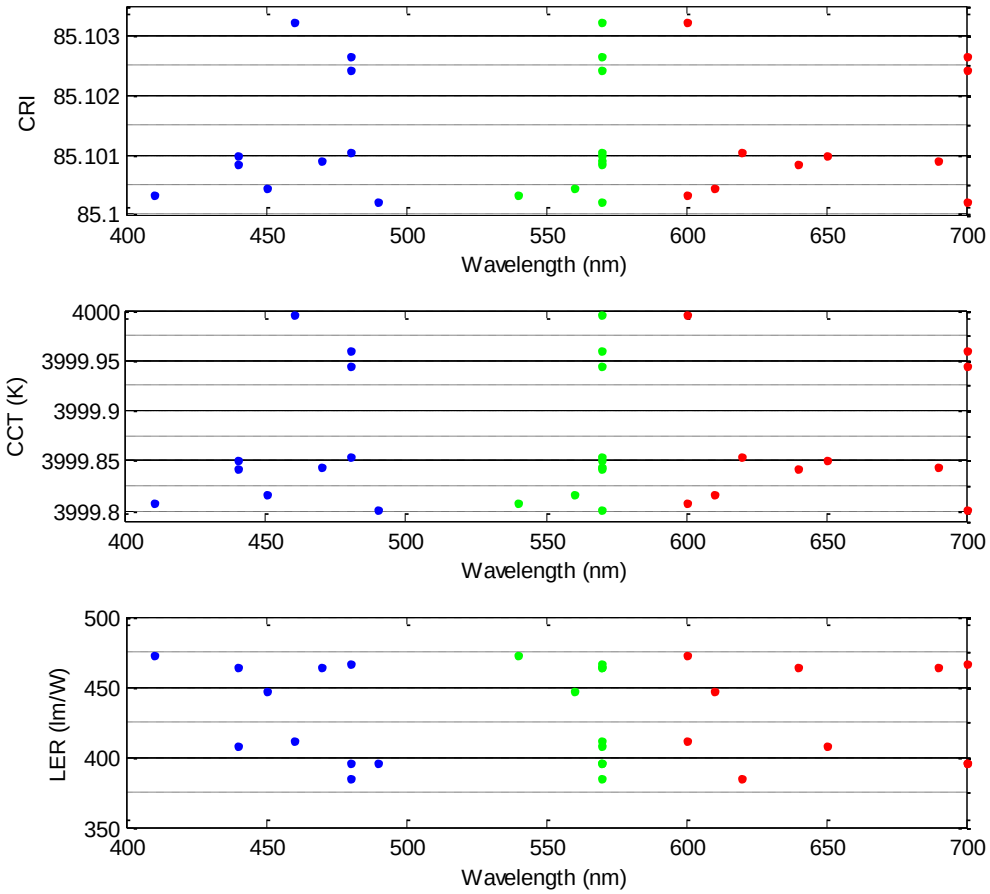

Figure 2.4.2.4.4 For filtered data (CCT<4000K, LER>380lm/W and CRI≥85.1 in white region), relation between peak emission wavelength and CRI/CCT/LER in three-color mixing

Fig. 2.4.2.4.4 represents the combinational results of CRI, CCT and LER which gives at least 85.1 CRI value and their dependence on the peak emission wavelength. As can be seen in Fig. 2.4.2.4.4, for blue and red emitters, using all wavelengths that have been simulated works to reach high CRI levels whereas in green emitter using 570nm peak emission wavelength increases the probability to achieve higher quality white light.

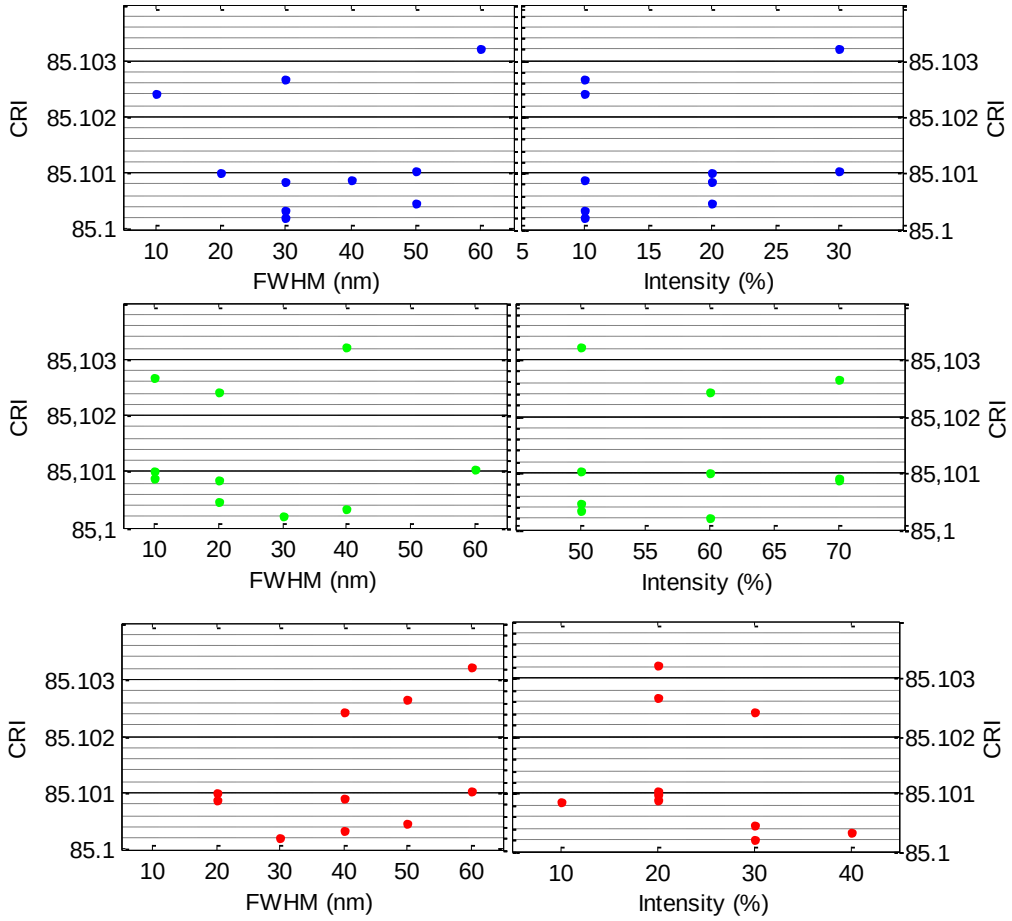

Figure 2.4.2.4.5 The relations between FWHM values and CRI in filtered data (CCT<4000K, LER>380lm/W and CRI≥85.1 in white region)

In Fig. 2.4.2.4.5 the relation between FWHM and CRI has been given for three color components in left side. For blue, having a FWHM parameter at all ranges provides high performance white light, as the FWHM value increases the probability increases as expected. Using green emitter with FWHM less than 50nm gives more chance to get higher quality. For the red, from 20nm to 50nm FWHM range is optimal for the high quality white color and increasing the FWHM red, increases the CRI as expected.

In Fig. 2.4.2.4.5, the effect of intensity percentage on CRI also has been given in right side. As can be seen maximum 30% intensity is optimal for blue whereas

up to 50% for red and higher than 50% for green provides the higher results in three-color mixing.

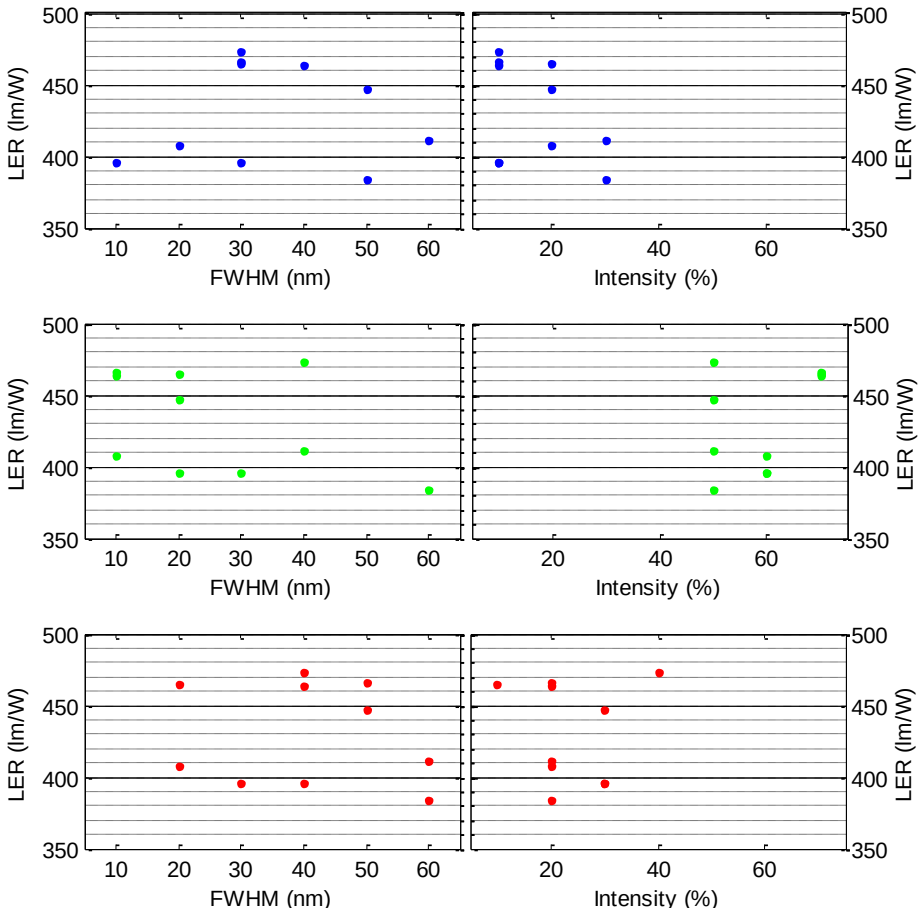

Figure 2.4.2.4.6 LER-FWHM/Intensity relation for filtered data (CCT<4000K, LER>380lm/W and CRI≥85.1 in white region)

In Fig. 2.4.2.4.6 the relation between LER and FWHM of three primaries has been given in left side. For blue, having a FWHM parameter from 10nm to 60nm provides the higher performance white light whereas 30nm is the highest one. Using green emitter with FWHM less than 50nm gives more chance to get higher results. For red emitter, FWHM range from 20nm to 50nm is optimal for the high quality white color. It may be expected that increasing the FWHM has to increase the CRI due to the area under spectrum would be increased when FWHM had been increased but one also needs to take into account the intensity of the emitter in the analysis. Increasing the intensity with the same FWHM

increases the CRI but increasing the intensity while decreasing the FWHM may not affect the CRI.

For an LER value higher than 380lm/W_{opt}, the intensity of blue has to be approximately lower than 40%. The green percentage higher than 40% applies the high quality white conditions. Up to 40% intensity for red component ensures the higher quality white light.

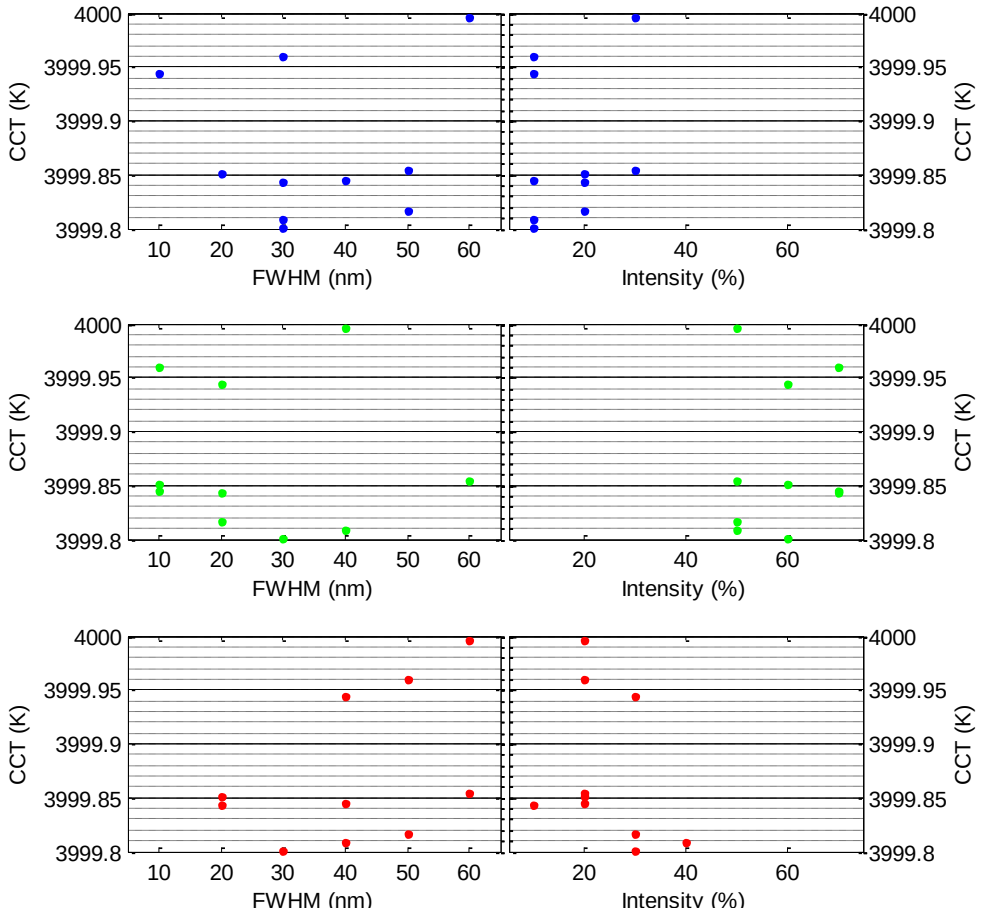

Figure 2.4.2.4.7 CCT-FWHM/Intensity relation for filtered data (CCT<4000K, LER>380lm/W and CRI≥85.1 in white region)

In Fig. 2.4.2.4.7, the relation between FWHM and CCT has been given in left side. All the inferences in CRI and LER relations for spectrum parameters are apply in CCT requirement. In three color mixing, maximum 30% blue intensity and for the rest, green dominance provides the higher results.

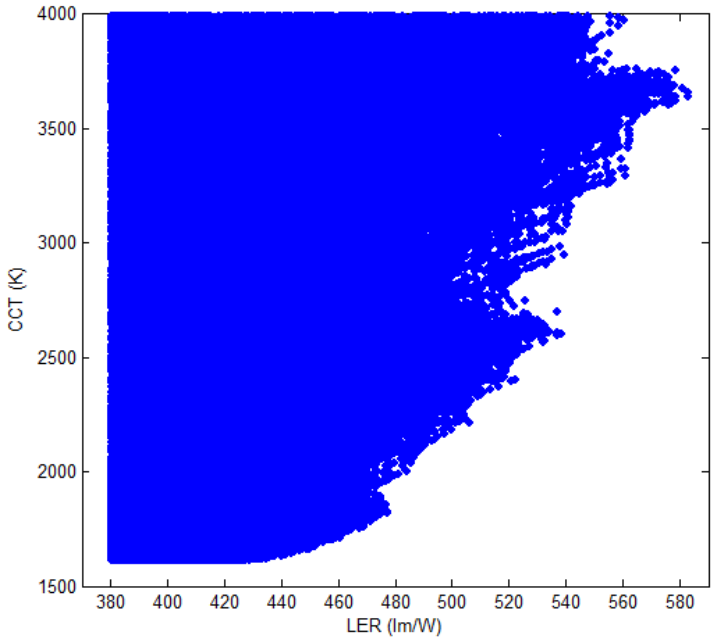

Figure 2.4.2.4.8 LER-CCT relation using filtered data (CCT<4000K, LER>380lm/W and CRI≥85.1 in white region) for three-color mixing

In Fig. 2.4.2.4.8, the relation between LER and CCT has been given. As can be seen, as LER has been increased, the CCT increases. Because of CCT can get maximum 4000K to ensure high quality parameter, LER is limited by CCT.

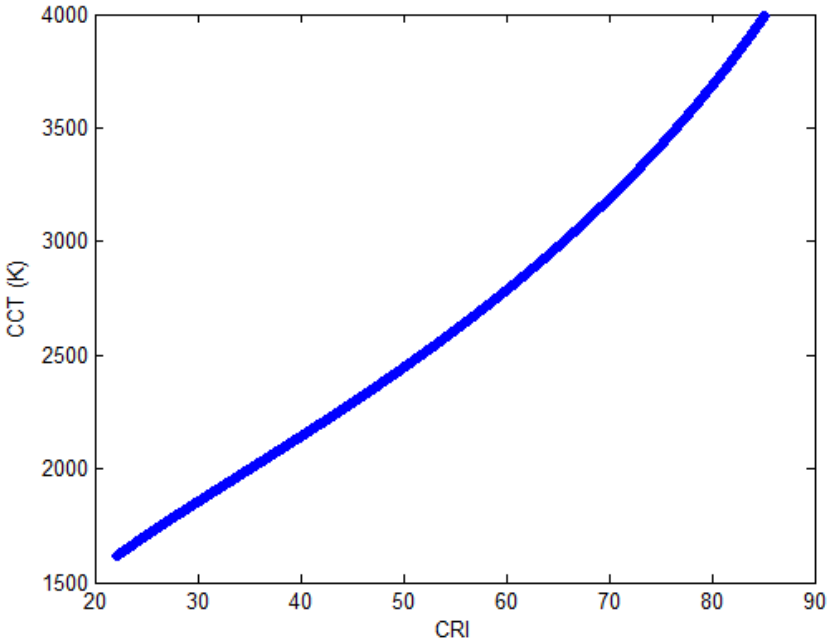

Figure 2.4.2.4.9 CRI-CCT relation using filtered data (CCT<4000K, LER>380lm/W and CRI≥85.1 in white region) for three-color mixing

As it is given in Fig. 2.4.2.4.9, an increment on CRI triggers the increase on CCT. It is clear that higher CRI levels are possible to reach but CCT requirement limits further increase.

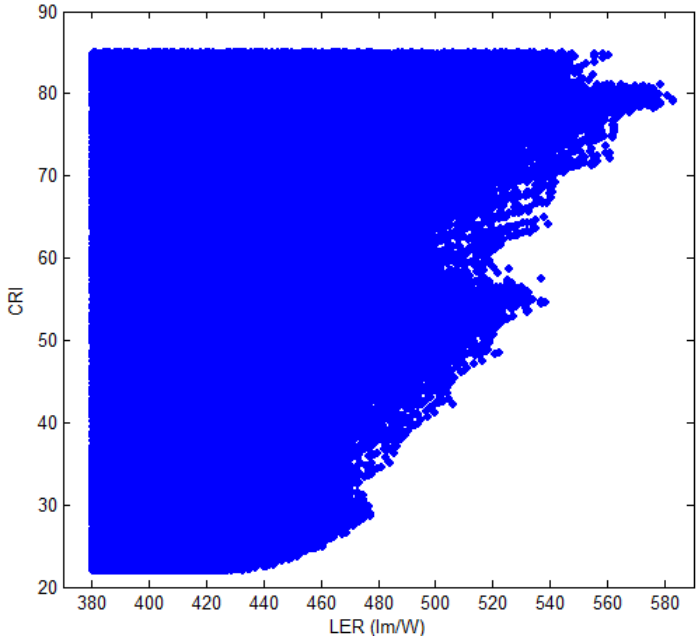

Figure 2.4.2.4.10 LER-CRI relation using filtered data (CCT<4000K, LER>380lm/W and CRI≥85.1 in white region) for three-color mixing

In Fig. 2.4.2.4.10, the relation between CRI and LER has been given. As can be seen in figure, if CRI increases, LER increases. At the CRI value under approximately 80, the LER can reached up to approximately 580lm/W whereas when the CRI is higher than 80, the LER level is to reach around 550 lm/W_{opt}. The data given have been filtered considering white region.

In the filtered results, by CCT<4000K, LER>380lm/W in white region requirements have been analyzed. In filtered parameter sets, using the data having at least 85.1 CRI is used to investigate the input situations for getting higher performance. The 10 proper sets that gave more than 85.1 CRI in defined limitations as given in Table 2.4.2.4.2

CRI	CCT (K)	LER (lm/W)	λ_{peak} blue (nm)	FWHM Blue (nm)	Intensity blue (%)	λ_{peak} green (nm)	FWHM Green (nm)	Intensity green (%)	λ_{peak} red (nm)	FWHM Red (nm)	Intensity red (%)	x coordinate	y coordinate
85,1	4000	395	490	30	10	570	30	60	700	30	20	0,31	0,33
85,1	4000	473	410	30	10	540	40	50	600	40	30	0,38	0,36
85,1	4000	447	450	50	20	560	20	50	610	50	40	0,35	0,29
85,1	4000	465	440	30	20	570	20	70	640	20	30	0,38	0,30
85,1	4000	464	470	40	10	570	10	70	690	40	10	0,31	0,35
85,1	4000	408	440	20	20	570	10	60	650	20	20	0,38	0,37
85,1	4000	384	480	50	30	570	60	50	620	60	20	0,37	0,44
85,1	4000	396	480	10	10	570	20	60	700	40	20	0,35	0,32
85,1	4000	466	480	30	10	570	10	70	700	50	30	0,34	0,26
85,1	4000	412	460	60	30	570	40	50	600	60	20	0,36	0,39

Table 2.4.2.4.2 The parameter sets that provides the CCT and LER requirements in white region and have CRI>40 in two-color mixing

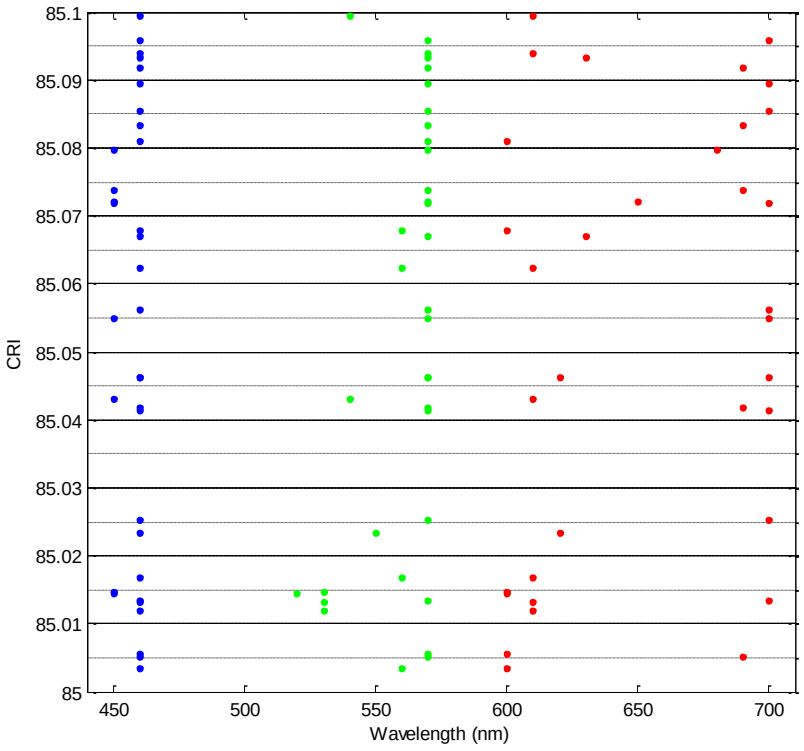

Figure 2.4.2.4.11 Based on commercial blue LED, relation between peak emission wavelength and CRI in three-color mixing for raw data

Regarding an application on commercial blue LED in three-color mixing, the raw data filtered considering the limitations of blue LED, and also considering white region, CCT, LER limitations, the relation between spectral input parameters, peak emission wavelength, have been given in Fig. 2.4.2.4.11. The maximum CRI value, taking the commercial blue LED and quality restrictions into account, is 85,09. In Fig. 2.4.2.4.12, the relation between FWHM and intensities of three primaries has been given.

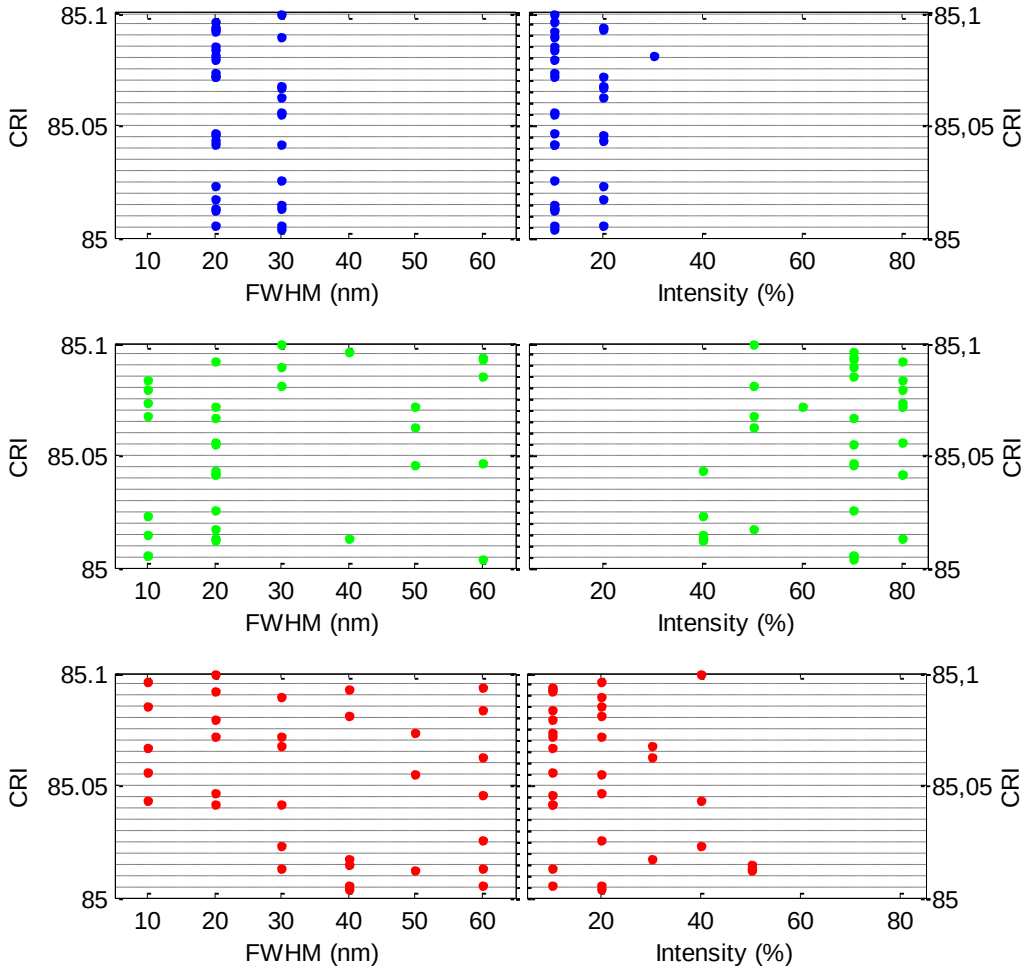

Figure 2.4.2.4.12 Based on commercial blue LED, relation between FWHM, intensity and CRI in three-color mixing for raw data

Following the horizontal lines for each color in same CRI level, the parameters of FWHM and intensity can be seen for their combination. The peak emission wavelengths also can be used from Fig. 2.4.1.10.

Due to the limited performance of three-color mixing on color quality of white, and also the issue of providing all the requirements using the same parameter set, the addition of forth color component, yellow, has been simulated and analyzed. The addition of forth color component would increase the color rendering ability because the total area under spectra of color components would be increased since there will be more spectral content under white light zone.

2.4.3 Four-color mixing

In this part of the thesis, the effect of forth component in mixing will be analyzed. Since the spectral area under Gaussians are not enough to provide all three requirements for high quality white light, a forth color, yellow has been added to the combination.

In three-color mixing, only missing part was CRI. Actually that is possible to achieve results that have higher than 90 in terms of CRI however the CCT or LER level decreases the white light quality in that situation. As has been mentioned before, high quality white light requires all necessities to be met the same time.

2.4.3.1 Definition of simulation parameters

The visible light spectrum range was divided into four parts, that 400nm-490nm, 500nm-540nm, 550nm-590nm and 600nm-700nm for blue, green, yellow, and red respectively.

The FWHM ranges have been simulated between 10nm-60nm as in three-color mixing. Using that range makes it easy to check the effect of both ultra-narrow (FWHM between 10nm-20nm) and narrow emitters (FWHM between 30nm-60nm) possible. Intensity of the color components in mixing have been simulated with 10% ranges with 10nm intervals for other parameters.

2.4.3.2 Simulation methodology

In four-color mixing, spectrum parameters that are peak emission wavelength, FWHM and intensity for blue, green, yellow, and red have been used in nested loops respectively. All of the possible combinations in defined ranges have been controlled in terms of whether they provide requirements or not.

2.4.3.3 Four-color mixing simulation

Using four color components' spectrum to generate white color is the only difference between four-color and two/three color mixing application. The MATLAB code has been given below for that simulation.

```
gaussw=gaussb+gaussg+gaussy+gaussr;    %blue,    green,
yellow, and red summation
```

2.4.3.4 Four-color mixing results

The results have been filtered with the conditions of high quality parameters. Different from three-color mixing, this time there were 29 results which provide all of the limitations providing CRI>90, CCT<4000 K and LER>380 lm/W_{opt} in white region. All data presented in four-color mixing results part ensure the requirements including white region for the same parameter set.

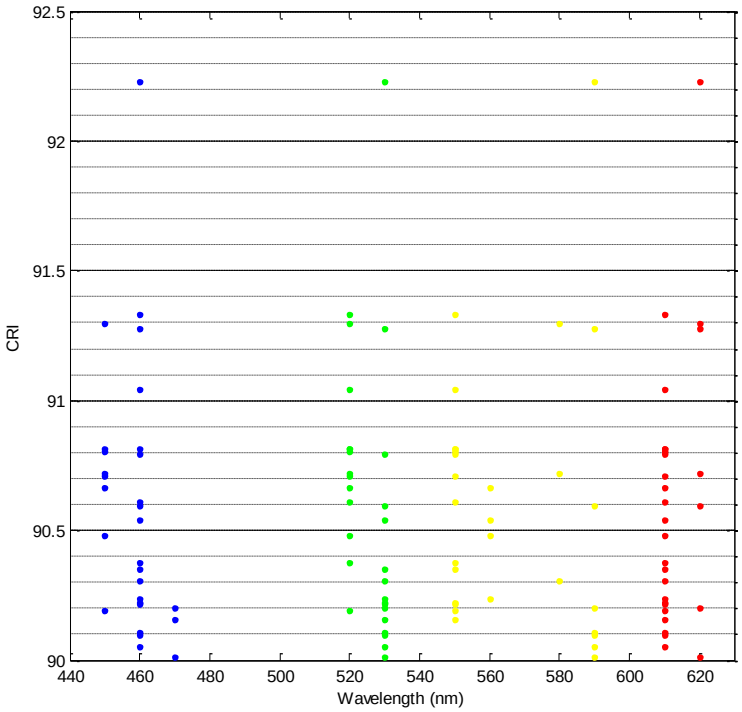

Figure 2.4.3.4.1 Wavelength-CRI relation for high quality white light in four-color mixing

In Fig. 2.4.3.4.1, the relation between peak emission wavelength and CRI has been presented. All of the dots are appropriate to the limitations. However, using peak emission wavelength of 460nm for blue, 530nm for green, 590nm for yellow and 620nm for red give the best CRI result of 92,23.

If four-color is used instead of three, the CRI would increase up to 92.23 in our simulation range. For that value, the CCT is 3791K and LER is 381,1lm/W that provides the high quality white light limitations.

In 62.832.000 results, all the appropriate ones belong to the narrow emitters (FWHM between 30nm-60nm). Having no proper results in the ultra-narrow emitter range due to the emission thickness was an expected situation.

The predetermined high quality white light can be achieved using 610nm-620nm for red, 550nm-590nm range (except from 570nm) for yellow, 520nm-530nm for green and 450-470nm for blue emitter as given in Fig. 2.4.3.4.1.

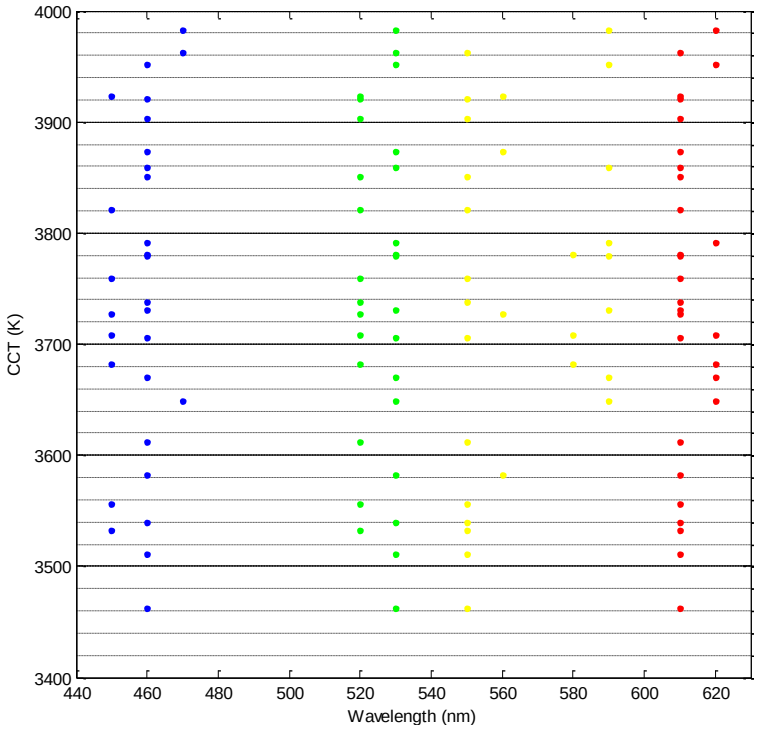

Figure 2.4.3.4.2 Wavelength-CCT relation for high quality white light in four-color mixing

In Fig. 2.4.3.4.2., The CCT below 4000K can be achieved using defined spectral wavelength ranges above for four-color mixing. For higher LER results, as given in Fig. 2.4.3.3., all ranges apply again whereas using 450nm and 470nm for blue, 520nm and 530nm for green, 550nm and 590nm for yellow and 610nm-620nm provide noticeably higher results in their combinations.

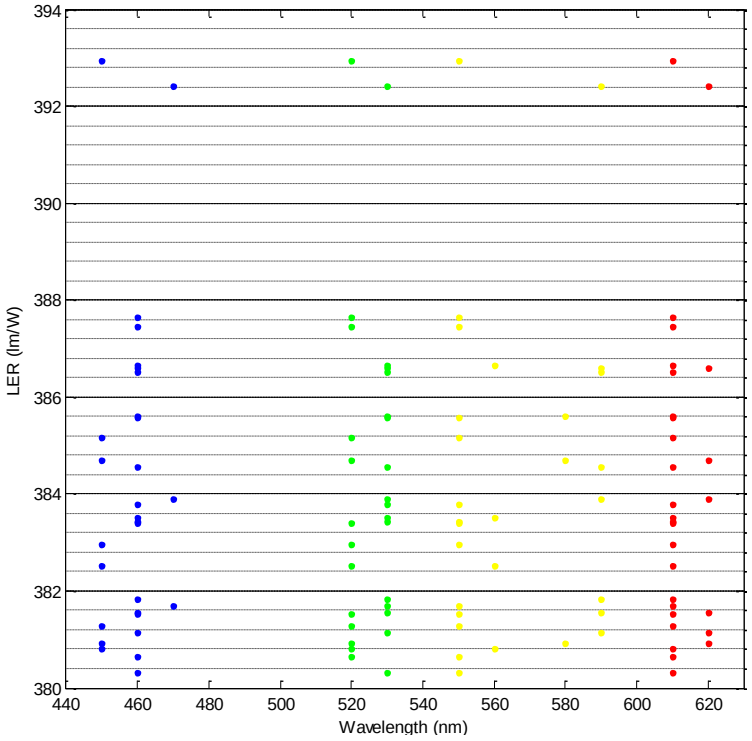

Figure 2.4.3.4.3 Wavelength-LER relation for high quality white light in four-color mixing

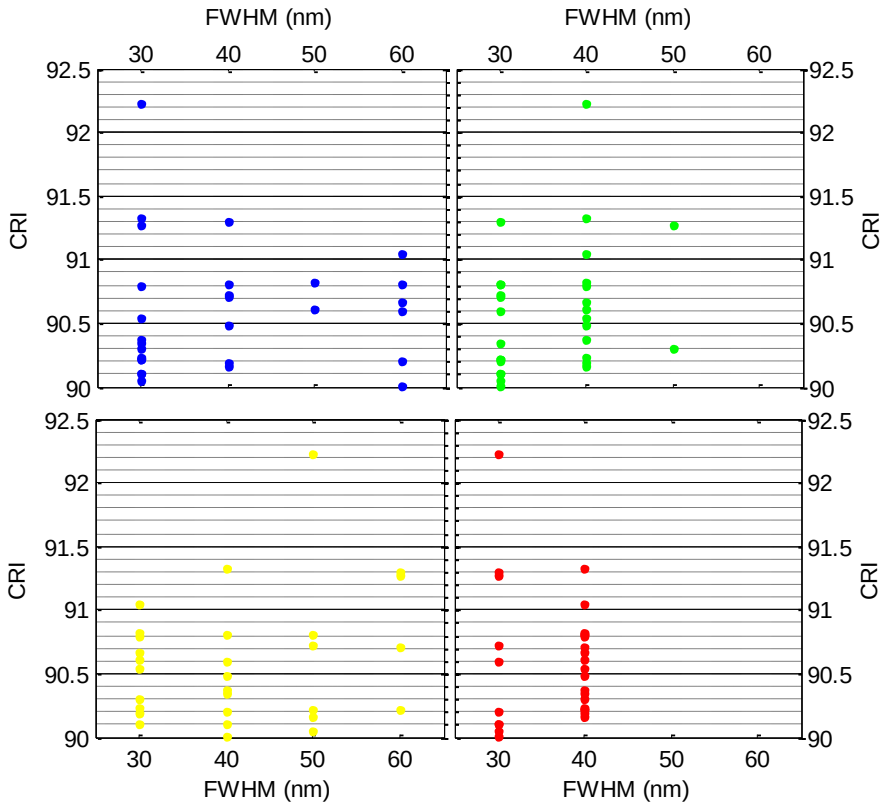

Figure 2.4.3.4.4 FWHM-CRI relation for high quality white light

In Fig. 2.4.3.4.4, the FWHM parameters of color components that provide the high quality white light parameters are given for CRI. According to the figures, only red and green have some limitations for the narrow emitter range simulated. The FWHM for red below 50nm and for green below 60nm are found to be optimal. As has been mentioned before, since the spectral area under color components are limited when ultra-narrow emitters used, for high quality white light, none of appropriate results can be achieved using ultra-narrow FWHM range. The highest CRI value has been achieved using 30nm blue, 40nm green, 50nm yellow and 30nm red FWHM.

Fig. 2.4.3.4.5 indicates that the proper FWHM values for CRI are also applicable for LER, too. Where blue and yellow can provide higher LER levels, the red emitter can have a maximum 40nm FWHM. For CCT, all comments have been done for CRI and LER are valid as can be seen in Fig. 2.4.3.4.6.

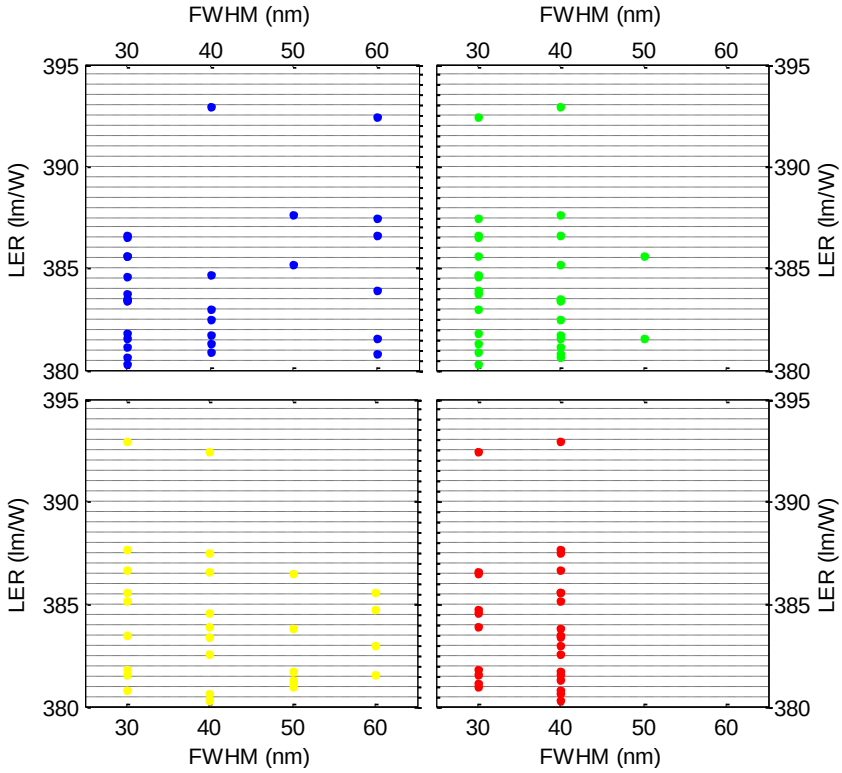

Figure 2.4.3.4.5 FWHM-LER relation for high quality white light

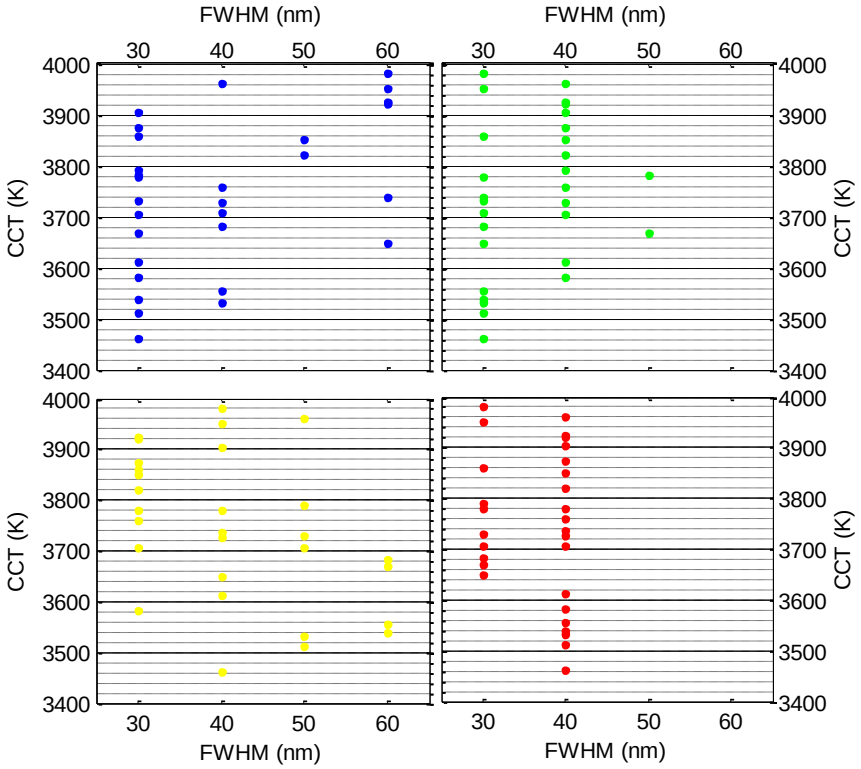

Figure 2.4.3.4.6 FWHM-CCT relation for high quality white light

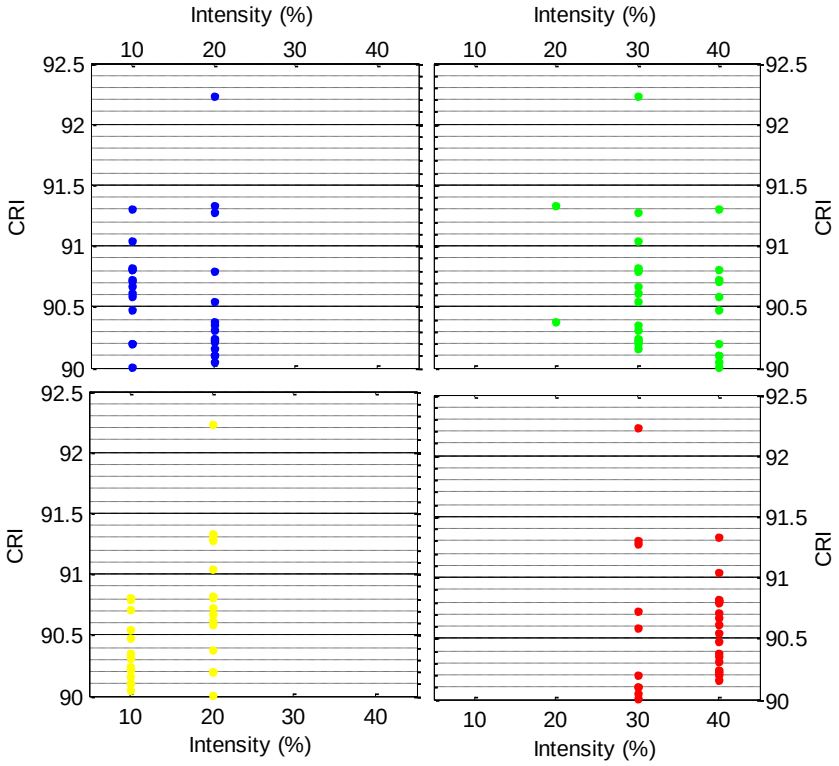

Figure 2.4.3.4.7 Intensity-CRI relation for high quality white light

The relationship between the intensity of four color components with CRI, LER and CCT parameters have been given from Fig. 2.4.3.4.7 to Fig. 2.4.3.4.9. As can be seen from these figures, when there are four color components in mixing for white, blue and yellow get the lower percentages compared to the red and green.

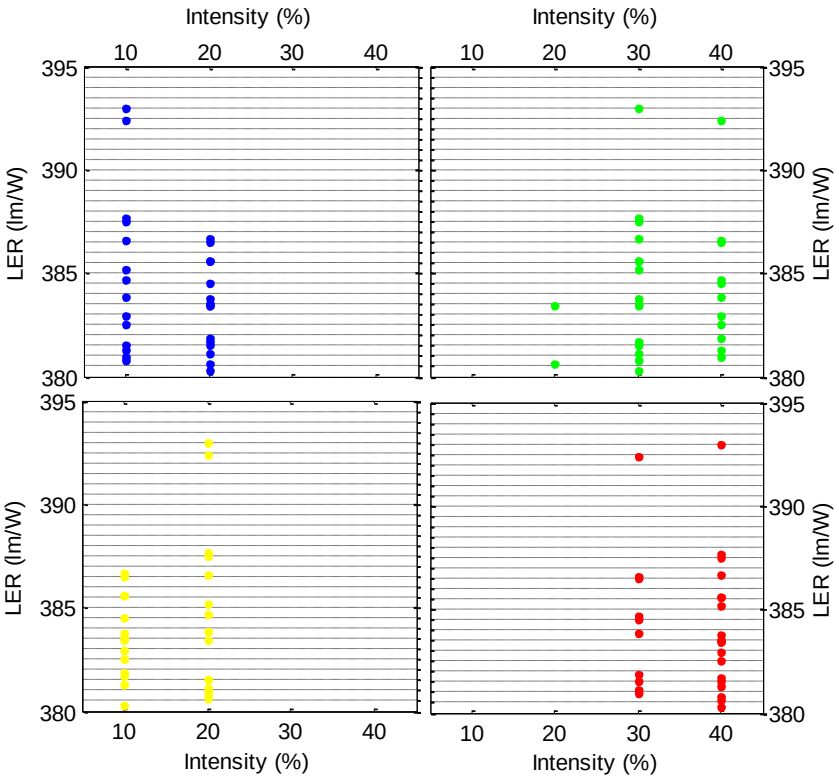

Figure 2.4.3.4.8 Intensity-LER relation for high quality white light

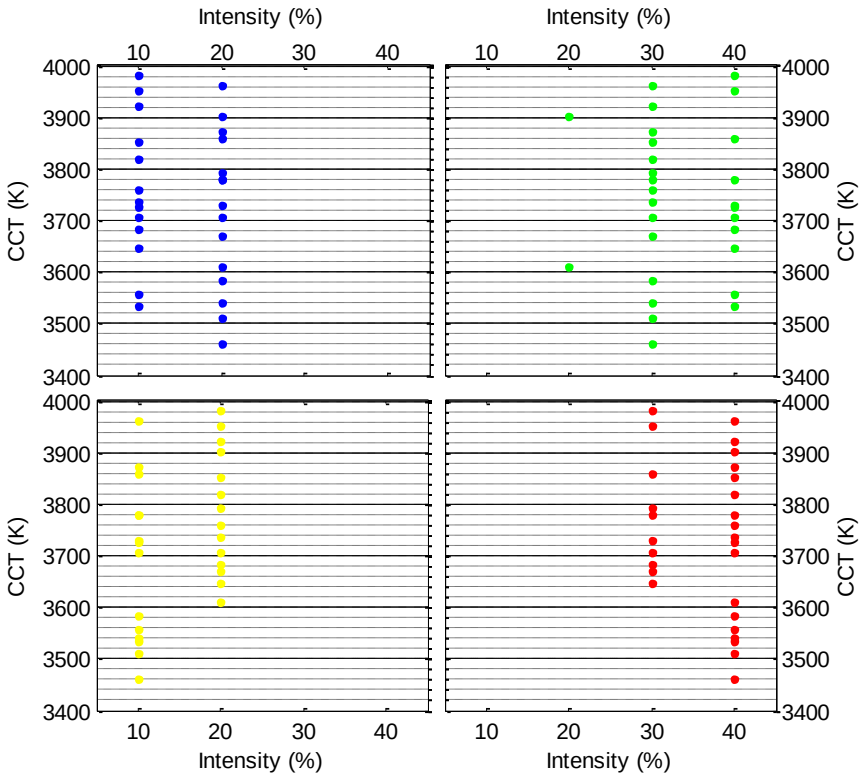

Figure 2.4.3.4.9 Intensity-CCT relation for high quality white light

Using green and red intensities around 30%-40% and blue and yellow around 10%20% provides the achievement of high quality white light. All of these ranges in terms of intensity ensure the CCT, CRI and LER requirements.

CRI	CCT (K)	LER (lm/W)	λ_{peak} blue (nm)	FWHM blue (nm)	Intensity blue (nm)	λ_{peak} green (nm)	FWHM green (nm)	Intensity green (nm)	λ_{peak} yellow (nm)	FWHM yellow (nm)	Intensity yellow (nm)	λ_{peak} red (nm)	FWHM red (nm)	Intensity red (nm)	x coord.	y coord.
90,0	3648	384	470	60	10	530	30	40	590	40	20	620	30	30	0,40	0,44
90,1	3731	387	460	30	20	530	30	40	590	50	10	610	30	30	0,37	0,41
90,1	3859	382	460	30	20	530	30	40	590	30	10	610	30	30	0,36	0,41
90,1	3780	385	460	30	20	530	30	40	590	40	10	610	30	30	0,37	0,41
90,2	3963	382	470	40	20	530	40	30	550	50	10	610	40	40	0,38	0,43
90,2	3759	393	450	40	10	520	40	30	550	30	20	610	40	40	0,40	0,45
90,2	3983	392	470	60	10	530	30	40	590	40	20	620	30	30	0,40	0,44
90,2	3511	384	460	30	20	530	30	30	550	50	10	610	40	40	0,40	0,41
90,2	3539	386	460	30	20	530	30	30	550	60	10	610	40	40	0,40	0,41
90,2	3583	384	460	30	20	530	40	30	560	30	10	610	40	40	0,40	0,41
90,3	3781	386	460	30	20	530	50	30	580	30	10	610	40	40	0,40	0,41
90,4	3462	380	460	30	20	530	30	30	550	40	10	610	40	40	0,40	0,40
90,4	3612	381	460	30	20	520	40	20	550	40	20	610	40	40	0,39	0,41
90,5	3727	383	450	40	10	520	40	40	560	40	10	610	40	40	0,39	0,45
90,5	3873	387	460	30	20	530	40	30	560	30	10	610	40	40	0,40	0,41
90,6	3952	387	460	60	10	530	30	40	590	40	20	620	30	30	0,40	0,43
90,6	3851	388	460	50	10	520	40	30	550	30	20	610	40	40	0,39	0,45
90,7	3924	381	450	60	10	520	40	30	560	30	20	610	40	40	0,40	0,43
90,7	3556	383	450	40	10	520	30	40	550	60	10	610	40	40	0,40	0,45
90,7	3708	381	450	40	10	520	30	40	580	50	20	620	30	30	0,39	0,44
90,8	3706	383	460	30	20	530	40	30	550	30	10	610	40	40	0,39	0,41
90,8	3533	381	450	40	10	520	30	40	550	50	10	610	40	40	0,40	0,44
90,8	3738	387	460	60	10	520	30	30	550	40	20	610	40	40	0,40	0,44

Tablo 2.4.3.4.1 The parameters sets for high quality white light in four-color mixing

CRI	CCT (K)	LER (lm/W)	λ_{peak} blue (nm)	FWHM blue (nm)	Intensity blue (nm)	λ_{peak} green (nm)	FWHM green (nm)	Intensity green (nm)	λ_{peak} yellow (nm)	FWHM yellow (nm)	Intensity yellow (nm)	λ_{peak} red (nm)	FWHM red (nm)	Intensity red (nm)	x coord.	y coord.
90,8	3821	385	450	50	10	520	40	30	550	30	20	610	40	40	0,39	0,44
91,0	3921	382	460	60	10	520	40	30	550	30	20	610	40	40	0,39	0,44
91,3	3670	382	460	30	20	530	50	30	590	60	20	620	30	30	0,39	0,42
91,3	3682	385	450	40	10	520	30	40	580	60	20	620	30	30	0,40	0,45
91,3	3903	383	460	30	20	520	40	20	550	40	20	610	40	40	0,39	0,41
92,2	3791	381	460	30	20	530	40	30	590	50	20	620	30	30	0,40	0,41

Tablo 2.4.3.4.1 (continue) The parameters sets for high quality white light in four-color mixing

The application of white color based on commercial blue LED has been simulated and it was shown that it is possible using blue LED such as InGaN to reach high quality white light parameters. On a blue LED, using green, yellow and red emitters with 520nm-530nm, 550nm-590nm and 610nm-620nm as peak emission wavelength respectively gives the highest CRI value that 92,23 as given Fig. 2.4.3.4.10.

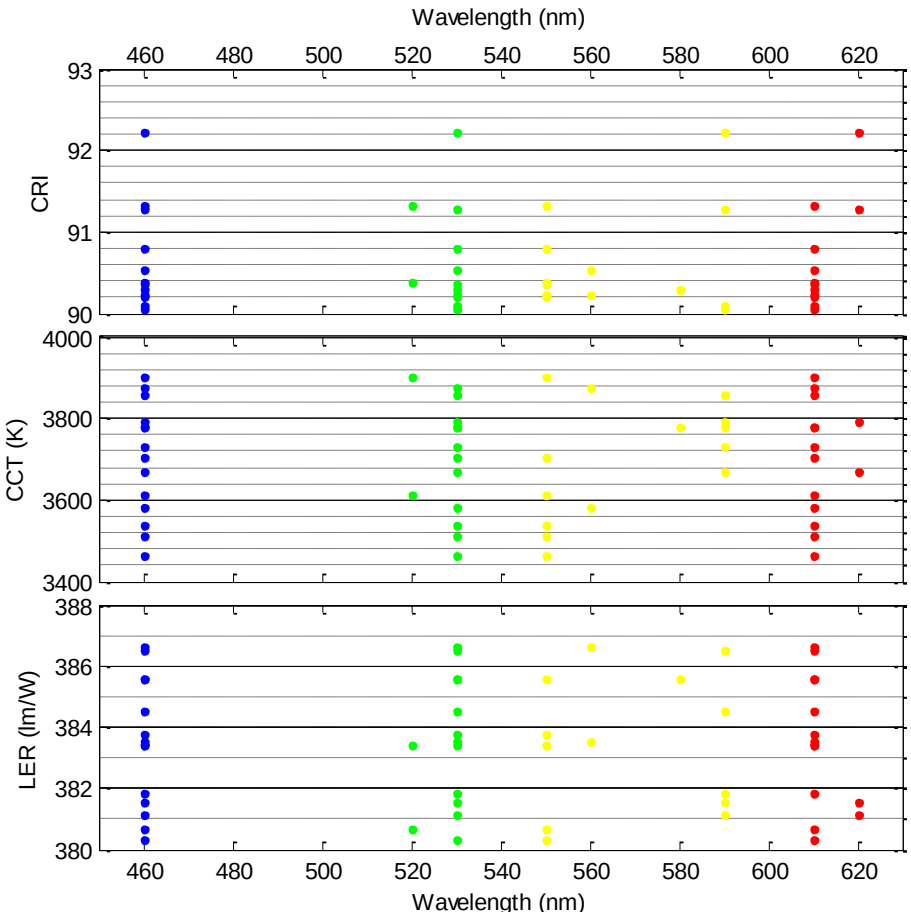

Figure 2.4.3.4.10 Based on commercial blue LED, relation between peak emission wavelength and CRI/CCT/LER in four-color mixing.

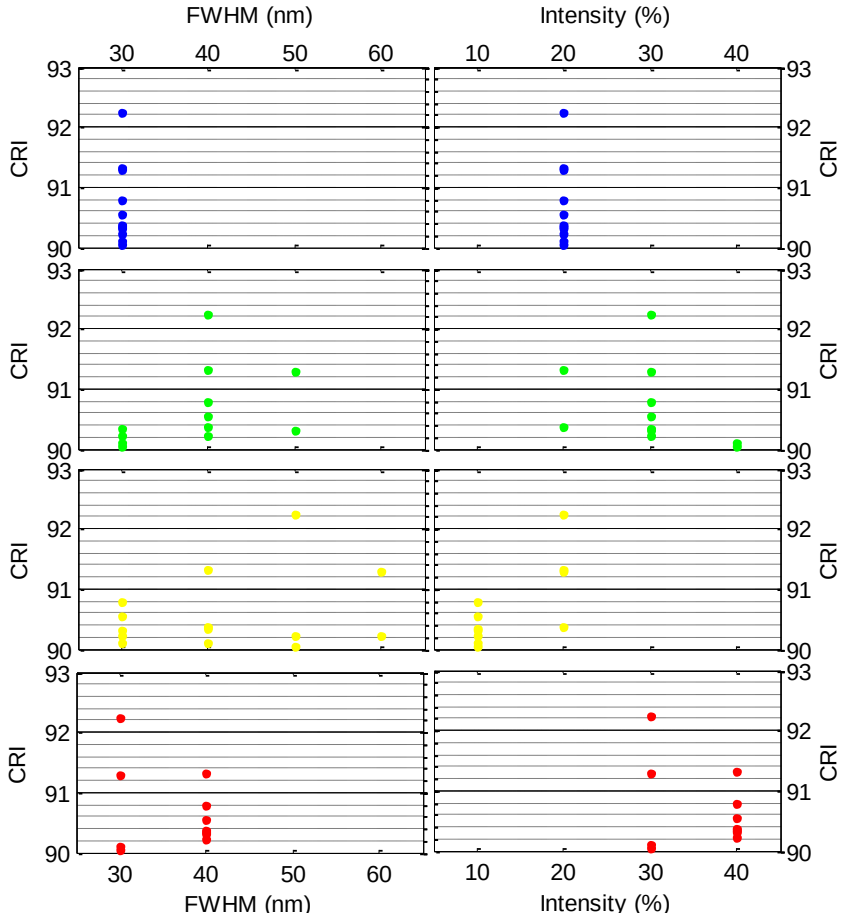

Figure 2.4.3.4.11 Based on commercial blue LED, relation between FWHM/Intensity and CRI in four-color mixing.

As it is given in Fig. 2.4.3.4.11 to achieve high quality white light using commercial InGaN blue LED, 20% of blue intensity is needed. A low yellow intensity as in blue and higher green and red percentages are applicable to obtain the high performance. In terms of FWHM, narrow yellow emitters are proper whatever the value is. Red FWHM can have 30nm or 40nm thickness where for green 50nm can be used additionally.

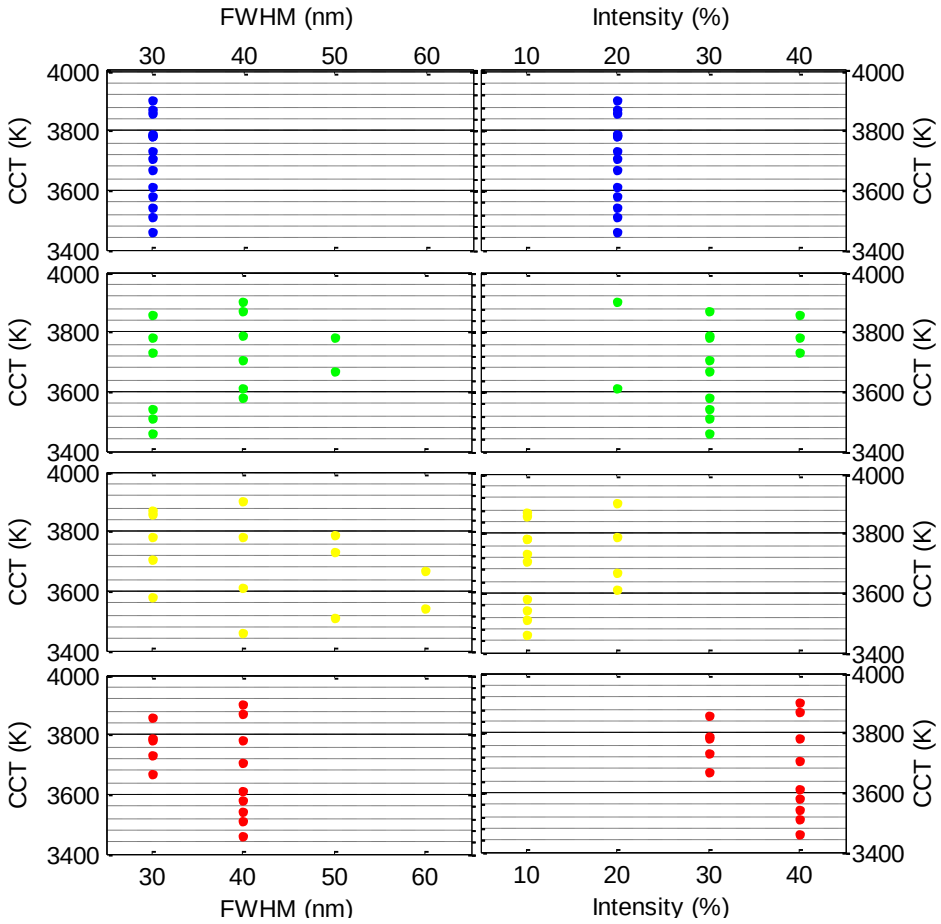

Figure 2.4.3.4.12 Based on commercial blue LED, relation between FWHM/Intensity and CCT in four-color mixing.

Using 20% and 10%-20% yellow intensity provides requirements where red and green ratios have to be higher. Having more possibility in yellow and green components in terms of FWHM may be seen as a chance but using 30nm-40nm FWHM values for all components ensure the high quality necessities as can be seen in Fig. 2.4.3.4.12.

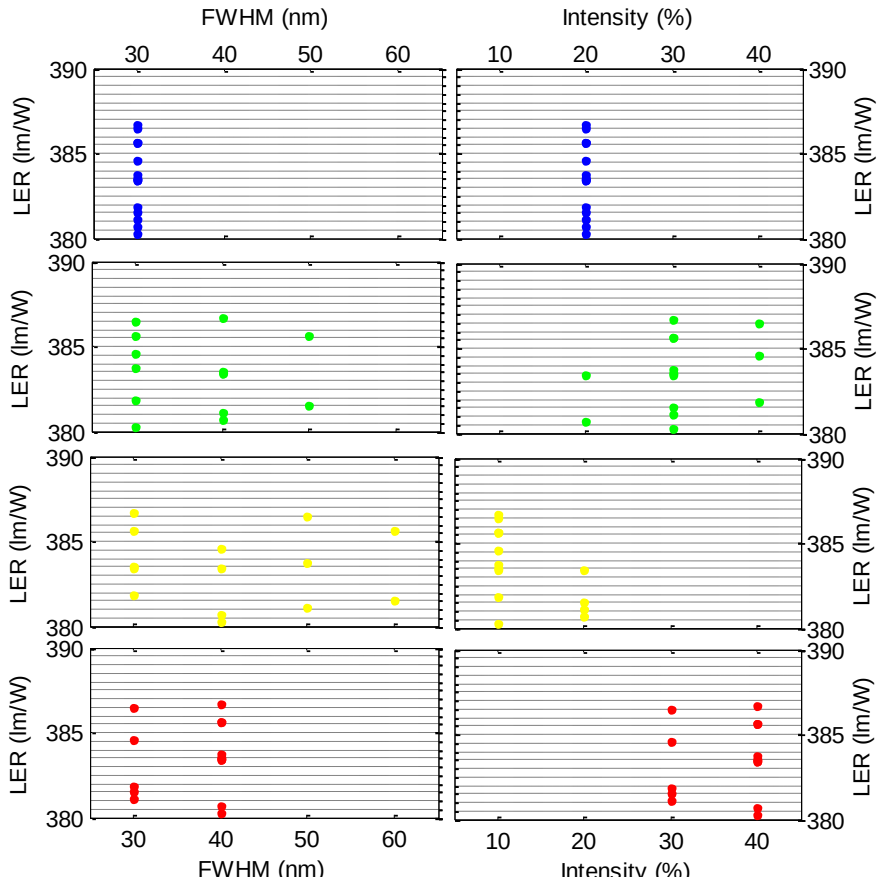

Figure 2.4.3.4.13 Based on commercial blue LED, relation between FWHM/Intensity and LER in four-color mixing.

Obtaining high LER value requires the same levels of FWHM and intensity parameters as in CRI and CCT as given in Fig 2.4.3.4.13. In white region, all requirements in terms of CCT, CRI and LER have to be procured in same time. Having similar levels of FWHM and intensity for blue, green, red, and yellow colors indicate that results are consistent.

The white light, whose spectrum is given in Fig. 2.4.3.4.14, has been generated using green, yellow and red polymeric films based on colloidal quantum dots onto blue InGaN LED in laboratory [60]. Addition of yellow component provides a warm white light with 88.6 CRI, 2763K CCT and 290lm/W_{opt} LER.

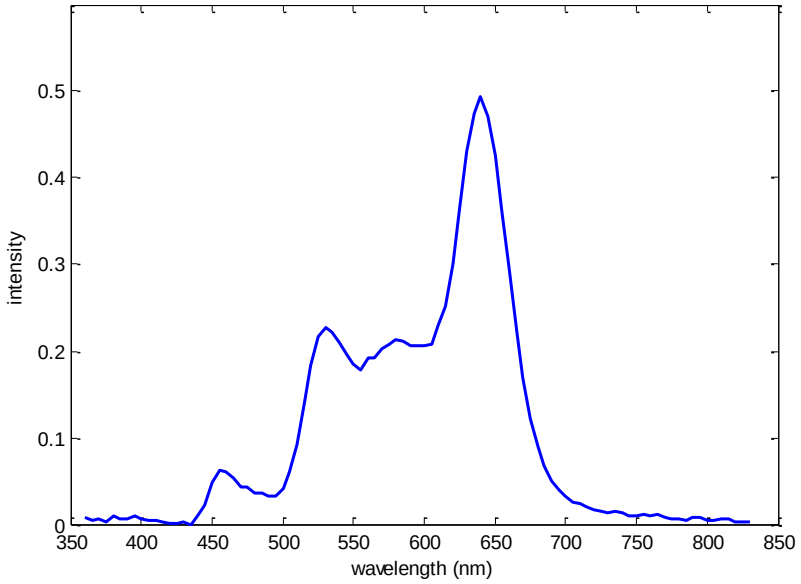

Figure 2.4.3.4.14 The spectrum of white light synthesized in laboratory

The investigation of high quality white light which requires a CRI>90, a CCT<4000K and LER>380lm/W_{opt} is the main aim of this chapter. Two-color mixing is not an efficient way in terms of the performance of white light due to the limited are under blue and yellow spectra. Increasing the performance needs more color components in the visible range so that more than two colors combined to achieve high quality white light.

High quality white light has to follow those requirements at the same time so that especially in three-color mixing even it is possible to achieve high CRI levels, CCT and LER requirements limit that increment.

Adding a forth component, yellow, to fulfill the gap in visible region resulted well. Accessing more colors under the white spectrum provides high quality white light parameters as has been discussed in this chapter.

Chapter 3

Investigation of Color Quality on Displays

LCD backlight systems had a great improvement from CCFL to LEDs in order to save energy, minimize the device thickness and enhance the color quality [25]. As a first step of moving towards LED backlights, the RGB LEDs were used and 105% NTSC 1931 color gamut ratio was achieved and that ratio was approximately corresponding to 150% compared to the television display technology of that era [54,55]. However, their poor power efficiency and high cost had directed the industry to the use of white LEDs using color converters. While the cost had been decreased using white LEDs [9] based on phosphor emitters, the broad emissions of white LEDs led to a decrease on the color quality of displays. The achieved color gamut was approximately 70% in areal scale compared to the NTSC color gamut in CIE 1931 [56,57]. To enhance the white backlighting units, QDs have started to emerge as promising agents for backlight in LCDs [58,59,60]. In addition to LCDs, white OLEDs based on colloidal quantum dots have also started to emerge as promising building blocks for the next generation displays [58]. However, in 2012 Japan Broadcasting Corporation (NHK) declared a new reference, Rec.2020, has a wider color gamut area than NTSC triangle. In this Chapter, the requirements to cover Rec.2020 color gamut while maintaining the NTSC triangle will be investigated and analyzed.

3.1 Color Gamut

In CIE diagram, the color space that includes all visible colors by human eye, the triangle in which the colors of a display are located, is called color gamut. Different color gamuts have been declared as reference to compare the proposed

design. In 1953 National Television System Committee defined a reference color gamut which has 47,3% of CIE 1931 as can be seen in Fig. 3.1.1.

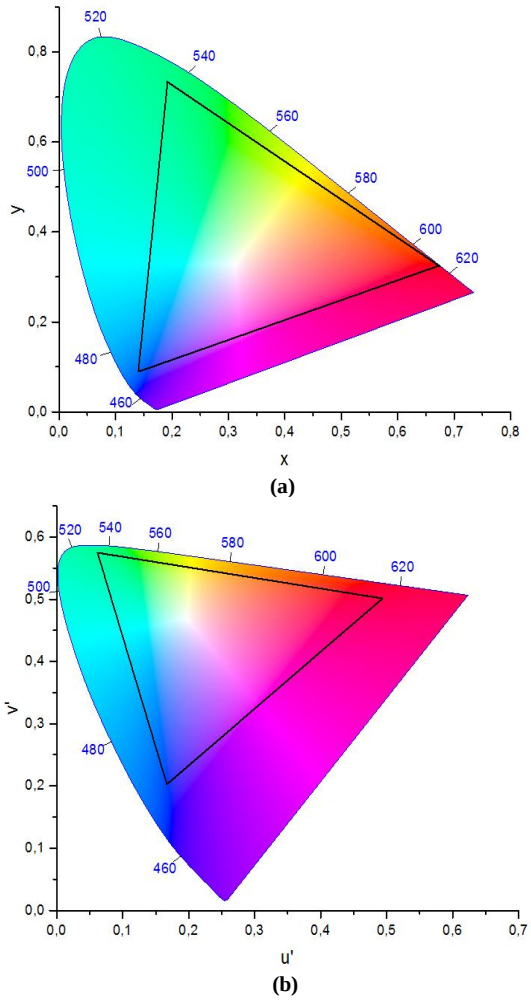

Figure 3.1.1 (a) CIE 1931 color space, (b) CIE 1976 color space [61]

Although there were areas had not been covered in xy color space, for a display NTSC triangle was too wide to cover in that era. In 1996 sRGB color gamut was created by HP and Microsoft [62]. It has 33,51% of all colors in CIE xy color space. Then Adobe Systems announced a new reference Adobe RGB triangle that wider than sRGB and covers 45,21% of the CIE, in 1998 [63]. The wider color gamut the more different colors on displays and Adobe RGB gamut has more colors on green part of the space. But for that era, a new design that reaches the area of NTSC triangle was so difficult. In some studies the higher

result was declared between CIE 1931 and CIE 1976 color spaces. The NTSC, Adobe RGB and sRGB triangles are shown in Fig. 3.1.1.and in Table 3.1.1 the corner coordinates of these triangles are given.

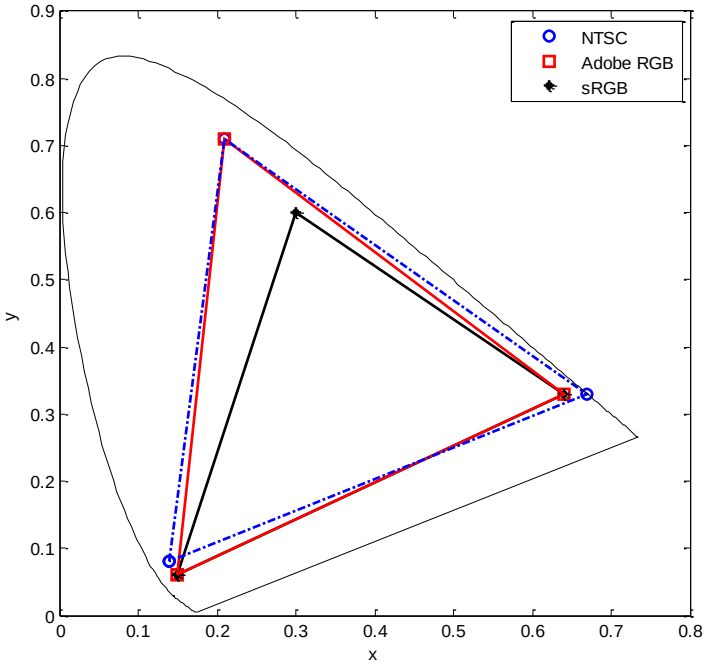

Figure 3.1.2 NTSC, Adobe RGB and sRGB color gamuts on CIE 1931

Color Triangle	Red Coordinate	Green Coordinate	Blue Coordinate
NTSC	(0,67, 0,33)	(0,21 , 0,71)	(0,14 , 0,08)
Adobe RGB	(0,64 , 0,33)	(0,21 , 0,71)	(0,15 , 0,06)
sRGB	(0,64 , 0,33)	(0,30 , 0,60)	(0,15 , 0,06)

Table 3.1.1 The red, green and blue coordinates of NTSC, Adobe RGB and sRGB color spaces

From the beginning of reference color gamut declaration each of them was wider than previous one. Research efforts have been focused on reaching sRGB, followed by Adobe RGB and finally NTSC. Higher coverage more than 100% of NTSC triangle announced however mostly they were areal comparisons. However, Japan Broadcasting Corporation (NHK) defined a new and wider color gamut and CIE recommended called ITU-R BT2020 (Rec.2020) given in Fig. 3.1.2 with other basic color spaces [64].

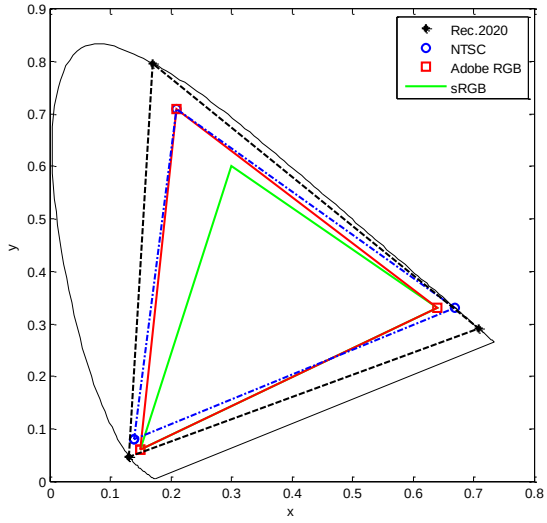

Figure 3.1.3 Relation between reference color gamuts

Color Triangle	Red Coordinate	Green Coordinate	Blue Coordinate
Rec.2020	(0,708 , 0,292)	(0,170 , 0,797)	(0,131 , 0,046)

Table 3.1.2 The red, green and blue coordinates of Rec.2020 color space

Although the spectral coverage enhancement is possible for Rec.2020, it comes with the cost of sacrificing from its existing colors because of having all of its corner coordinates on spectral locus given in Table 3.1.2. Another limit due to its corners lying on locus, it is impossible to work on broadening higher than 100% in terms of coverage ratio. Having larger triangles than Rec.2020 is possible but this would not be able to cover the Rec 2020. Thus the main aim for the thesis in terms of a wide color gamut is to define the color parameters to achieve Rec.2020. The parameters of FWHM and peak emission wavelength must be optimized at the same time to obtain the color gamut [65]. It is known that the peak emission wavelength located on the border of spectral locus and changes on that scale which means increasing the peak emission wavelength moves the color coordinate from blue range towards red area so FWHM is important to determine.

3.1.1 The effect of FWHM on chromaticity coordinate

Color gamut can be broadened by having three primaries' coordinates closer to the borders of spectral locus in corners. The color coordinates closer to the border of locus result in purer colors. It is easy to change the emission wavelength by checking the CIE 1931 and on a specific peak emission wavelength, if the FWHM is changed systematically the effect of FWHM can be explored analyzing the chromaticity coordinates.

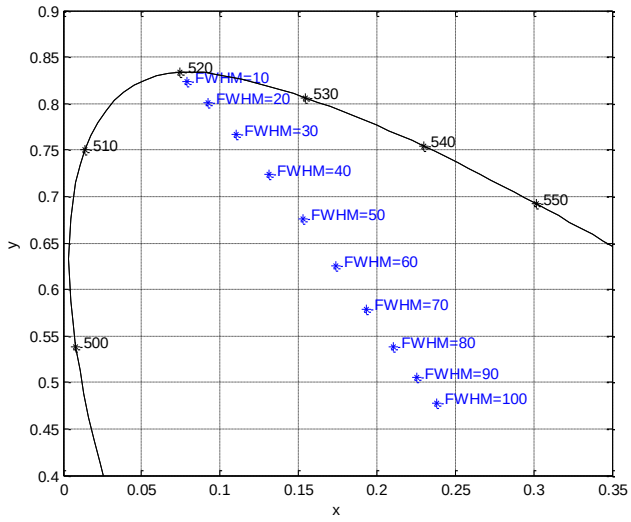

Figure 3.1.1.1 The effect of FWHM change on chromaticity coordinate

In Fig. 3.1.1.1, the effect of FWHM change has analyzed. On a constant peak emission wavelength, 520nm, the FWHM values had changed between 10nm and 100nm with 10nm increments. It can be seen in Fig. 3.1.1.1 that if the FWHM of spectrum shrinks, the chromaticity coordinate moves towards the border of the spectral locus.

3.1.2 Areal percentage vs. Coverage Percentage

One of the important problems is the spectral coverage area announced for the proposed system. In previous studies, the areal comparison is used and announced, however for a logical development the reference must be covered to provide any missing color while enhancement of the reference such as NTSC

triangle. Unfortunately in literature there are many studies that use areal comparison [55,56,58]. The difference between areal and coverage percentage is given in Eq. 3.1.1 and 3.1.2 [66].

$$\text{Areal Percentage}=\frac{A_{proposed}}{A_{reference}}*100 \tag{3.1.1}$$

$$\text{Coverage Percentage}=\frac{A_{proposed}\cap A_{reference}}{A_{reference}}*100 \tag{3.1.2}$$

In this study, all percentage values were given in terms of coverage type if it is not specified as areal. The main reason for that is that, for a logical broadening the new triangle must cover the reference. Only the coverage can lead a meaningful enhancement and development.

3.1.3 CIE 1931-CIE 1976 Relation

In literature, there are many studies that the gamut area had been declared due to the gamut area percentage. If the percentage of CIE 1931 was higher it was used or vice versa [67]. A scientist from NHK, Masaoka, revealed the independence between these two color spaces [68]. His research proved that, a wider color gamut than reference in one color space may not extend the reference in other color space. For instance a coverage higher than 100% in CIE 1931, may give a result in 80% CIE 1976. The identification of a metric is needed therefore he suggested to use CIE 1931 color space because the colors covered in that space also mostly covered in other color spaces such as CIECAM02 Ja_cb_c, CIELAB L*a*b* and CIELUV L*u*v* [69]. According to Fig. 3.1.3.1, the relation between coverage ratio in CIE 1931 and CIE 1976 is not linear. While CIE 1931 is coverage increasing, CIE 1976 percentage may increase or decrease.

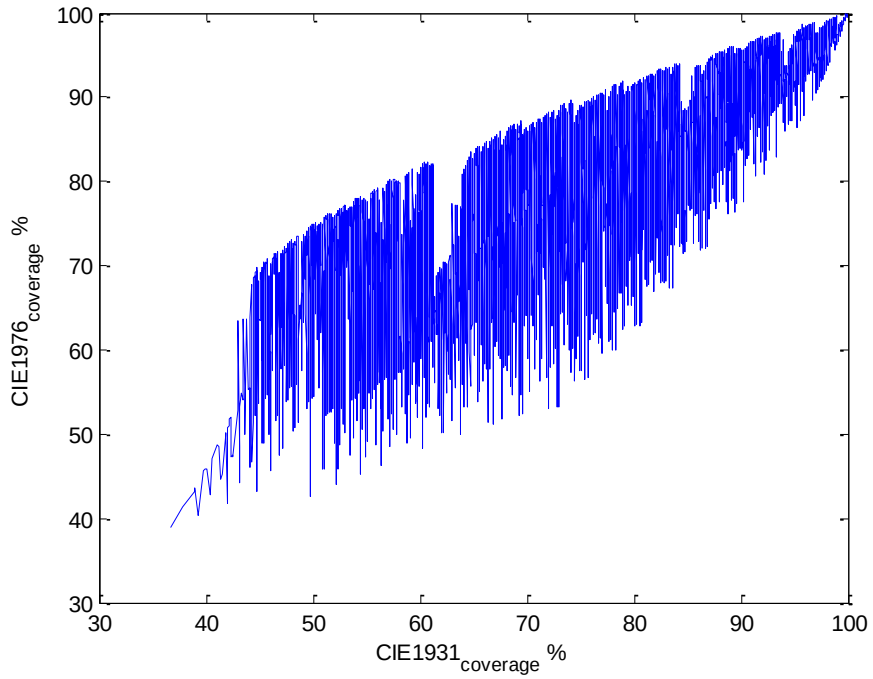

Figure 3.1.3.1 The relation between CIE 1931 coverage and CIE 1976 coverage ratios

3.2 Ultra-narrow Emitters for Wide Color Gamut

In the previous part, it is shown that for a wider color gamut, the coordinates of three primaries must be closer to the spectral locus. FWHM value of the emission must be narrow to have an appropriate coordinate so that narrow emitters such as quantum dots were started to be used for backlight technology. Their narrow emission spectra, energy efficient performance and ease in controllability revealed them as promising devices [70,71,72]. NTSC triangle may be achieved using narrow emitters such as quantum dots however for reaching Rec.2020 color gamut to the highest degree, emitters having FWHM narrower than 10nm are required. QDs are possible materials to get wider coverage ratios with filter engineering for Rec. 2020. However, new filter design is an important issue as well to be considered. For the time being, reaching the borders of Rec.2020 looks not available with QDs [73].

Rec.2020 has all of its corners almost on spectral locus and nowadays laser diodes may provide that narrow enough emissions [74]. In the near future use of laser as backlight sources may be available and for the time being ultra-narrow emitters such as colloidal nanoplatelets may address that need. Ultra-narrow emitters that have emission spectra with less than 10nm FWHM were simulated and 6-7nm emission bandwidth has been found as appropriate reference level [75,76,77]. Decreasing the FWHM for an emitter moves the chromaticity coordinate towards borders of spectral locus so that using colloidal nanoplatelets will increase the color gamut area as expected.

3.3 Simulation Study

In this thesis, the main aim is to figure out the parameters of color components to cover the Rec.2020 triangle. However, it has been considered that coverage of NTSC has to be controlled at the same time. The reason is, although a wider reference, Rec.2020, has been declared, NTSC color gamut is still a widely accepted reference in the literature.

In simulation methodology, as it has been done in high quality white light simulation, using defined parameter ranges as the starting and ending values of nested for loops, all probabilities have been investigated. Different from white light application, in display color quality process, intensities of color components are not important to define the chromaticity coordinate of components as can be seen in Eq. 1.4.10 and 1.4.11. However, the desired white light for backlight units is achieved by arranging the intensities of color components.

Comparison of simulated triangle's corners and reference color gamut's corners provides information about triangle's ratio. In coverage percentages, only intersected areas have been measured whereas for areal results, all achieved area has been presented. All calculations have been done using CIE 1931 color space.

3.3.1 Three-color combination

Using blue, green and red emitters, the achievement of Rec.2020 while covering the NTSC has been investigated in this part of the thesis. As expected, three-color combination can cover the reference triangle since reference triangle also has three primary color components. However, in next part, 3.3.2, the effect of adding forth color components will be analyzed using best coverage parameters of three-color combination.

In simulation steps, peak emission wavelengths were defined using the NTSC triangles lines. By extending them through spectral locus, the intersection points of the lines with locus give information about the simulation range. With a minor extra range from left and right side, the limits of peak emission wavelengths to enlarge the NTSC can be defined [78]. With this method, peak emission wavelength ranges have been defined as 451nm-475nm for blue, 514nm-540nm for green and 610-700nm for red with 2nm increments as given in Fig. 3.3.1.1.

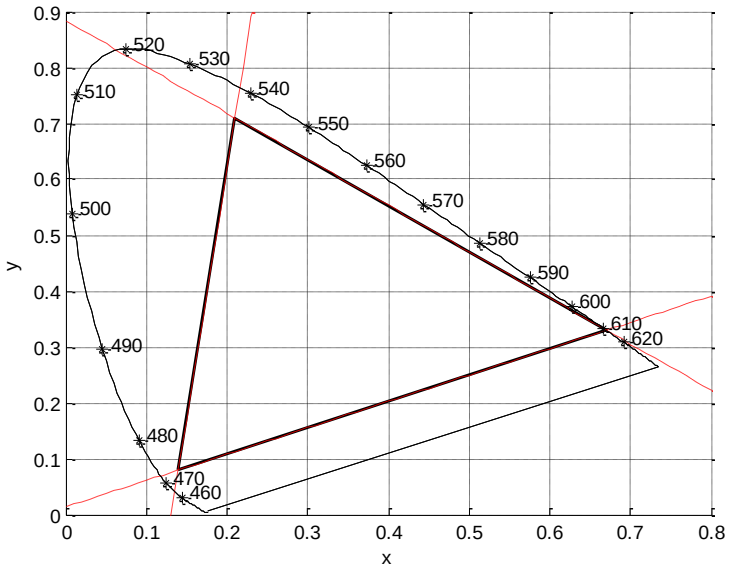

Figure 3.3.1.1 The extended lines to determine peak emission wavelengths for simulation ranges.

The FWHM ranges have been determined using chromaticity coordinates for varied FWHM values from 30nm to 90nm for each color component. By doing

so, it has been shown that up to 50nm FWHM is applicable for green, maximum 70nm FWHM for blue are necessary to cover NTSC triangle whereas the red FWHM can get many values due to the narrow area for red in color space on that region as given in Fig. 3.3.1.2.

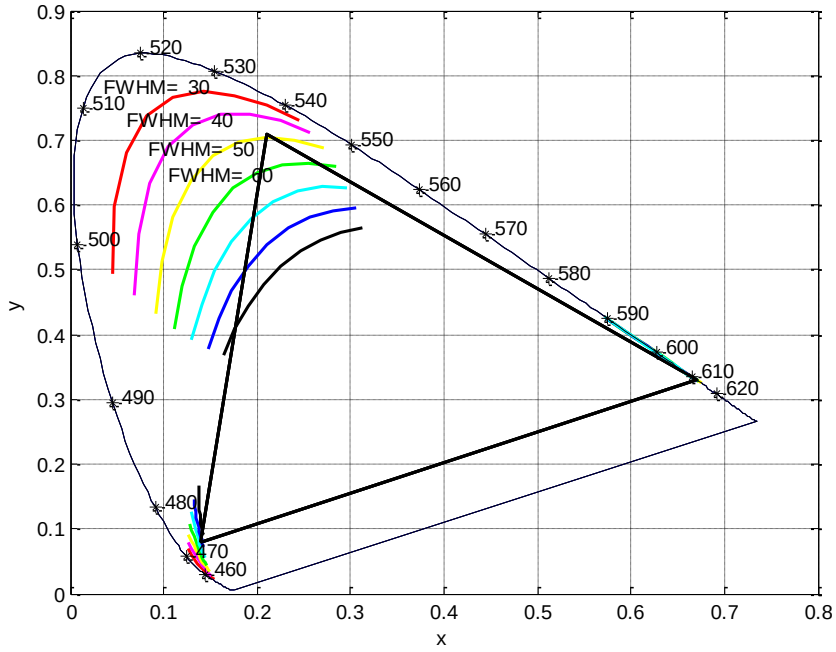

Figure 3.3.1.2 The effect of FWHM on chromaticity coordinates

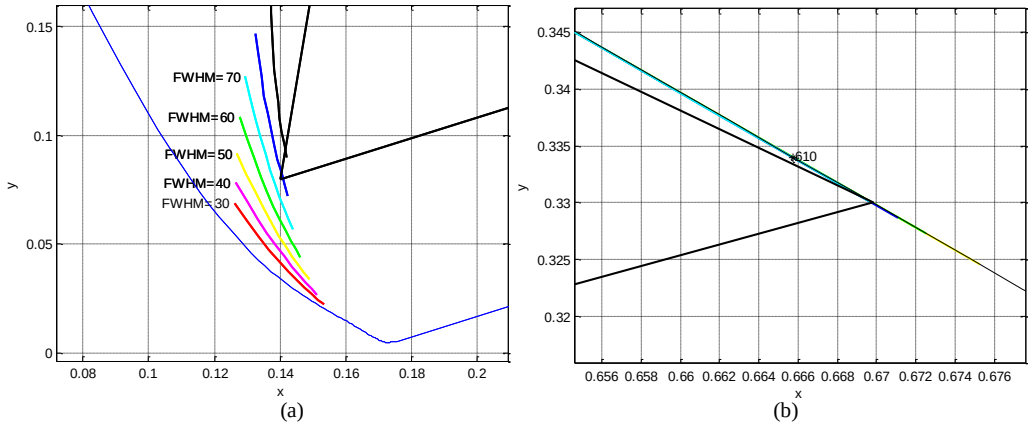

Figure 3.3.1.3 The effect of FWHM on blue(a) and red(b) chromaticity coordinate

In simulation steps, the FWHM ranges have been defined as 6nm-30nm for three primaries to cover ultra-narrow emitters, too. The chromaticity coordinates of red is almost on spectral locus so that the change on peak emission

wavelength and FWHM does not affect the coordinate too much as given in Fig. 3.3.1.3.

In Fig. 3.3.1.4, the simulation areas for three primaries' coordinate have been visualized with their colors. If the coordinates are in the areas, the coverage of the NTSC would provide more than 90% coverage.

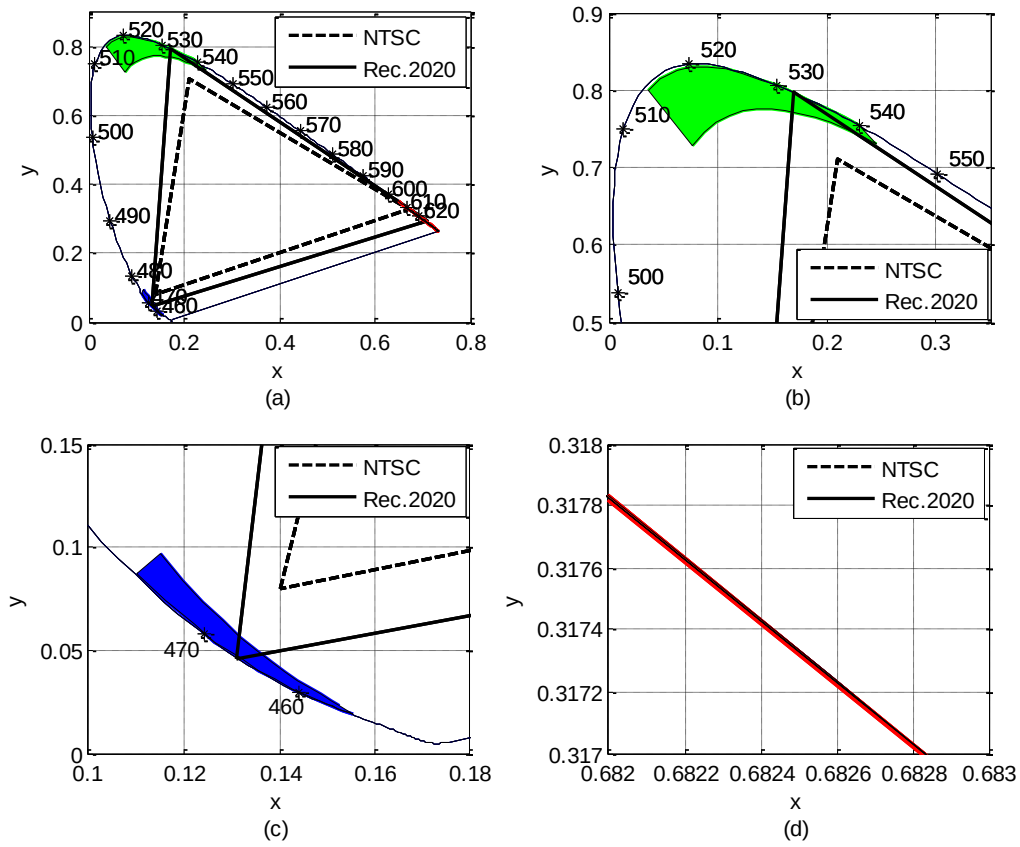

Figure 3.3.1.4 Possible chromaticity coordinate areas for our simulation

In more than 130 million results (130.312.500) the maximum Rec.2020 coverage ratio was 99,7%. The color spectrum parameters for red, green and blue were 632nm, 532nm and 467nm for peak emission wavelengths and 11nm, 6nm 7nm for FWHM respectively. Those parameters extend the NTSC triangle up to 133,7%, with coverage of more than 99.98% as can be seen in Fig. 3.3.1.5. The parameters also cover the sRGB and Adobe RGB triangles.

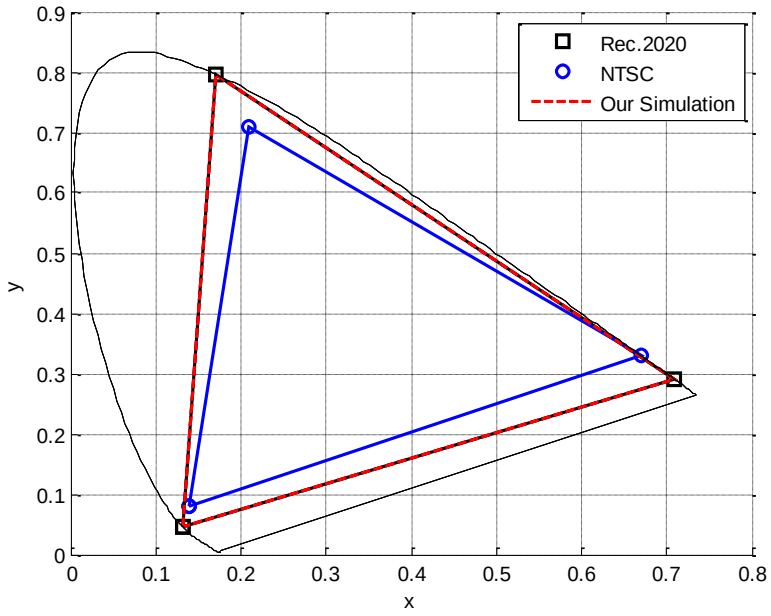

Figure 3.3.1.5 Rec.2020, NTSC and our simulated color triangles on CIE 1931

In Table 3.3.1.1, the distribution of results in terms of Rec.2020 coverage is given. As can be seen on the table, our estimation for the ranges worked properly, thus almost 98% of the results covered more than 80% of Rec.2020 triangle.

Coverage Ratio (C.R.)	Number of Data Sets	% of Data Sets
C.R. ≥99%	219.697	<1%
99%>C.R.≥95%	24.945.483	19%
95%>C.R.≥90%	48.826.342	37%
90%>C.R.≥80%	53.778.719	41%
80%>C.R.≥70%	2.537.438	2%

Table 3.3.1.1 Distribution of results considering the coverage ratio on Rec.2020

The relationship of peak emission wavelength and Rec.2020 coverage ratio has been given in Fig. 3.3.1.6. In the range of 460nm-470nm for blue and 530nm-535nm for green are critical for Rec.2020 coverage. Red peak emission wavelength can vary in many different points whereas 630nm-635nm gives

better performance. After that small range, increasing the peak emission wavelength further decreases the coverage percentage.

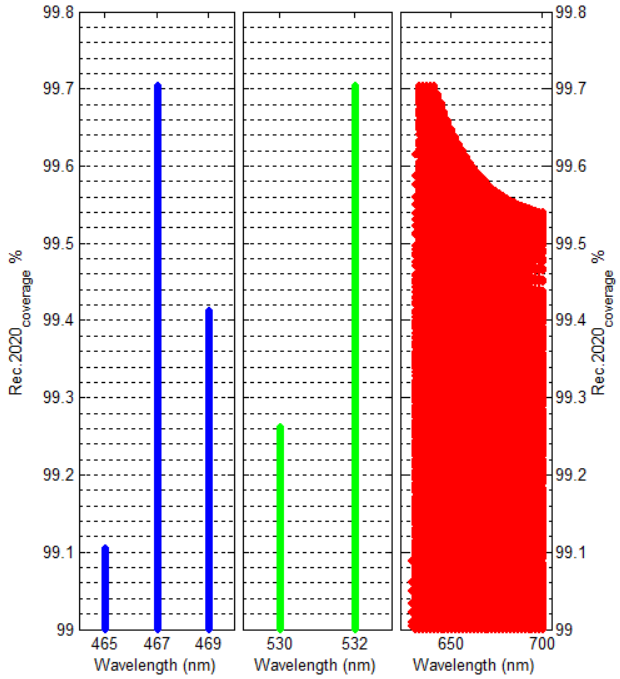

Figure 3.3.1.6 Filtered data providing higher than 99% Rec.2020 coverage ratio

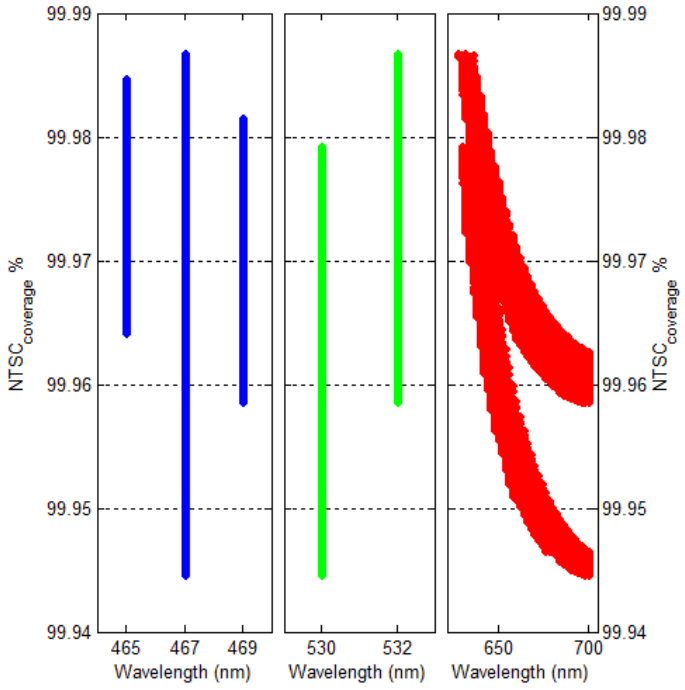

Figure 3.3.1.7 For Rec.2020 coverage≥99%, NTSC coverages achieved

Fig. 3.3.1.7 indicates that all of data sets cover Rec. 2020 more than 99% also cover the NTSC about more than 99,95%. In these results, using red emitter with peak emission wavelength smaller than 650nm increases the probability of having higher coverage ratio. As for Rec.2020, 467nm blue and 532nm green peak emission wavelengths were determined to provide optimal results.

Different from coverage ratio, another figure of merit, the triangle area is used to describe the color gamut. Areal comparison of color gamut with a reference such as CIE 1931 or NTSC gamut explains how the gamut is wide. The improvement of color quality in terms of achieved color scale requires the coverage of reference, so that using coverage ratio term looks more appropriate [66].

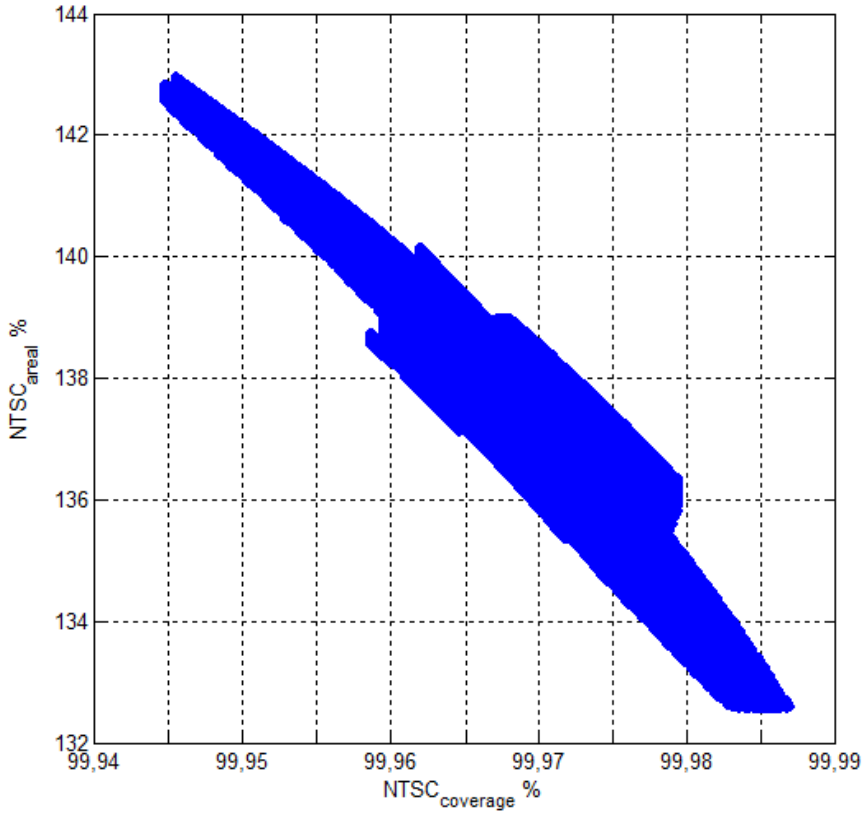

Figure 3.3.1.8 Relation of NTSC coverage and NTSC areal percentages for data have higher than 99% for Rec.2020 coverage

In Fig. 3.3.1.8, the areal comparison of simulated color gamut with NTSC triangle coverage ratio has been presented. Having meaningful color coordinates on red, green and blue corners can enhance the triangle while covering it.

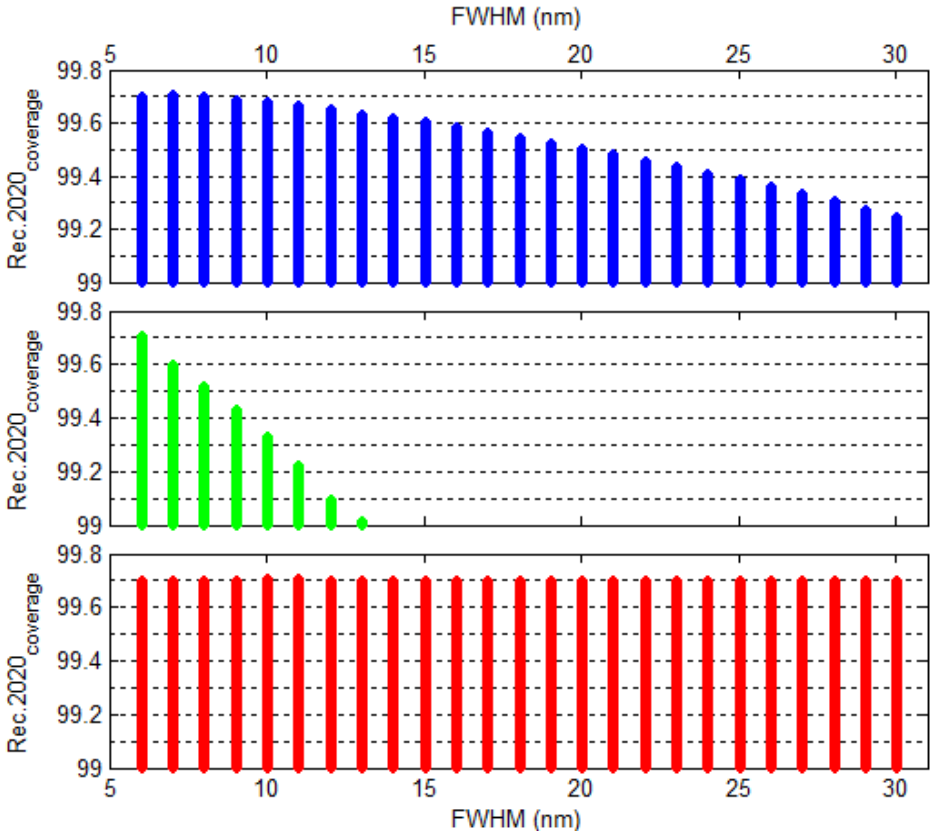

Figure 3.3.1.9 FWHM-Rec.2020 coverage relation for Rec.2020 coverage≥99%

As can be seen in Fig. 3.3.1.9, all of FWHM values in defined range are appropriate for red whereas green can only get up to 13nm for a coverage ratio that higher than 90%. Blue tends to decrease while increasing the FWHM although all of the range is possible.

Considering commercial blue LED with 450nm-460nm peak emission wavelength and 20nm-30nm FWHM parameters, maximum 98,2% coverage of Rec.2020 is possible while NTSC coverage is more than 99% as given in Fig. 3.3.1.10. 459nm for blue and 530nm for green are essential values in terms of

peak emission wavelength. The red emitter can get values approximately from 630nm up to 685nm as given in Fig. 3.3.1.10.

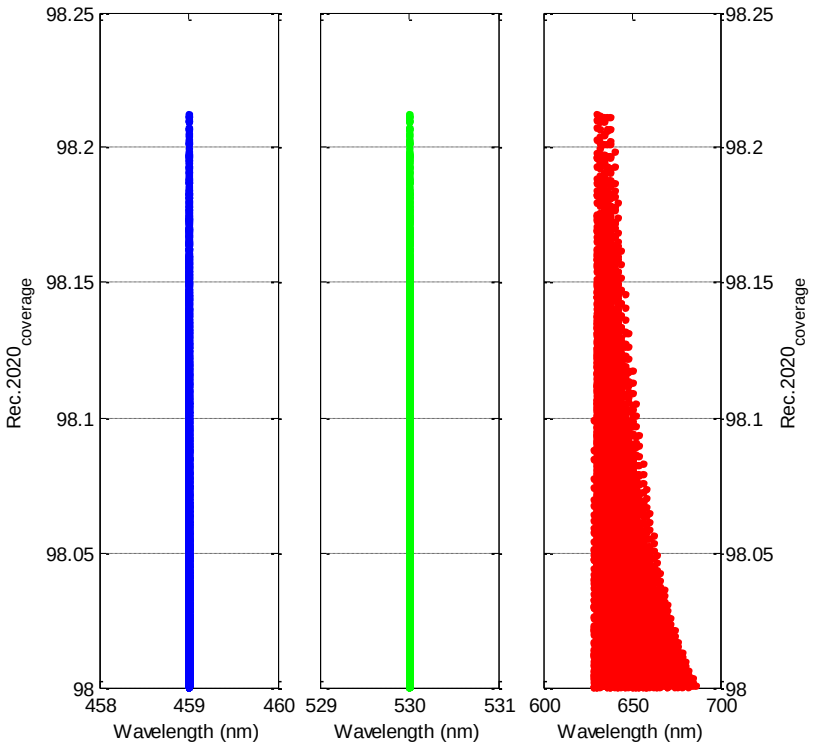

Figure 3.3.1.10 Wavelength-Rec.2020 coverage ratio relation for commercial blue LED application using results that have more than 99% NTSC coverage

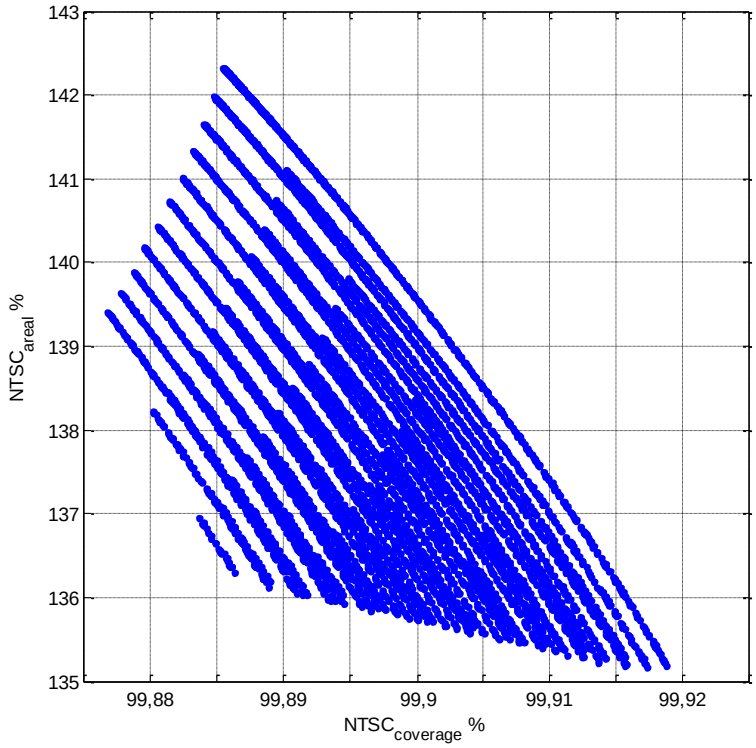

Figure 3.3.1.11 Relation of NTSC coverage and NTSC areal percentages using commercial blue LED

Fig. 3.3.1.11 shows that increasing the NTSC coverage decreases the achieved areal percentage. It seems logical because of the NTSC triangle location in CIE 1931. If a coverage is required, the green peak emission wavelength is limited around 520nm-530nm. However, using a green peak emission wavelegth about 510nm increases the covered area due to the blue-green chromaticity coordinates' slope.

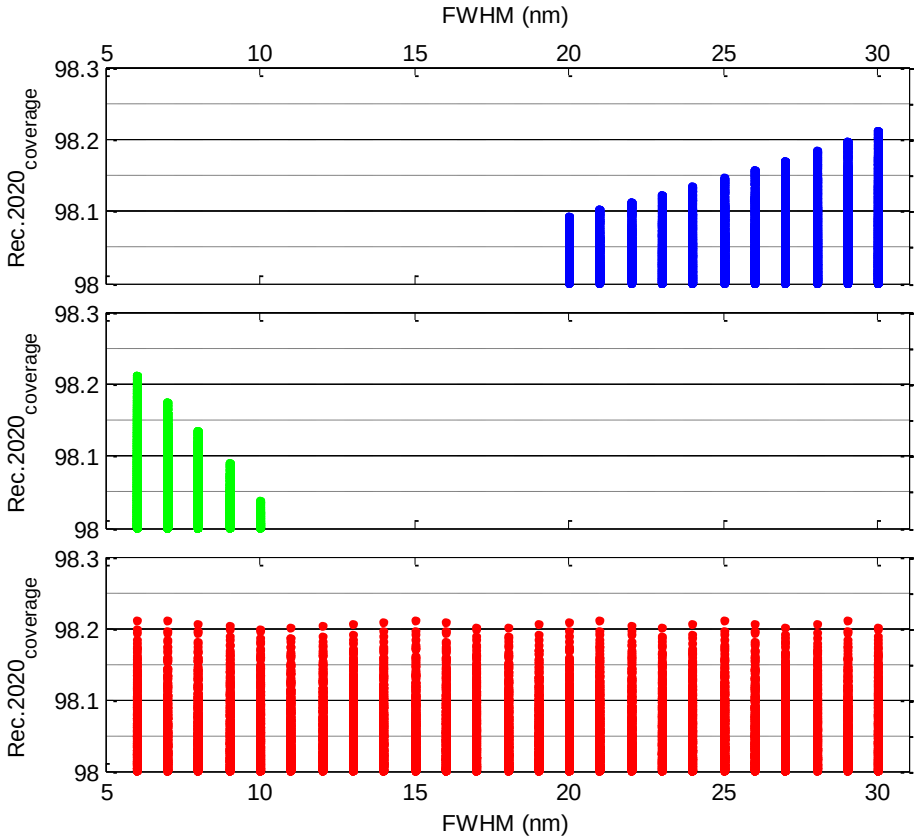

Figure 3.3.1.12 FWHM-Rec.2020 coverage relation for commercial blue LED application using results that have more than 99% NTSC coverage

As can be seen in Fig. 3.3.1.12, increasing blue FWHM in the range that can be found in technology market, increases the achieved Rec.2020 coverage level whereas green can be maximum 10nm. FWHM red can get all values in defined range.

In an experimental work, the synthesis of green and red colloidal quantum dots and hybridizing them on to commercial blue InGaN LED has given us a chance to get white light with three-color mixing approach. The peak emission wavelengths and FWHMs were 456nm-28nm for blue LED, 527nm-37nm for green and 629nm-33nm for red emitter. Because of the intensity value of a spectrum does not affect the chromaticity coordinate, spectrum of combination that has equal levels of color components is given in Fig. 3.3.1.13.

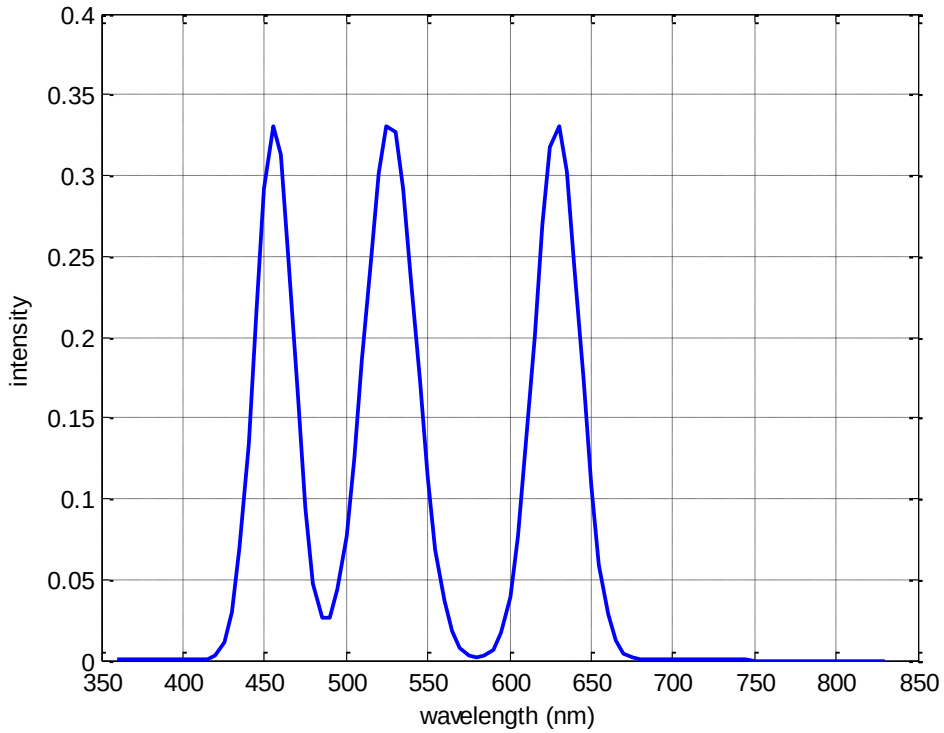

Figure 3.3.1.13 For equal intensities, the emission spectra of the synthesized green and red color components along with the blue InGaN LED

In Fig. 3.3.1.14, the color gamut relation between experimentally achieved white light and NTSC triangle is given in CIE 1931color space. The percentage of the gamut area in comparison with NTSC is 122,5% with 99,5% coverage ratio. The parameter set also covers the 89,9% of Rec.2020. All relations are given in Fig. 3.3.1.14.

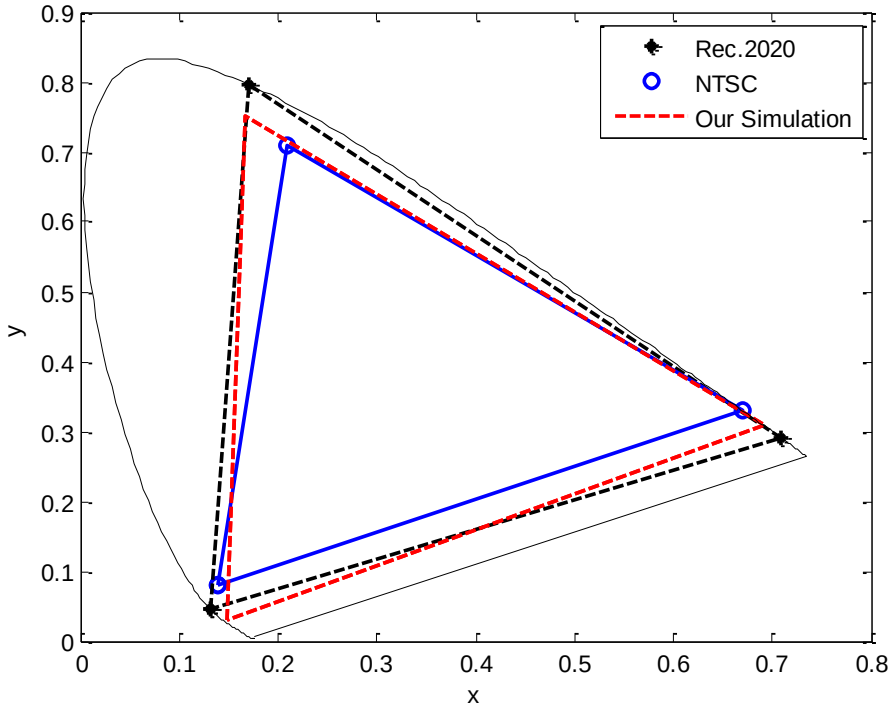

Figure 3.3.1.14 The relation of color gamut based on synthesized emitters and reference color triangles

3.3.2 Four-color combination

In previous part, using three color components, it is almost possible with ultra-narrow emitters to cover Rec.2020. The percentage is 99.7, which will be tried to increase adding a forth color, cyan.

Using the parameters of best result in three-color combination the ranges of cyan parameters that 510nm-528nm peak emission wavelength and 6nm-30nm for FWHM have been analyzed to check the maximum Rec.2020 coverage.

The parameter set in three-color combination, 467nm-7nm for blue, 532nm-6nm for green and 632nm-11nm for red as peak emission wavelength and FWHM respectively, with cyan parameters 506nm-6nm has increased the result from 99,70% to 99,87% as can be seen in Fig. 3.3.1.1. The set also increases the area on CIE 1931 to 171,05% with more than 99,99% of NTSC coverage.

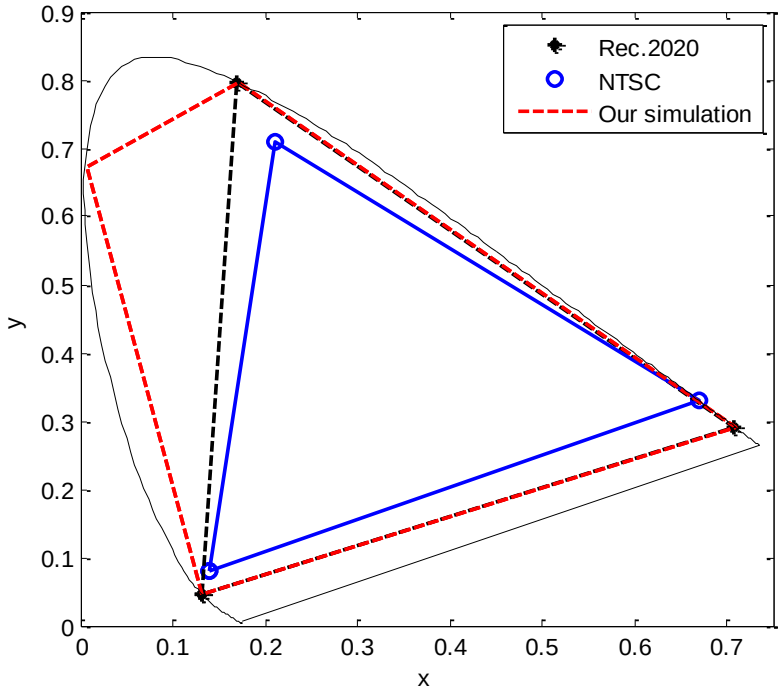

Figure 3.3.2.1 Rec.2020 coverage after addition of cyan component to the parameters of best set in three-color combination

In another simulation, instead of using the best data set, all data that have higher than 99% coverage in three color combination have been used with 510nm-528nm peak emission wavelength with 2nm intervals and 6nm-30nm FWHM range to search for maximum Rec.2020 coverage ratio. In more than 14 million results; the highest achievable value was 99,89% of Rec.2020 as given in Fig. 3.3.2.2. The parameters were 467nm-6nm for blue, 510nm-6nm for cyan 532nm-6nm for green and 632m-14nm for red as peak emission wavelength and FWHM respectively. The set also increases the area on CIE 1931 to 169,55% with more than 99,98% of NTSC coverage.

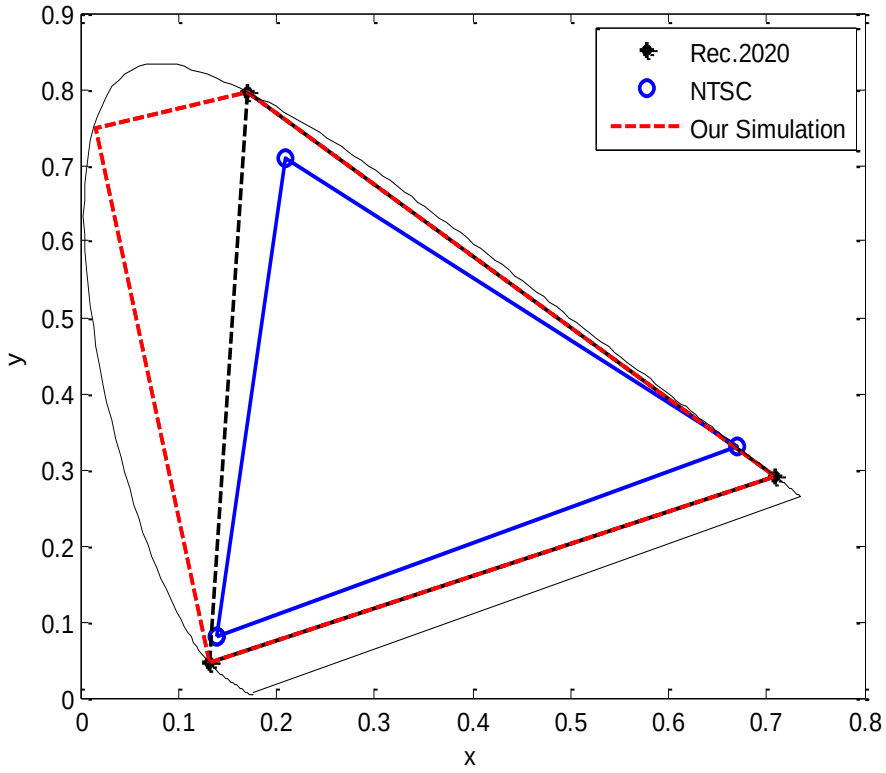

Figure 3.3.2.2 Rec.2020 coverage after addition of cyan component to the parameters that have more than 99% coverage in three-color combination

Chapter 4

Conclusions

Energy efficient technologies are extremely important especially for the future. In every aspect of life, designing energy saving devices is the main topic of the industry. In this thesis, to save energy and improve the quality of lighting and display applications, the parameters of light are optimized.

Starting from two color components, the performance of the light sources have been simulated and analyzed in terms of color rendering ability, color temperature and luminous efficacy of optical radiation.

Up to four-color mixing, it is proved that to obtain a high quality white light that has a color rendering index (CRI) value higher than 90, a correlated color temperature (CCT) value lower than 4000K and a luminous efficacy of optical radiation (LER) value higher than 380lm/W is needed. In this thesis, the emission parameters of a color source, peak emission wavelength, full width at half maximum (FWHM) and intensity, have been engineered to provide the high quality white light parameters.

As it has been stated, the three-color mixing is not enough to obtain the high quality white. It provides the LER and CCT conditions whereas the CRI was 85.1. Four-color mixing gave the appropriate results and it was proved that it is possible to reach limitations using four color components.

Display technology requires different spectral content in the color scale that matches the visible colors perceived by the human eye. Increment on the

number of colors on display is possible by enlargement of the color gamut that includes colors on display. Using ultra-narrow emitters instead of narrow emitters, it is possible to reach last announced reference triangle, Rec.2020 reaching up to 99.82% coverage which corresponds to 99.99% NTSC color gamut coverage and 171.05% areal enlargement of NTSC.

Consequently, in this thesis all parameters for applications of both lighting and display technology have been filtered and the quality of applications has been increased to address for enhanced energy efficiency and color quality.

BIBLIOGRAPHY

[1] D.B. Judd, G. Wyszecki, “Color in business, science, and industry, 3rd. Ed.” John Wiley & Sons Inc. (1975).

[2] Electromagnetic Spectrum, http://en.citizendium.org/images/8/8a/Electromagnetic-Spectrum.png (last accessed: 09-Sep-2016).

[3] Basic Visual Pathways, http://www.bioon.com/bioline/neurosci/course/basvis.html (last accessed: 11-Nov-2016).

[4] Parts of the Ascending Visual Pathway, http://academic.udayton.edu/gregelvers/psy323/labels/pathway.jpg. (last accessed: 10-Sep-2016).

[5] Human Eye Anatomy and Eye Surgery Types, http://www.healthpages.org/health-a-z/human-eye-anatomy-surgery-types/ (last accessed: 10-Sep-2016).

[6] Simple Anatomy of Retina by Helga Kolb, http://webvision.med.utah.edu/book/part-i-foundations/simple-anatomy-of-the-retina/ (last accessed: 11-Sep-2016).

[7] G. Wyszecki, W. S. Stiles, “Color science: Concepts and methods, quantitative data and formulae, 2nd. Ed.” John Wiley & Sons Inc. (2000).

[8] What is the difference between rod and cone type of cells?, https://www.quora.com/What-is-the-difference-between-rod-and-cone-type-of-cells (last accessed: 13-Sep-2016).

[9] E. F. Schubert, “Light-emitting diodes, 2nd. Ed.” Cambridge University Press (2006).

[10] Introduction-Lumens, Lux and Candelas http://sound.whsites.net/lamps/lumen-lux-candela.html (last accessed: 11-Sep-2016).

[11] E. F. Schubert/Light Emitting Diodes, https://www.ecse.rpi.edu/homepages/schubert/Light-Emitting-Diodes-dot-org/chap16/chap16.htm (last accessed: 15-Sep-2016)

[12] N. Ohta, A. R. Robertson, “Colorimetry- Fundamentals and applications,” John Wiley & Sons Inc. (2005).

[13] R. W. G. Hunt, “The reproduction of the color,” John Wiley & Sons Inc. 6th Edt. (2004).

[14] Cones and Waves, http://www.boronine.com/2012/03/26/Color-Spaces-for-Human-Beings/ (last accessed: 15-Sep-2016).

[15] E. Reinhard, E. A. Khan, A. O. Akyüz, G. M. Johnson, “Color imaging-Fundamentals and applications,” A. K. Peters Ltd. (2008).

[16] R. G. Kuehnl, “Color space and its devisions-Color order from antiquity to the present,” John Wiley & Sons Inc. (2003).

[17] Introduction to color theory, http://kcchao.wikidot.com/color-space (last accessed: 17-Sep-2016).

[18] J. Morovic, “Color gamut mapping,” John Wiley & Sons Inc. (2008).

[19] W. D. Wright, “The graphical representation of small color differences,” J. Opt. Soc. Am., 33, 632-636 (1943).

[20] CIE Luv, http://dba.med.sc.edu/price/irf/Adobe_tg/models/cieluv.html (last accessed: 22-Sep-2016).

[21] D. L. MacAdam, “Visual sensitivities to color differences in daylight,” J. Opt. Soc. Am., 32, 247-274 (1942).

[22] E. F. Schubert/Light Emitting Diodes, https://www.ecse.rpi.edu/~schubert/Light-Emitting-Diodes-dot-org/chap17/chap17.htm (last accessed: 22-Sep-2016).

[23] P. Goldstein, “Non-MacAdam color discrimination ellipses,” Proc. SPIE Novel Optical Systems Design and Optimization XV, 8487, A1-A13 (2012).

[24] R. W. G. Hunt, M. R. Pointer, “Measuring colour,” John Wiley & Sons Inc. 4th Edt. (2011).

[25] S. Kobayashi, S. Mikoshiba, S. Lim, “LCD backlights,” John Wiley & Sons Inc. (2009).

[26] Color gamut & Correlated color temperature, http://lumenhub.com/color-and-cct/ (last accessed: 13-Nov-2016).

[27] A. R. Robertson, “Computation of correlated color temperature and distribution temperature,” J. Opt. Soc. Am. 58(11), 1528-1535 (1968).

[28] Y. Ohno, “Practical use and calculation of CCT and Duv.” NIST, 47-55 (2013).

[29] Color temperature, https://en.wikipedia.org/wiki/Color_temperature (last accessed: 18-Sep-2016).

[30] Correlated Color Temperature, https://www.iluxz.com/blog/correlated-color-temperaturecct/ (19-Nov-2016).

[31] T. Erdem, S. Nizamoğlu, H. V. Demir, “Computational study of power conversion and luminous efficiency performance for semiconductor quantum dot nanophosphors on light-emitting diodes,” Opt. Express, 20(3), 3275-3295 (2012).

[32] S. Nizamoğlu, T. Erdem, X. W. Sun, H. V. Demir, “Warm-white light-emitting diodes integrated with colloidal quantum dots for high luminous efficacy and color rendering,” Opt. Letters, 35(20), 3372-3374 (2010).

[33] S. Nizamoğlu, G. Zengin, H. V. Demir, “Color-converting combinations of nanocrystal emitters for warm-white light generation with high color rendering index,” Appl. Phys. Lett., 92, 031102 (2008).

[34] T. Erdem, S. Nizamoğlu, X. W. Sun, H. V. Demir, “A photometric investigation of ultra-efficient LEDs with high color rendering index and high luminous efficacy employing nanocrystal quantum dot luminophores,” Opt. Express, 18(1), 340-347 (2009).

[35] Color Rendering Index (CRI), http://www.luxtg.com/color-rendering-index-cri/ (last accessed: 15-Nov-2016).

[36] W. Davis, Y. Ohno, “Approaches to color rendering measurement,” J. Mod. Opt., 56(13), 1412-1419 (2009).

[37] LEDs: Decoding Color Performance, http://www.archlighting.com/technology/leds-decoding-color-performance_o (last accessed: 27-Sep-2016).

[38] E. F. Schubert/Light Emitting Diodes, https://www.ecse.rpi.edu/~schubert/Light-Emitting-Diodes-dot-org/chap19/chap19.htm (last accessed: 23-Sep-2016).

[39] The only LED lights, http://greensavingsolution.com/home.html (last accessed: 12-Nov-2016).

[40] T. Erdem, H. V. Demir, “Color science of nanocrystal quantum dots for lighting and displays,” Nanophotonics 2(1), 57-81 (2012).

[41] R. Peon, G. Doluweera, I. Platonova, D. I. Halliday, G. I. Halliday, "Solid state lighting for developing world-The only solution," Optics&Photonics 2005, Proc. SPIE 5941, 109-123 (2005).

[42] R. Haitz, J. Y. Tsao, "Solid state lighting: 'The case' 10 years after and future prospects," Phys. Status Solidi A, 208(1),17-29 (2011).

[43] D. C. Agraval, H. S. Leff, V. J. Menon, "Efficiency and efficacy of incandescent lamps," Am. J. Phys., 64(5), 649-654 (1996).

[44] J. M. Phillips, M. F. Coltrin, M. H. Crawford, A. J. Fischer, M. R. Krames, R. Mueller-Mach, G. O. Mueller, Y. Ohno, L. E. S. Rohwer, J. A. Simmons, J. Y. Tsao, "Research challenges to ultra-efficient inorganic solid-state lighting," Laser&Photon. Rev., 1(4) 307-333 (2007).

[45] P. Raynham, T. Saksvrikronning, "White light and facial recognition," The Lighting Journal, 68(1), 29-33 (2003).

[46] H. V. Demir, "Quality LED lighting and display using nanocrystals," IEEE International Photonics Conference (2013).

[47] M. Özdemir, S. Genç, R. Özdemir, Y. Altıntas, M. Çıtır, Ü. Şen, E. Mutlugün, H. Usta, "Trans-cis isomerization assisted synthesis of solution-processable yellow fluorescent maleic anhydrides for white-light generation," Synthetic Met., 210(B), 192-200 (2015).

[48] M. H. Crawford, "LEDs for Solid-State Lighting: Performance Challenges and Recent Advances," IEEE Journal of Selected Topics in Quantum Electronics 15(4), 1028-1040 (2009).

[49] J. Shinar, "Organic light-emitting devices," Springer (2004).

[50] S. Kim, S. H. Im, S. W. Kim, "Performance of light-emitting-diode based on quantum dots," Nanoscale, 5, 5205-5214 (2013).

[51] P. Zhong, G. He, M. Zhang, "Optimal spectra of white light-emitting diodes using quantum dot nanophosphors," Opt. Express, 20(8), 9122-9134 (2012).

[52] J. Ziegler, S. Xu, E. Kucur, F. Meister, M. Batentschuk, F. Gindele, T. Nann, "Silica-coated InP/ZnS nanocrystals as converter materialin White LEDs," Adv. Mater 20, 4068-4073 (2008).

[53] W. S. Song, H. Yang, "Efficient white-light-emitting diodes fabricated from highly fluorescent copper indium sulfide core/Shell quantum dots," Chem. Mater. 24, 1961-1967 (2012).

[54] K. Kakinuma, “Technology of wide color gamut backlight with light-emitting-diode for liquid crystal display television,” Jpn. J. Appl. Phys., 45(5) 4330-4334 (2006).

[55] J. Chen, V. Hardev, J. Hartlove, J. Hofler, E. Lee, “A high-efficiency wide-color-gamut solid-state backlight system for LCDs using quantum dot enhancement film,”SID Symposium Digest of Technical Papers, 43(1), 895–896 (2012).

[56] R. J. Xie, N. Hirosaki, T. Takeda, “Wide color gamut backlight for liquid crystal displays using three-band phosphor-converted white light-emitting diodes,” Appl. Phys. Express **2**(2), 022401 (2009).

[57] S. C. Sullivan, W. Liu, P. Allen, J. S. Steckel, “Quantum dots for LED downconversion in display applications,” Journal of Solid State Science and Tech., 2(2), R3026-R3030 (2013).

[58] S. H. Lee, K. H. Lee, J. H. Jo, B. Park, Y. Kwon, H. S. Jang, H. Yang, “Remote-type, high-color gamut white light-emitting diode based on InP quantum dot color converters,” Opt. Mater. Express 4(7), 1297-1302 (2014).

[59] Z. Luo, D. Xu, S.T. Wu “Emerging quantum-dots-enhanced LCDs,” J. Display Tech. 10(7), 526-539 (2014).

[60] Y. Altıntas, S. Genç, M. Y. Talpur, E. Mutlugün, "CdSe/ZnS quantum dot films for high performance flexible lighting and display applications," Nanotechnology, 27, 1-9 (2016).

[61] Chromaticity Diagram Template, http://www.originlab.com/fileExchange/details.aspx?fid=168 (last accessed: 1-Dec-2016).

[62] ITU-R Recommendation BT.709-5, “Parameter values for HDTV standards for production and international programme exchange,” (2002).

[63] Adobe Systems Inc., “Adobe RGB (1998) Color Image Encoding,” (2005).

[64] ITU-R Recommendation BT.2020-1, “Parameter values for ultra-high definition television systems for production and international programme exchange,” (2014).

[65] S. Wen, “A method for selecting display primaries to match a target color gamut,” Journal of SID, 15(12), 1015-1022 (2007).

[66] K. Masaoka, "Single display gamut size metric," Journal of the SID, 24(7), 419-423 (2016).

[67] K. Masaoka, Y. Nishida, M. Sugawara, “Designing display primaries with currently available light sources for UHDTV wide-gamut system colorimetry,” Opt. Express 22(16), 19069-19077 (2014).

[68] K. Masaoka, Y. Nishida, “Metric of color-space coverage for wide-gamut displays,” Opt. Express 23(6), 7802-7808 (2015).

[69] K. Masaoka, “Display gamut metrology using chromaticity diagram,” IEEE Access 4(16), 3878-3886 (2016).

[70] J. S. Steckel, J. Ho, C. Hamilton, J. Xi, C. Breen, W. Liu, P. Allen, S. C. Sullivan, “Quantum dots: The ultimate down-conversion material for LCD displays,” Journal of SID 23(7), 294-305 (2015).

[71] Z. Luo, Y. Chen, S.T. Wu “Wide color gamut LCD with a quantum dot backlight,” Opt. Express 21(22), 26269-26284 (2013).

[72] E. Jang, S. Jun, H. Jang, J. Lim, B. Kim, Y. Kim “White-light-emitting diodes with quantum dot color converters for display backlights,” Adv. Mater., 22, 3076-3080 (2010).

[73] R. Zhu, Z, Luo, H. Chen, Y. Dong, S. T. Wu, “Realizing Rec.2020 color gamut quantum dot displays,” Opt. Express 23(18), 23680-23693 (2015).

[74] K. V. Chellappan, E, Erden, H. Urey, "Laser based displays: a review," Applied optics, 49(25), F79-F98 (2010).

[75] S. Ithurria, G. Bousquet, B. Dubertret, “Continuous transition from 3D to 1D confinement observed during the formation of CdSe nanoplatelets,” J. Am. Chem. Soc. 133(9), 3070-3077 (2011).

[76] S. Ithurria, B. Dubertret, “Quasi colloidal CdSe platelets with thicknesses controlled at the atomic level,” J. Am. Chem. Soc., 130, 16504-16505 (2008).

[77] M. Artemyev, A. Prudnikau, A. Antanovich, “New type of quantum confined semiconductor nanostructures: 2D colloidal nanoplatelets,” Physics, Chemistry and App. of Nanostructures, 257-263 (2015).

[78] K. Masaoka, Y. Nishida, M. Sugawara, E. Nakasu, “Design of primaries for a wide-gamut television colorimetry,” IEEE Trans. On Broad., 56(4), 452-457 (2010).

APPENDIX A

x, y, z Color Matching Functions

λ (nm)	$\bar{x}(\lambda)$	$\bar{y}(\lambda)$	$\bar{z}(\lambda)$
380	0,001368	0,000039	0,006450
385	0,002236	0,000064	0,010550
390	0,004243	0,000120	0,020050
395	0,007650	0,000217	0,036210
400	0,014310	0,000396	0,067850
405	0,023190	0,000640	0,110200
410	0,043510	0,001210	0,207400
415	0,077630	0,002180	0,371300
420	0,134380	0,004000	0,645600
425	0,214770	0,007300	1,039050
430	0,283900	0,011600	1,385600
435	0,328500	0,016840	1,622960
440	0,348280	0,023000	1,747060
445	0,348060	0,029800	1,782600
450	0,336200	0,038000	1,772110
455	0,318700	0,048000	1,744100
460	0,290800	0,060000	1,669200
465	0,251100	0,073900	1,528100
470	0,195360	0,090980	1,287640
475	0,142100	0,112600	1,041900
480	0,095640	0,139020	0,812950
485	0,057950	0,169300	0,616200
490	0,032010	0,208020	0,465180
495	0,014700	0,258600	0,353300
500	0,004900	0,323000	0,272000
505	0,002400	0,407300	0,212300
510	0,009300	0,503000	0,158200
515	0,029100	0,608200	0,111700
520	0,063270	0,710000	0,078250
525	0,109600	0,793200	0,057250
530	0,165500	0,862000	0,042160
535	0,225750	0,914850	0,029840
540	0,290400	0,954000	0,020300
545	0,359700	0,980300	0,013400
550	0,433450	0,994950	0,008750
555	0,512050	1,000000	0,005750
560	0,594500	0,995000	0,003900
565	0,678400	0,978600	0,002750
570	0,762100	0,952000	0,002100
575	0,842500	0,915400	0,001800
580	0,916300	0,870000	0,001650
585	0,978600	0,816300	0,001400
590	1,026300	0,757000	0,001100
595	1,056700	0,694900	0,001000
600	1,062200	0,631000	0,000800
605	1,045600	0,566800	0,000600
610	1,002600	0,503000	0,000340
615	0,938400	0,441200	0,000240
620	0,854450	0,381000	0,000190
625	0,751400	0,321000	0,000100
630	0,642400	0,265000	0,000050
635	0,541900	0,217000	0,000030
640	0,447900	0,175000	0,000020
645	0,360800	0,138200	0,000010
650	0,283500	0,107000	0,000000
655	0,218700	0,081600	0,000000
660	0,164900	0,061000	0,000000
665	0,121200	0,044580	0,000000
670	0,087400	0,032000	0,000000
675	0,063600	0,023200	0,000000
680	0,046770	0,017000	0,000000
685	0,032900	0,011920	0,000000
690	0,022700	0,008210	0,000000
695	0,015840	0,005723	0,000000
700	0,011359	0,004102	0,000000
705	0,008111	0,002929	0,000000
710	0,005790	0,002091	0,000000
715	0,004109	0,001484	0,000000
720	0,002899	0,001047	0,000000
725	0,002049	0,000740	0,000000
730	0,001440	0,000520	0,000000
735	0,001000	0,000361	0,000000
740	0,000690	0,000249	0,000000
745	0,000476	0,000172	0,000000
750	0,000332	0,000120	0,000000
755	0,000235	0,000085	0,000000

λ (nm)	$\bar{x}(\lambda)$	$\bar{y}(\lambda)$	$\bar{z}(\lambda)$
760	0,000166	0,000060	0,000000
765	0,000117	0,000042	0,000000
770	0,000083	0,000030	0,000000
775	0,000059	0,000021	0,000000
780	0,000042	0,000015	0,000000

APPENDIX B

Spectral Reflection Data for 14 Test Color Samples

TCS1: light greyish red
TSC2: dark greyish yellow
TCS3: strong yellow green
TCS4: moderate yellowish green
TCS5: light bluish green
TCS6: light blue
TCS7: light violet
TCS8: light reddish purple
TCS9: strong red
TCS10: strong yellow
TCS11: strong green
TCS12: violet blue
TCS13: skin color
TCS14: leaf of tree

λ (nm)	TCS 1	TCS 2	TCS 3	TCS 4	TCS 5	TCS 6	TCS 7	TCS 8	TCS 9	TCS 10	TCS 11	TCS 12	TCS 13	TCS 14
360	116	53	58	57	143	79	150	75	69	42	74	189	71	36
365	136	55	59	59	187	81	177	78	72	43	79	175	76	36
370	159	59	61	62	233	89	218	84	73	45	86	158	82	36
375	190	64	63	67	269	113	293	90	70	47	98	139	90	36
380	219	70	65	74	295	151	378	104	66	50	111	120	104	36
385	239	79	68	83	306	203	459	129	62	54	121	103	127	36
390	252	89	70	93	310	265	524	170	58	59	127	90	161	37
395	256	101	72	105	312	339	546	240	55	63	129	82	211	38
400	256	111	73	116	313	410	551	319	52	66	127	76	264	39
405	254	116	73	121	315	464	555	416	52	67	121	68	313	39
410	252	118	74	124	319	492	559	462	51	68	116	64	341	40
415	248	120	74	126	322	508	560	482	50	69	112	65	352	41
420	244	121	74	128	326	517	561	490	50	69	108	75	359	42
425	240	122	73	131	330	524	558	488	49	70	105	93	361	42
430	237	122	73	135	334	531	556	482	48	72	104	123	364	43
435	232	122	73	139	339	538	551	473	47	73	104	160	365	44
440	230	123	73	144	346	544	544	462	46	76	105	207	367	44
445	226	124	73	151	352	551	535	450	44	78	106	256	369	45
450	225	127	74	161	360	556	522	439	42	83	110	300	372	45
455	222	128	75	172	369	556	506	426	41	88	115	331	374	46
460	220	131	77	186	381	554	488	413	38	95	123	346	376	47
465	218	134	80	205	394	549	469	397	35	103	134	347	379	48

λ (nm)	TCS 1	TCS 2	TCS 3	TCS 4	TCS 5	TCS 6	TCS 7	TCS 8	TCS 9	TCS 10	TCS 11	TCS 12	TCS 13	TCS 14
470	216	138	85	229	403	541	448	382	33	113	148	341	384	50
475	214	143	94	254	410	531	429	366	31	125	167	328	389	52
480	214	150	109	281	415	519	408	352	30	142	192	307	397	55
485	214	159	126	308	418	504	385	337	29	162	219	282	405	57
490	216	174	148	332	419	488	363	325	28	189	252	257	416	62
495	218	190	172	352	417	469	341	310	28	219	291	230	429	67
500	223	207	198	370	413	450	324	299	28	262	325	204	443	75
505	225	225	221	383	409	431	311	289	29	305	347	178	454	83
510	226	242	241	390	403	414	301	283	30	365	356	154	461	92
515	226	253	260	394	396	395	291	276	30	416	353	129	466	100
520	225	260	278	395	389	377	283	270	31	465	346	109	469	108
525	225	264	302	392	381	358	273	262	31	509	333	90	471	121
530	227	267	339	385	372	341	265	256	32	546	314	75	474	133
535	230	269	370	377	363	325	260	251	32	581	294	62	476	142
540	236	272	392	367	353	309	257	250	33	610	271	51	483	150
545	245	276	399	354	342	293	257	251	34	634	248	41	490	154
550	253	282	400	341	331	279	259	254	35	653	227	35	506	155
555	262	289	393	327	320	265	260	258	37	666	206	29	526	152
560	272	299	380	312	308	253	260	264	41	678	188	25	553	147
565	283	309	365	296	296	241	258	269	44	687	170	22	582	140
570	298	322	349	280	284	234	256	272	48	693	153	19	618	133
575	318	329	332	263	271	227	254	274	52	698	138	17	651	125
580	341	335	315	247	260	225	254	278	60	701	125	17	680	118
585	367	339	299	229	247	222	259	284	76	704	114	17	701	112
590	390	341	285	214	232	221	270	295	102	705	106	16	717	106
595	409	341	272	198	220	220	284	316	136	705	100	16	729	101
600	424	342	264	185	210	220	302	348	190	706	96	16	736	98
605	435	342	257	175	200	220	324	384	256	707	92	16	742	95
610	442	342	252	169	194	220	344	434	336	707	90	16	745	93
615	448	341	247	164	189	220	362	482	418	707	87	16	747	90
620	450	341	241	160	185	223	377	528	505	708	85	16	748	89
625	451	339	235	156	183	227	389	568	581	708	82	16	748	87
630	451	339	229	154	180	233	400	604	641	710	80	18	748	86
635	451	338	224	152	177	239	410	629	682	711	79	18	748	85
640	451	338	220	151	176	244	420	648	717	712	78	18	748	84
645	451	337	217	149	175	251	429	663	740	714	78	18	748	84
650	450	336	216	148	175	258	438	676	758	716	78	19	748	84

λ (nm)	TCS 1	TCS 2	TCS 3	TCS 4	TCS 5	TCS 6	TCS 7	TCS 8	TCS 9	TCS 10	TCS 11	TCS 12	TCS 13	TCS 14
655	450	335	216	148	175	263	445	685	770	718	78	20	748	84
660	451	334	219	148	175	268	452	693	781	720	81	23	747	85
665	451	332	224	149	177	273	457	700	790	722	83	24	747	87
670	453	332	230	151	180	278	462	705	797	725	88	26	747	92
675	454	331	238	154	183	281	466	709	803	729	93	30	747	96
680	455	331	251	158	186	283	468	712	809	731	102	35	747	102
685	457	330	269	162	189	286	470	715	814	735	112	43	747	110
690	458	329	288	165	192	291	473	717	819	739	125	56	747	123
695	460	328	312	168	195	296	477	719	824	742	141	74	746	137
700	462	328	340	170	199	302	483	721	828	746	161	97	746	152
705	463	327	366	171	200	313	489	720	830	748	182	128	746	169
710	464	326	390	170	199	325	496	719	831	749	203	166	745	188
715	465	325	412	168	198	338	503	722	833	751	223	210	744	207
720	466	324	431	166	196	351	511	725	835	753	242	257	743	226
725	466	324	447	164	195	364	518	727	836	754	257	305	744	243
730	466	324	460	164	195	376	525	729	836	755	270	354	745	260
735	466	323	472	165	196	389	532	730	837	755	282	401	748	277
740	467	322	481	168	197	401	539	730	838	755	292	446	750	294
745	467	321	488	172	200	413	546	730	839	755	302	485	750	310
750	467	320	493	177	203	425	553	730	839	756	310	520	749	325
755	467	318	497	181	205	436	559	730	839	757	314	551	748	339
760	467	316	500	185	208	447	565	730	839	758	317	577	748	353
765	467	315	502	189	212	458	570	730	839	759	323	599	747	366
770	467	315	505	192	215	469	575	730	839	759	330	618	747	379
775	467	314	510	194	217	477	578	730	839	759	334	633	747	390
780	467	314	516	197	219	485	581	730	839	759	338	645	747	399
785	467	313	520	200	222	493	583	730	839	759	343	656	746	408
790	467	313	524	204	226	500	585	731	839	759	348	666	746	416
795	466	312	527	210	231	506	587	731	839	759	353	674	746	422
800	466	312	531	218	237	512	588	731	839	759	359	680	746	428
805	466	311	535	225	243	517	589	731	839	759	365	686	745	434
810	466	311	539	233	249	521	590	731	838	758	372	691	745	439
815	466	311	544	243	257	525	590	731	837	757	380	694	745	444
820	465	311	548	254	265	529	590	731	837	757	388	697	745	448
825	464	311	552	264	273	532	591	731	836	756	396	700	745	451
830	464	310	555	274	280	535	592	731	836	756	403	702	745	454

APPENDIX C

CIE Daylight Components

λ (nm)	$S_0(\lambda)$	$S_1(\lambda)$	$S_2(\lambda)$
300	0,04	0,02	0,00
305	3,02	2,26	1,00
310	6,00	4,50	2,00
315	17,80	13,45	3,00
320	29,60	22,40	4,00
325	42,45	32,20	6,25
330	55,30	42,00	8,50
335	56,30	41,30	8,15
340	57,30	40,60	7,80
345	59,55	41,10	7,25
350	61,80	41,60	6,70
355	61,65	39,80	6,00
360	61,50	38,00	5,30
365	65,15	40,20	5,70
370	68,80	42,40	6,10
375	66,10	40,45	4,55
380	63,40	38,50	3,00
385	64,60	36,75	2,10
390	65,80	35,00	1,20
395	80,30	39,20	0,05
400	94,80	43,40	-1,10
405	99,80	44,85	-0,80
410	104,80	46,30	-0,50
415	105,35	45,10	-0,60
420	105,90	43,90	-0,70
425	101,35	40,50	-0,95
430	96,80	37,10	-1,20
435	105,35	36,90	-1,90
440	113,90	36,70	-2,60
445	119,75	36,30	-2,75
450	125,60	35,90	-2,90
455	125,55	34,25	-2,85
460	125,50	32,60	-2,80
465	123,40	30,25	-2,70
470	121,30	27,90	-2,60
475	121,30	26,10	-2,60
480	121,30	24,30	-2,60
485	117,40	22,20	-2,20
490	113,50	20,10	-1,80
495	113,30	18,15	-1,65
500	113,10	16,20	-1,50
505	111,95	14,70	-1,40
510	110,80	13,20	-1,30
515	108,65	10,90	-1,25
520	106,50	8,60	-1,20
525	107,65	7,35	-1,10
530	108,80	6,10	-1,00
535	107,05	5,15	-0,75
540	105,30	4,20	-0,50
545	104,85	3,05	-0,40
550	104,40	1,90	-0,30
555	102,20	0,95	-0,15
560	100,00	0,00	0,00
565	98,00	-0,80	0,10
570	96,00	-1,60	0,20
575	95,55	-2,55	0,35
580	95,10	-3,50	0,50
585	92,10	-3,50	1,30
590	89,10	-3,50	2,10
595	89,80	-4,65	2,65
600	90,50	-5,80	3,20
605	90,40	-6,50	3,65
610	90,30	-7,20	4,10
615	89,35	-7,90	4,40
620	88,40	-8,60	4,70
625	86,20	-9,05	4,90
630	84,00	-9,50	5,10
635	84,55	-10,20	5,90
640	85,10	-10,90	6,70
645	83,50	-10,80	7,00
650	81,90	-10,70	7,30
655	82,25	-11,35	7,95
660	82,60	-12,00	8,60
665	83,75	-13,00	9,20
670	84,90	-14,00	9,80

λ (nm)	$S_0(\lambda)$	$S_1(\lambda)$	$S_2(\lambda)$
675	83,10	-13,80	10,00
680	81,30	-13,60	10,20
685	76,60	-12,80	9,25
690	71,90	-12,00	8,30
695	73,10	-12,65	8,95
700	74,30	-13,30	9,60
705	75,35	-13,10	9,05
710	76,40	-12,90	8,50
715	69,85	-11,75	7,75
720	63,30	-10,60	7,00
725	67,50	-11,10	7,30
730	71,70	-11,60	7,60
735	74,35	-11,90	7,80
740	77,00	-12,20	8,00
745	71,10	-11,20	7,35
750	65,20	-10,20	6,70
755	56,45	-9,00	5,95
760	47,70	-7,80	5,20
765	58,15	-9,50	6,30
770	68,60	-11,20	7,40
775	66,80	-10,80	7,10
780	65,00	-10,40	6,80
785	65,50	-10,50	6,90
790	66,00	-10,60	7,00
795	63,50	-10,15	6,70
800	61,00	-9,70	6,40
805	57,15	-9,00	5,95
810	53,30	-8,30	5,50
815	56,10	-8,80	5,80
820	58,90	-9,30	6,10
825	60,40	-9,55	6,30
830	61,90	-9,80	6,50

APPENDIX D

MATLAB codes

The first part of the MATLAB codes which is used for the calculation of a chromaticity coordinate that belongs green color with 35nm FWHM and 525nm peak emission wavelength is given below:

```
wlg=525;
FWHMgreen=35;
wavel=360:5:830;

gaussg=normpdf(wavel,wlg,FWHMgreen/ro);
gaussg=peakg*gaussg./max(gaussg);
spdg=gaussg';

Xg = trapz(wavel,spdg.*xcol');
Yg = trapz(wavel,spdg.*ycol');
Zg = trapz(wavel,spdg.*zcol');
xg = Xg/(Xg+Yg+Zg);
yg = Yg/(Xg+Yg+Zg);
```

where "xcol", "ycol", and "zcol" are the x,y,z color matching functions from table and xg, yg are chromaticity coordinates.

The calculation of coordinates is enough for the LER. The equation has been given below:

```
LER=683*(trapz(wavel,spd'.*esf))/(trapz(wavel,spd));
```

where "esf" stands for eye sensitivity function.

After the coordinates of a spectrum have been calculated, using these coordinates and constant corner coordinates of any reference triangle, the intersection are can be calculated as given below:

```
[intxNTSC, intyNTSC] = polybool('intersection', xour,
your, cons31x,cons31y);
```

```
coverNTSC=polyarea(intxNTSC,intyNTSC)/polyarea(cons31
x,cons31y)*100;
```

where "intxNTSC", "intyNTSC" are the intersection coordinates of borders with our triangle (xour,your) and reference triangle (NTSC) and "coverNTSC" is the coverage ratio of our triangle on NSTC.

The MATLAB codes for the calculation of CCT value for a spectrum have given below.

```
% Data of isotemperature lines

dwl = wl(2)-wl(1); % wavelength increment = 1 nm

ucol = (2/3)*xcol;
vcol = ycol;
wcol = -0.5*xcol + (3/2)*ycol + 0.5*zcol;
h = 6.6260693e-34; % Planck's constant
c = 299792458; % speed of light
k = 1.3806505e-23; % Boltzmann constant
c1 = 2*pi*h*c^2;
c2 = h*c/k;

MK = [0.01 1:600]; % MIRED values
T = 1./(MK*1e-6);
for i = 1:length(T)
   spdref = c1 * (1e-9*wl).^-5 ./ (exp(c2./…
(T(i).* 1e-9*wl)) - 1);
   spdref = spdref/max(spdref);  %normalization
   wave = wl*1e-9;

   U = sum(spdref.*ucol);
   V = sum(spdref.*vcol);
   W = sum(spdref.*wcol);
   R = U+V+W;
   u(i) = U/R;
   v(i) = V/R;

   Upr = c1*c2*(T(i))^-2*sum(wave.^-
6.*ucol.*exp(c2./(wave.*T(i))).*(exp(c2./(wave.*…
(T(i))))-1).^-2)*dwl;
```

```
   Vpr = sum(c1*c2*T(i)^-2*wave.^-
6.*vcol.*exp(c2./(wave.*T(i))).*(exp(c2./(wave.*…
(T(i))))-1).^-2)*dwl;
   Wpr = sum(c1*c2*T(i)^-2*wave.^-
6.*wcol.*exp(c2./(wave.*T(i))).*(exp(c2./(wave.*…
(T(i))))-1).^-2)*dwl;
   Rpr = Upr+Vpr+Wpr;

   sl(i) = (Vpr*R-V*Rpr)/(Upr*R-U*Rpr);
   m(i) = -1/sl(i);
end
ut = u;
vt = v;
tt = m;
isoTempLinesTable = [T' u' v' m'];

% CCT Calculation

%Robertson Method
% Find adjacent lines to (us, vs)

u = 4*x/(-2*x+12*y+3);
v = 6*y/(-2*x+12*y+3);
 index = 0;
 d1 = ((v-vt(1)) - tt(1)*(u…
-ut(1)))/sqrt(1+tt(1)*tt(1));
 for i=2:length(T)
     d2 = ((v-vt(i)) - tt(i)*(u…
-ut(i)))/sqrt(1+tt(i)*tt(i));
     if (d1/d2 < 0)
         index = i;
         break;
     else
         d1 = d2;
     end
 end
 if index == 0
     Tc = -1; % Not in range
     fprintf(1,'Not able to calculate CCT, u, v
coordinates outside range.\n');
 else
     % Interpolation between isotemperature lines
     Tc = 1/(1/T(index-1)+d1/(d1-d2)*(1/T(index)…
-1/T(index-1)));
     fprintf(1,'CCT(x,y) = %.1fK\n',Tc);
 end
```

The CCT value can be calculated also using the McCamy equation which has been given below:

```
n=(x-0.3320)/(0.1858-y);
CCT= 449*nn^3+3525*nn^2+6823.3*nn+5520.33;
```

where n is found using chromaticity coordinates and using n the CCT can be calculated. Although it is much easier compared to the classical method, it has error in the levels of one to ten Kelvin degrees.

The codes for the calculation of CRI are as the followings;

```
if (Tc < 5000)
    c1 = 3.7418e-16;
    c2 = 1.4388e-2;
    spdref = c1 * (1e-9*wavel).^-5 ./ (exp(c2./…
(Tc.* 1e-9*wavel)) - 1);
else
    if (Tc <= 25000)

        S0=CIEDay(:,2); % The table has been given in
Appendix C.
        S1=CIEDay(:,3);
        S2=CIEDay(:,4);

        if (Tc <= 7000)
            xd = -4.6070e9 / Tc.^3 + 2.9678e6 / …
Tc.^2 + 0.09911e3 / Tc + 0.244063;
        else
            xd = -2.0064e9 / Tc.^3 + 1.9018e6 / …
Tc.^2 + 0.24748e3 / Tc + 0.237040;
        end
        yd = -3.000*xd*xd + 2.870*xd - 0.275;
        M1 = (-1.3515 - 1.7703*xd + 5.9114*yd)…
 / (0.0241 + 0.2562*xd - 0.7341*yd);
        M2 = (0.0300 - 31.4424*xd + 30.0717*yd)…
 / (0.0241 + 0.2562*xd - 0.7341*yd);
        spdref = S0 + M1*S1 + M2*S2;
        spdref = interp1(wl,spdref,wavel);
        spdref(isnan(spdref)) = 0.0;
    else
        R = -1;
        Ra=-1;
```

```
disp('CCT is higher than 25000K so the CRI have not
been calculated.\n');
    end
end

% Interpolate TCS values from 5 nm to spd increments
TCS_1 = zeros(length(wavel),14);
for i = 1:14
    TCS_1(:,i) =
interp1(TCS(:,1),TCS(:,i+1),wavel,'linear',0);
end

% u, v chromaticity coordinates under test
illuminant, (uk, vk) and reference illuminant, (ur,
vr)
uki = zeros(1,14);
vki = zeros(1,14);
uri = zeros(1,14);
vri = zeros(1,14);
X = trapz(wavel,spd .* xcol);
Y = trapz(wavel,spd .* ycol);
Z = trapz(wavel,spd .* zcol);
Yknormal = 100 / Y;
Yk = Y*Yknormal;
uk = 4*X/(X+15*Y+3*Z);
vk = 6*Y/(X+15*Y+3*Z);
X = trapz(wavel,spdref .* xcol);
Y = trapz(wavel,spdref .* ycol);
Z = trapz(wavel,spdref .* zcol);
Yrnormal = 100 / Y;
Yr = Y*Yrnormal;
ur = 4*X/(X+15*Y+3*Z);
vr = 6*Y/(X+15*Y+3*Z);
for i = 1:14
    X = trapz(wavel,spd .* TCS_1(:,i) .* xcol);
    Y = trapz(wavel,spd .* TCS_1(:,i) .* ycol);
    Z = trapz(wavel,spd .* TCS_1(:,i) .* zcol);
    Yki(i) = Y*Yknormal;
    uki(i) = 4*X/(X+15*Y+3*Z);
    vki(i) = 6*Y/(X+15*Y+3*Z);
    X = trapz(wavel,spdref .* TCS_1(:,i) .* xcol);
    Y = trapz(wavel,spdref .* TCS_1(:,i) .* ycol);
    Z = trapz(wavel,spdref .* TCS_1(:,i) .* zcol);
    Yri(i) = Y*Yrnormal;
    uri(i) = 4*X/(X+15*Y+3*Z);
    vri(i) = 6*Y/(X+15*Y+3*Z);
end
```

```
% Color tolerance
DC = sqrt((uk-ur).^2 + (vk-vr).^2);

% Color shift
ck = (4 - uk - 10*vk) / vk;
dk = (1.708*vk + 0.404 - 1.481*uk) / vk;
cr = (4 - ur - 10*vr) / vr;
dr = (1.708*vr + 0.404 - 1.481*ur) / vr;

for i = 1:14
    cki = (4 - uki(i) - 10*vki(i)) / vki(i);
    dki = (1.708*vki(i) + 0.404 - 1.481*…
uki(i)) / vki(i);
    ukip(i) = (10.872 + 0.404*cr/ck*cki …
- 4*dr/dk*dki) / (16.518 + 1.481*cr/ck*cki -
dr/dk*dki);
    vkip(i) = 5.520 / (16.518 + 1.481*cr/ck*…
cki - dr/dk*dki);
end
%  Into 1964 Uniform space coordinates.
for i = 1:14
    Wstarr(i) = 25*Yri(i).^.333333 - 17;
    Ustarr(i) = 13*Wstarr(i)*(uri(i) - ur);
    Vstarr(i) = 13*Wstarr(i)*(vri(i) - vr);

    Wstark(i) = 25*Yki(i).^.333333 - 17;
    Ustark(i) = 13*Wstark(i)*(ukip(i) - ur);
    Vstark(i) = 13*Wstark(i)*(vkip(i) - vr);
end

% Delta E calculation
deltaE = zeros(1,14);
R = zeros(1,14);
for i = 1:14
    deltaE(i) = sqrt((Ustarr(i) - Ustark(i)).^2…
+ (Vstarr(i) - Vstark(i)).^2 + (Wstarr(i) -
Wstark(i)).^2);
    R(i) = 100 - 4.6*deltaE(i);
end
Ra = sum(R(1:8))/8;
fprintf(1,'CRI(x,y) = %.1f\n',Ra);
```